U. S. ARMY
TRANSPORTATION RESEARCH COMMAND
FORT EUSTIS, VIRGINIA

TRECOM Technical Report 63-17

OPTIMIZATION OF SILICON-GERMANIUM THERMOELECTRIC MODULES FOR TRANSPORTATION CORPS SILENT BOAT DESIGN

Task 1D010501A01408
(Formerly Task 9R99-20-001-08)
Contract DA 44-177-TC-857

May 1963

prepared by:

RADIO CORPORATION OF AMERICA
Harrison, New Jersey

DISCLAIMER NOTICE

THIS DOCUMENT IS BEST QUALITY PRACTICABLE. THE COPY FURNISHED TO DTIC CONTAINED A SIGNIFICANT NUMBER OF PAGES WHICH DO NOT REPRODUCE LEGIBLY.

HEADQUARTERS
U. S. ARMY TRANSPORTATION RESEARCH COMMAND
Fort Eustis, Virginia

This report reviews and summarizes the work performed under Contract DA 44-177-TC-857 for the U. S. Army Transportation Research Command.

Work on this project was carried out in the Electron Tube Division, Radio Corporation of America, Harrison, New Jersey, from July 1962 to December 1962, under the over-all direction of Dr. A. G. F. Dingwall.

The purpose of this study was to determine the feasibility of developing a 30-kw generator using SiGe alloy thermoelements and to develop a preliminary design. This effort was satisfactorily accomplished.

The conclusion reached in this report is concurred in by this command.

FOR THE COMMANDER:

KENNETH B. ABEL
Captain, TC
Adjutant

APPROVED BY:

JAMES P. WALLER
USATRECOM Project Engineer

Task 1DO10501A01406
(Formerly Task 9R99-20-001-08)
Contract DA 44-177-TC-857
TRECOM Technical Report 63-17
May 1963

OPTIMIZATION OF SILICON-GERMANIUM THERMOELECTRIC MODULES FOR TRANSPORTATION CORPS SILENT BOAT DESIGN

Prepared by

Radio Corporation of America
Direct Energy Conversion Department
Thermoelectric Products Engineering
Electron Tube Division
Harrison, New Jersey

for

U. S. ARMY TRANSPORTATION RESEARCH COMMAND
FORT EUSTIS, VIRGINIA

PREFACE

This is a report to the U. S. Army Transportation Research Command, Fort Eustis, Va., on the optimization of silicon-germanium thermoelectric modules for a Transportation Corps' silent boat design. The work referred to in this report was carried on by RCA in the Direct Energy Conversion Department at Harrison, N. J., and in the DEP Applied Research group at Camden, N. J.

This report was prepared by Dr. A. G. F. Dingwall, Project Engineer, and approved by W. F. Lawrence, Leader, Thermoelectric Device Design. USATRECOM Project Supervisors were Dr. R. L. Echols and J. P. Waller.

CONTENTS

Page

Section IV: 30-KW Thermoelectric Converter Design Study

ILLUSTRATIONS

LIST OF SYMBOLS

A	Area
d	Separation between legs of thermocouple (cm)
E	Voltage
h	Planck constant
h	Film coefficient (BTU/hr-ft^2-^{o}R)
I	Electric current (amp)
K	Thermal conductance (watt/^{o}C)
k	Boltzmann constant
L	Length (cm)
M	Dimensionless parameter characterizing performance of thermoelectric material = $(1 + ZT_{avg})^{1/2}$
m*	Effective mass of charge carriers
n	Carrier concentration
P	Electric power (watts)
Q	Thermal power (watts)
R	Resistance (ohm)
r	A number depending on the type of scattering which a carrier experiences as it moves through the lattice
S	Seebeck coefficient (volt/^{o}C)
T	Temperature (^{o}K)
T_{avg}	Average temperature (^{o}K)

T_C	Cold junction temperature (^oK)
T_H	Hot junction temperature (^oK)
T'	Temperature (^oR)
Z	Figure-of-merit of a thermoelectric material ($^oC^{-1}$)
α	Coefficient of thermal expansion ($^oC^{-1}$)
$\Delta\epsilon$	Elongation (inch)
ΔT	Temperature difference (^oC)
ϵ	Efficiency
ϵ_A	Emissivity of adsorber
ϵ_R	Emissivity of radiator
η	Carnot efficiency
K	Thermal conductivity (watt/cm-^oC)
μ	Mobility
ρ	Electrical resistivity (ohm-cm)
σ	Stefan-Boltzmann constant

SUMMARY

The TRECOM evaluation project encompassed a four and one-half month period of engineering effort to evaluate, by life test, optimum design factors for a silicon-germanium (SiGe) thermoelectric alloy converter. The overall technical objective of this study has been to design, fabricate and evaluate water-cooled thermoelectric modules which will operate in an air environment, in line with TRECOM requirements, for a silent-boat power source, utilizing RCA-developed SiGe alloys and assembly techniques.

All major technical objectives contained in the original proposal appear to have been met or exceeded, namely:

1. RCA-developed SiGe water-cooled thermoelectric modules have been successfully operated in air for prolonged periods at hot junction temperatures up to and including 1050°C with no signs of deterioration.

2. Stable thermocouple conversion efficiency values of 10.0 per cent at a hot junction temperature of 1020°C were demonstrated. To RCA's knowledge, this figure represents the highest long-term efficiency value actually obtained for thermoelectric devices, and represents a major breakthrough in the thermoelectric art.

3. A simple, yet rugged, basic module configuration has been developed by RCA. Among the unique features of the construction means are the use of continuous metallurgical joints throughout (i.e., no pressure contacts required) and a rigid construction in which no provision for flexible joints is necessary.

4. The RCA-developed configuration has been demonstrated to be mechanically rugged. Thermocouples, previously operated at 1050°C, have successfully withstood 100-g shock tests and 60-g vibration tests over the frequency spectrum 20-3000 cycles per second. In addition, the basic thermocouple modules have been temperature-cycled many times between 1000°C and room temperature with no evidences of deterioration.

5. The initial feasibility study of a 30-KW generator using SiGe thermoelements for a silent-boat power source has been completed. This analysis indicates that construction of such a generator using diesel oil or gasoline as a fuel supply is technically feasible within a weight limit of 1000 pounds and a total volume limit of 12 cubic feet.

RECOMMENDATIONS

The successful completion of this initial phase of the TRECOM feasibility study has demonstrated the efficiency and reliability of SiGe thermoelectric materials. RCA considers that the logical continuation of the present effort should be the construction of a prototype SiGe power generator of modest output. Such a fully working power source would provide important intermediate-stage engineering data necessary for the construction of a full 30-KW silent-boat power source. A convenient generator size of approximately 600 watts capacity would simulate the basic modular units in the 30-KW silent-boat design.

Electric power generated by a thermoelectric device for military applications affords several distinct advantages over more conventional methods of power generation. On a weight and volume basis, a 1000-pound thermoelectric generator with a 30-KW output will be more compact than gasoline and diesel motor-generator units. In addition, the thermoelectric generator has no moving parts, will operate silently, is free from vibration, and requires little or no attendance.

Incorporation of the new proven TRECOM thermocouple design into a compact, silent, power source will require extensive engineering development of the fossil-fuel burner-regenerator system and other associated hardware within which the thermoelectric units must be housed. It is anticipated, however, that construction and delivery of a working prototype generator can be completed by the end of 1963, representing a year's engineering effort.

SECTION I

BASIC THERMOELECTRIC CONSIDERATIONS

INTRODUCTION

Electrical power, at the present time, is generated by machines with moving parts. In such devices, thermal energy is converted into mechanical energy and thence into electrical energy. Recent advances in solid-state physics, however, have made practicable direct conversion of heat into electricity by thermoelectric power generators. Such thermoelectric generators can have significant advantages in the low- and medium-power fields. These advantages include portability, lack of noise associated with moving machinery, and no fundamental requirements for lubrication or mechanical adjustment which might limit long periods of unattended operation.

The basic phenomena that form the basis of operation of a thermoelectric generator have been known for many years. The Seebeck effect discovered in 1822 consists essentially of the fact that, if a closed circuit be made of two conductors of different materials and if one junction is maintained at a higher temperature than the other junction, then current will flow in the closed circuit. Practical advantage is taken of these basic phenomena by the use of the output voltage of thermocouples for temperature measurements. Although thermocouples of the type used for temperature measurement produce electrical energy, their efficiency is invariably quite low (a few tenths of a per cent). Significant efficiencies require the use of semiconducting alloys. The general principles of device operation are, however, the same in both cases.

The recent development of silicon-germanium (SiGe) semiconductor alloys by RCA represents a major development in the thermoelectric art. By use of this material, RCA has been able to construct and exhibit reliable, efficient, long-life, high-temperature thermoelectric power devices. In this section, consideration is given to a review of the physical factors involved in the selection of thermoelectric materials, the performance equations of a thermoelectric generator, and, finally, those factors which make the RCA-developed SiGe alloys especially favorable for use in practical power-producing devices.

* B. Abeles, D. S. Beers, G. D. Cody, J. P. Dismukes, "Thermal Conductivity of Ge-Si Alloys at High Temperature", Physical Review, Vol. 125, Jan. 1, 1962, p. 44.

REVIEW OF THERMOELECTRIC PHYSICS

Recent developments in solid-state theory have been successful in providing a semi-quantitative explanation of those thermoelectric effects in solids which permit the direct conversion of heat into electricity. The primary thermoelectric effect discovered by Seebeck is that a voltage is developed across a metal or semiconductor which is exposed to a temperature gradient. Essentially, the physical mechanism responsible for this effect (in n-type material) is that electrons at the "hot" end of a conductor have greater thermal energy than electrons at the "cold" end; the electron diffusion which tends to result produces charge movement. As a consequence of this charge movement, a potential gradient is established (negative at the cold end of n-type material) which eventually offsets the charge flow resulting from the thermal gradient. In p-type material, holes also tend to diffuse and produce a voltage of opposite sign.

An explicit approximation for the thermoelectric effect can be obtained, for example, by solving the Boltzmann equation and then substituting the resulting distribution function into the integral representing the current density. Detailed derivations of this and other more detailed solid-state computations may be found in the literature. The resulting expression for a non-degenerate* (i.e., not too highly doped) semiconductor is:

$$S = \pm \frac{k}{q}\left[(r+2) + \ln \frac{2}{n}\left(\frac{2\pi m^* kT}{h^2}\right)^{3/2}\right] \qquad (1)$$

where

- S is the Seebeck (thermoelectric) coefficient (volt/^{o}C)
- q is the electronic charge
- k is the Boltzmann constant
- h is the Planck constant
- n is the concentration of carriers per cubic centimeter
- m* is the effective mass of the charge carriers
- T is the absolute temperature
- r is a number which depends on the type of scattering which the carrier experiences as it moves through the lattice (r = 0 for a perfect covalent lattice, while in the presence of impurities, r = 2).

* It may be noted that thermoelectric semiconductors are normally "highly doped" to partial degeneracy and, in this region, classical computations such as Equation (1) should be regarded as approximations.

Some of the main factors which influence the selection of a thermoelectric material may be noted from examination of Equation (1). It is clear that the Seebeck thermoelectric voltage will depend on temperature and can be improved by substituting impurities into the lattice or, to a lesser extent, by choosing substances with large effective mass. It is important to note, however, that an increase in the number of carriers, n, results in a decrease of the Seebeck thermoelectric coefficient. It is basically for this cause that metals ($n \sim 10^{22}$) have a much lower Seebeck coefficient than optimum semiconductor thermoelectric materials ($n \sim 10^{19}$), and that the best thermoelectric materials are semiconductors. The number of carriers in a semiconductor material are, of course, adjusted experimentally to optimum levels by suitable doping techniques. n-type material is obtained by introduction of controlled amounts of doping agents which have a higher valence than the basic thermoelectric alloy. Conversely, p-type material is obtained by introducing controlled amounts of doping agents which have a lower valence than the basic thermoelectric alloy.

As shown in the following sections, high Seebeck coefficient, S, is not the only material property necessary for high thermoelectric performance. Analysis of generator efficiency equations shows that the necessary favorable combination of material properties can be expressed in terms of a figure-of-merit:

$$Z = \left[\frac{S^2}{\rho}\right]\left[\frac{1}{K}\right] \tag{2}$$

where

Z is the figure-of-merit
S is the Seebeck coefficient (volt/^{o}C)
ρ is the electrical resistivity (ohm-centimeter)
K is the thermal conductivity (watt/cm-^{o}C).

The electrical resistivity term in the figure-of-merit equation of a semiconductor depends on the carrier mobility and carrier concentration:

$$\frac{1}{\rho} = qn\mu \tag{3}$$

where

q is the electric charge
n is the concentration of carriers
μ is the mobility.

It will be noted from Equation (2) and Equation (3) that the most favorable values of electrical resistivity are obtained at high carrier concentrations as contrasted with the highest Seebeck coefficient values which are obtained at low carrier concentrations. Figure 1, after Joffe,* indicates the nature of these conflicting requirements. Theory predicts that optimum values of the S^2/ρ term in the figure-of-merit equation should occur at "intermediate" carrier concentrations of approximately 10^{19} per cubic centimeter in excellent agreement with experiment. These carrier concentration levels correspond to rather high doping levels and, therefore, efficient thermoelectric materials may be characterized as "degenerate" semiconductors.

Thermal conductivity is the final term appearing in Equation (2) for the figure-of-merit. To achieve highest values for figure-of-merit, the thermal conductivity term should be made as low as possible. Although several forms of thermal transport may contribute to heat flow, the observable thermal conductivity coefficient may be approximated as:

$$K = K_{lat} + K_{el} \tag{4}$$

where

K is the observed thermal conductivity
K_{lat} is the lattice component of thermal conductivity
K_{el} is the electronic component of thermal conductivity.

Equation (4) indicates that thermal transport includes contributions due to thermal vibrations of the lattice (i.e., phonons) as well as those due to the diffusion of charge carriers from the hot to cold ends of the thermoelectric material. In metals with high values of carrier concentration, n, the electronic component of conductivity invariably predominates and, as a result, the relationship between thermal conductivity and electrical conductivity is

* A. F. Joffe, Semiconductor Thermoelements and Thermoelectric Cooling, Infosearch Limited, London, 1957.

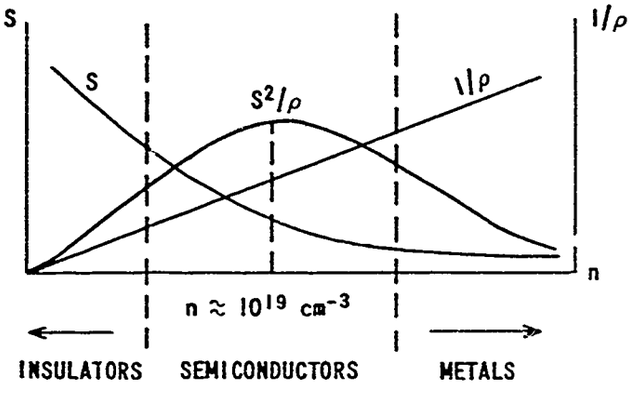

Figure 1. Theoretical Dependencies of Seebeck Coefficient, S, Electrical Resistivity, ρ, and S^2/ρ as a Function of Carrier Concentration, n.

normally well defined (Wiedemann-Franz ratio). In thermoelectric semiconductors with "intermediate" carrier concentrations, the lattice term is invariably the major contribution. Efficient thermoelectric materials must, therefore, be chosen from those semiconductors with a low value of lattice thermal conductivity. One of the most effective methods for achieving this result is to utilize solid solutions containing atoms of different mass (for example, silicon-germanium alloys). Under favorable circumstances, the alloys will have thermal conductivity values several-fold lower than that of either of the "pure" components. A second related effect is the introduction of impurity centers into the semiconductor lattice which are more effective in scattering phonons than electrons. Differences in the scattering behavior may be expected from the fact that most phonons have a wave length of the order of an atomic distance while that of a conductance electron is about ten times this value.

THERMOELECTRIC GENERATORS PERFORMANCE EQUATIONS

The basic theory of thermoelectric generators has been known for more than fifty years. In 1911, Altenkirch* derived the basic equations for thermoelectric power conversion and showed that materials were required with high Seebeck coefficients, high electrical conductivities to minimize Joule heating, and low thermal conductivities to reduce heat transfer losses. It is only since the advent of semiconductor thermocouples, however, that materials with the necessary favorable combination of thermoelectric properties have become available so that devices with significant efficiencies can be constructed.

While the efficiency of a thermoelectric generator depends, in theory, on only a few thermoelectric properties, in practice it is necessary that the thermoelectric material possess additional mechanical properties so that devices with good reliability can be constructed. The thermoelectric material should have reasonable strength, should be chemically stable at high temperatures, and should have low coefficient of thermal expansion to minimize thermal stresses across a thermoelement when one end is heated and the other end is cooled; in addition, means should be available for joining the thermoelectric material to other members of a thermoelectric structure so that efficient thermal and electric flux paths can be maintained. Silicon-germanium (SiGe) alloys represent a major contribution to the thermoelectric art in that they combine "good" thermoelectric properties with an extremely

* E. Altenkirch, Phys. Zeits., Vol. 12, 1911, p. 920.

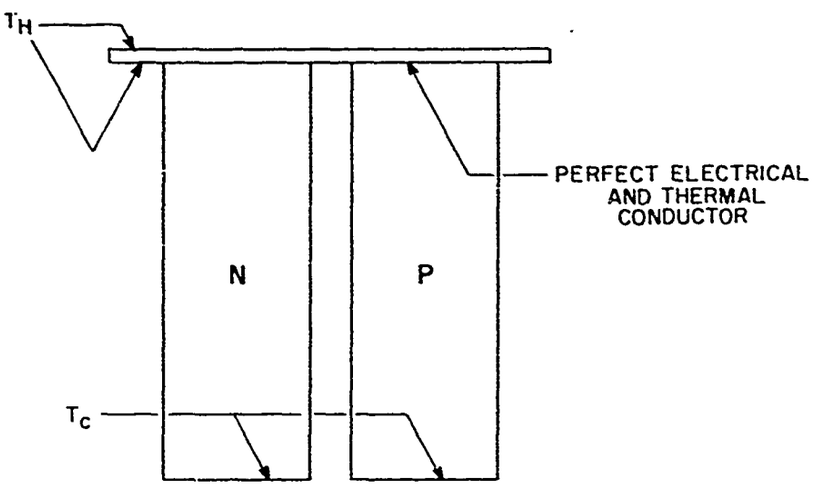

Figure 2. "Ideal" Thermocouple Construction.

favorable combination of mechanical properties, permitting construction of reliable devices with significant efficiency.

Customary efficiency computations utilize formulae derived under the assumption of temperature-independent parameters. Individual average material values over the temperature range of interest are then inserted into these relations. The results of more detailed averaging using more exact and complex formulae do not differ appreciably from the simpler approach which is, therefore, adopted in this section.

Figure 2 shows a schematic view of an "ideal" thermocouple with n-type and p-type arms joined by appropriate electrical conductors at the hot and cold junctions. If it is assumed that this thermocouple is without sources of loss (such as resistance contributions from the electrical conductors at the hot and cold junctions), the performance will depend only upon the properties of the thermoelectric materials. The total resistance of the ideal thermocouple will be given by:

$$R = \rho_n \frac{L_n}{A_n} + \rho_p \frac{L_p}{A_p} \qquad (5)$$

in which the subscripts "n" and "p" refer to the n and p arms respectively, and where

R is the resistance (ohm)
L is the length of the thermoelement arms (cm)
A is the cross-sectional area of the arms (cm^2)
ρ is the average resistivity of the thermoelement (ohm-cm).

The total thermal conductance of the two arms in parallel is

$$K = \frac{A_n K_n}{L_n} + \frac{A_p K_p}{L_p} \qquad (6)$$

where

K is the thermal conductance (watt/^oC)
K is the thermal conductivity of the thermoelements (watt/cm-^oC).

If the n and p arms of the thermocouple do not have identical thermoelectric properties, optimum performance results by selecting dimensions such that the following ratio is satisfied:

$$\frac{A_n}{A_p} = \left[\frac{L_n}{L_p}\right]\left[\frac{K_p \cdot \rho_n}{K_n \cdot \rho_p}\right]^{1/2} \tag{7}$$

The effective figure-of-merit for the n-p combination is then:

$$Z = \frac{(S_n + S_p)^2}{\left[(K_p \rho_p)^{1/2} + (K_n \rho_n)^{1/2}\right]^2} \tag{8}$$

where

Z is the effective figure-of-merit ($^{o}C^{-1}$).

It may be noted that because the properties of n- and p-type SiGe differ slightly, Equation (8) indicates that the areas of the n and p arms also should differ slightly for optimum performance. Detailed analysis indicates, however, that the present match is sufficiently close so that the resulting performance gains are negligible. For reasons of constructional simplicity, the dimensions of the n and p arms have been made the same for all thermocouple investigated in this study.

The heat balance in the thermoelements under load is the result of three terms:

1. Heat conducted through the thermoelement,
2. Peltier cooling at the hot junction,
3. Joule heating due to current flow through the thermocouple (half of the Joule heating finds its way back to the source).

The net rate of heat input is given as the sum of these three effects.

$$Q = K (T_H - T_C) + (S_n + S_p) T_H I - 1/2 I^2 R \tag{9}$$

where

Q is the rate of heat abstraction by the thermocouple (watt)
T_H is the hot junction temperature (^oK)
T_C is the cold junction temperature (^oK)
S is the Seebeck coefficient of the thermoelement (volt/^oK)
I is the current through the thermoelements (amp.).

For maximum power output from a given couple, the load resistance should be made equal to the generator resistance. The useful electrical energy transfer is then:

$$P_L = \frac{\left[(S_n + S_p)\ (T_H - T_C)\right]^2}{4R} = \frac{E_{oc}^2}{4R} \qquad (10)$$

where

P_L is the electrical energy output under a matched load (watt)
E_{oc} is the open circuit voltage of a thermocouple when hot junction temperatures are T_H and T_C.

The efficiency under matched load (i.e., at maximum power output) is given by:

$$\epsilon_L = \frac{P_L}{Q} = \frac{T_H - T_C}{2T_{avg} + \frac{T_H - T_C}{2} + 4/Z} \qquad (11)$$

in which

$$T_{avg} = \frac{T_H + T_C}{2} \qquad (12)$$

and where ϵ_L is the efficiency under matched load.

Although Equation (11) gives the expression for maximum thermocouple power output, it does not represent the normal operating point of maximum efficiency.

When maximum efficiency is desired, the load resistance should be adjusted to:

$$R_L = R\,M \tag{13}$$

in which

$$M = (1 + Z\,T_{avg})^{1/2} \tag{14}$$

The maximum thermoelectric conversion efficiency is then given by:

$$\epsilon_{max} = \left[\frac{T_H - T_C}{T_H}\right] \cdot \left[\frac{M - 1}{M + \frac{T_C}{T_H}}\right] \tag{15}$$

where ϵ_{max} is the maximum efficiency.

The first term of the above equation will be recognized as the familiar expression for Carnot efficiency, representing the maximum performance of an ideal thermodynamic heat engine operating between two temperature conditions. The second term in Equation (15) depends only on the effective figure-of-merit, Z, of the thermoelectric materials; and the temperatures of operation may be considered to indicate the relative performance of a thermoelectric device with respect to an ideal thermodynamic heat engine. For best device efficiency, both of the bracketed expressions in Equation (15) should be high.

For SiGe devices, the load conditions for matched load and optimum efficiency do not differ significantly. Consequently, most of the life test data in this report concerning the stability of SiGe thermocouple devices refer to matched load operation. This procedure not only facilitates the setup of life tests, but simplifies reporting of data. The basic voltage output and total resistance measurements of the test thermocouples can be used directly in Equation (10) to indicate power output levels without extensive numerical computations.

TECHNICAL DISCUSSION OF SiGe THERMOELECTRIC ALLOYS

The recent development of SiGe thermoelectric alloys by the RCA David Sarnoff Research Center and the establishment of manufacturing facilities for quantity production of this material at the RCA Thermoelectric Activity, Harrison, New Jersey, represent a major breakthrough in the thermoelectric art. With this

material, RCA has been able to build and exhibit practical devices which, to RCA's knowledge, have the highest long-term conversion efficiency yet obtained from thermoelectric devices. Such SiGe devices are not only electrically stable, mechanically rugged, and dimensionally compact, but also are suitable for unprotected operation in high-temperature vacuum and air environments. These unique properties have led to the extensive use of SiGe thermoelectric alloys for power generation in "space". In applications where reliability, unattended operation, low-weight, high-device efficiency and ability to operate in adverse high-temperature environments are important, SiGe thermoelectric devices are unmatched by any other competitive thermoelectric material available today.

The remarkable performance characteristics of SiGe devices result from an exceptional combination of desirable physical properties found in SiGe alloys. Among the unique features of the RCA SiGe thermoelectric alloys are:

1. High melting point (liquidus temperature in excess of 1300°C for the present alloys)

   The present SiGe alloys are inherently high-temperature materials which have the ability to operate at temperatures 500°C higher than previously available telluride thermoelectric materials. This high-temperature capability permits operation at high Carnot efficiency and enables significant device performance levels to be attained.

2. SiGe operates unprotected in air at high temperatures

   One of the major objectives of the TRECOM program was to determine the capabilities of SiGe alloys for unprotected operation in air. One thousand-hour life tests at 950°C and five hundred-hour life tests at 1025°C indicated that the SiGe alloys are essentially unaffected by operation in air at these temperatures. The upper limit for unprotected air operation of SiGe is not yet finalized but is probably in excess of 1100°C.

   The exceptional oxidation resistance of SiGe alloys is not unexpected from a metallurgical point of view. A frequently employed method for protecting non-noble metals from adverse high-temperature air environments is based on producing a silicon-rich alloy on all exposed surfaces. The silicon-rich areas on the surface then develop in air a protective, inert "film" of silica, SiO_2, which prevents oxidation of the substrate. By analogy, SiGe alloys themselves should be highly oxidation-resistant in air since they are silicon alloys throughout.

3. Excellent strength properties

Direct tensile strength measurements indicate that the basic stress capabilities of SiGe alloys are in excess of 7000 psi. This represents nearly ten times the tensile stress capabilities of telluride thermoelectric materials. These excellent mechanical strength properties permit, for the first time, the construction of truly reliable thermoelectric devices which can withstand the stresses caused by temperature gradients and temperature-cycled conditions of operation.

4. Light weight

The density (3.3 grams per cubic centimeter) of SiGe alloys is approximately one-third that of previously available lead tellurides.

5. SiGe alloys can be machined

SiGe alloys can be formed to any desired shape on standard metallurgical equipment. This permits SiGe components of a device to be made with any precise dimensional tolerances necessary for assembling arrays of thermocouples into a complete power-producing unit.

6. Extremely low coefficient of thermal expansion

The stresses arising from a given temperature gradient are proportional to the coefficient of thermal expansion. Because the thermal expansion coefficient of SiGe alloys is several-fold less than that of lead telluride materials, thermal stress problems are correspondingly reduced. As a consequence, SiGe devices have been successfully operated under temperature gradients exceeding $1000^{o}C$ per centimeter without degradation.

7. Ease of bonding

RCA has developed high-temperature bonding techniques which yield uniform, stable bonds between metal shoes and SiGe alloys with low contact resistance and excellent thermal contact which remain stable on life during high-temperature operation.

8. High figure-of-merit

Figures of merit of SiGe alloys in the temperature range of major device interest range from $0.60 \times 10^{-3}\ {}^{o}C^{-1}$ to $0.70 \times 10^{-3}\ {}^{o}C^{-1}$. Since maximum

Z values occur in the temperature range 400°C to 1000°C, this permits construction of thermoelectric devices with high material efficiency and high Carnot efficiency.

9. Exceptional shock-and-vibration resistance

SiGe thermoelectric devices can be constructed to meet severe shock and vibration specifications. For example thermocouples developed for the TRECOM application have been successfully tested without failure to vibration levels of 60 g in three mutually perpendicular directions over the frequency spectrum of 20 to 3000 cycles per second; 100-g shock tests have also been successfully passed. In addition, the basic TRECOM thermocouple configuration has been repeatedly temperature-cycled between room temperature and 1000°C with no evidences of degradation.

Because of the exceptional mechanical properties of SiGe materials, it becomes possible to construct devices in which essentially the full-power conversion capabilities of SiGe are attained. Among the unique features of the TRECOM module are use of continuous metallurgical joints throughout to ensure efficient thermal and electrical flux paths, and a design in which the basic SiGe thermocouple can be attached to any heat sink without need for flexible connectors. This results in a compact, rigid, efficient structure ensuring high-power output per unit weight or per unit volume.

As indicated in discussions of generator performance equations, it is necessary, in characterizing thermoelectric materials, to specify the Seebeck coefficient, the electrical resistivity and thermal conductivity, all of which combine to give the so-called "figure-of-merit". These properties determine the theoretical usefulness of the thermoelectric material. In combination with the above mechanical properties, they give the practical applicability of the alloy to any given thermoelectric conversion requirement.

Typical temperature-dependent characteristics of the RCA SiGe thermoelectric alloy 2213A, employed in TRECOM modules, are illustrated in Figure 3. The Seebeck coefficients of the n and p materials (referenced to platinum) are shown in Figure 3a. Corresponding values for electrical resistivity are shown in Figure 3b, and thermal conductivity values are shown in Figure 3c. The basic data are combined to give material figures-of-merit, Z, on a thermocouple basis in Figure 3d.

Depending on the level of doping, the individual resistivity and Seebeck coefficient curves are subject to slight variations for any given thermoelement. It

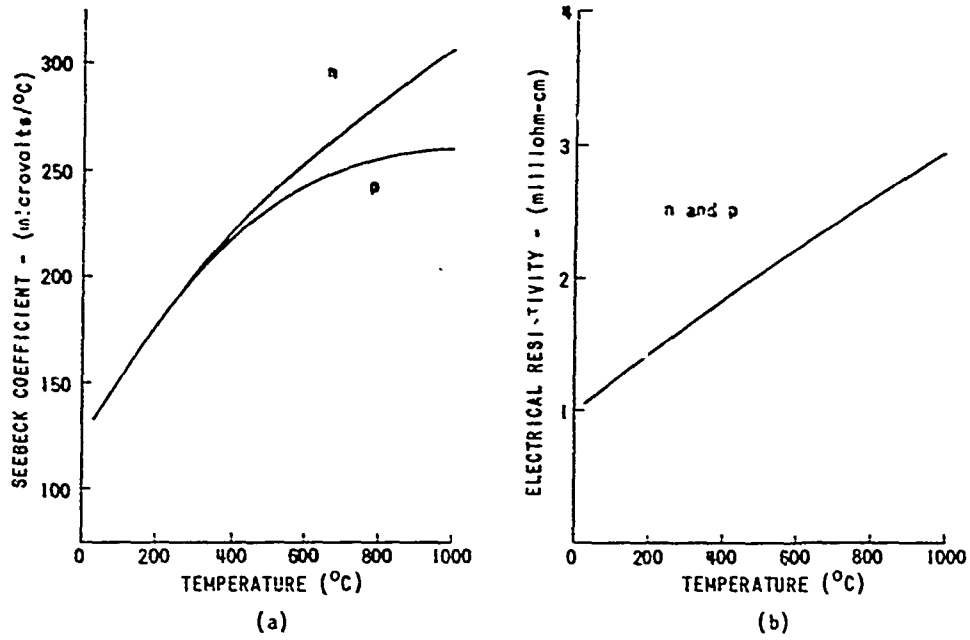

Figure 3. Typical Performance Characteristics of RCA Silicon-Germanium Alloy 2213A.

has been determined, however, that the figure-of-merit is relatively insensitive to such variations. Changes in one parameter (Seebeck coefficient) are effectively compensated for by corresponding changes in the other parameter (resistivity). The thermal conductivity is, at most, little affected by slight doping variations. Such relative constancy of figure-of-merit is a major factor in assuring stable power output, since the power output can be shown theoretically to depend almost entirely on the figure-of-merit under the usual matched load conditions.

RCA is continuing to concentrate effort toward optimization of thermoelectric alloy production techniques and, in particular, to detailed studies of doping additives. Significant improvements in the figure-of-merit are considered feasible.

SECTION II

INITIAL STUDIES

INTRODUCTION

Although RCA-sponsored studies preceding this contract had delineated the main lines of approach which were ultimately employed in developing TRECOM modules, many areas needed to be explored before optimum device features could be established. In particular, the performance of the silicon-germanium alloys, and bonds thereto, after long-term exposure to high-temperature air environments higher than 650°C was largely unknown; other areas of water-cooled module construction also remained correspondingly unexplored.

The technical objectives of the initial evaluation effort were four-fold:

1. To modify existing RCA life test facilities so that water-cooled TRECOM modules could be adequately life-tested and evaluated.

2. To survey the maximum temperature limits of the SiGe thermoelectric alloy materials.

3. To evaluate RCA-developed methods of module and thermocouple construction and determine those features most suitable to the TRECOM module.

4. To assess needs for oxidation protection for various members of the thermocouple exposed to high-temperature air environments.

The selection of present TRECOM thermocouple and module construction resulted from the evaluations conducted during this initial survey effort. The major task was to evaluate which of two basic RCA-developed approaches to SiGe thermocouple construction would be most suitable for TRECOM requirements that devices operate in adverse high-temperature air environments. Parallel engineering tests were run to evaluate the performance capabilities of each construction. The data generated by such evaluations are described in this section and in Section III. The major features of the two construction methods were found to be:

1. Tungsten hot-junction thermocouple construction

This construction, although most efficient at any temperature (approximately 95 per cent of theoretical material efficiency), resulted in high weight-to-power ratios and appeared less favorable with respect to maximum shock and vibration resistance due to the increase in moment of inertia associated with the dense metal parts cantilevered from the hot junction. Severe oxidation protection requirements for the tungsten hot-junction parts, at present, restrict maximum long-term operation in air to temperatures of the order of 700°C-750°C.

2. All-SiGe thermocouple construction

The all-SiGe construction operates at approximately 90 per cent of theoretical material efficiency; oxidation restrictions, however, no longer limit the maximum hot-junction temperature; 500-hour stable operation at 1025°C has been demonstrated. The higher temperature capability results in substantial net gains in power density and efficiency. Shock and vibration characteristics are excellent.

These initial survey studies, which are considered in detail in Section II, led to the selection of a TRECOM module which utilizes the all-SiGe thermocouple configuration. Detailed life performance data for this construction are described in Section III.

LIFE TEST FACILITIES

Special life test facilities were required to test the modules and SiGe material for this TRECOM study. While the basic facilities, including furnaces, recorders, temperature controllers, vacuum systems, and bell jar vacuum life test stations, were available, it was necessary to extensively modify existing RCA facilities to test water-cooled modules under the high hot-junction temperature considered in this study. Although such modifications now appear straightforward, it proved to be considerably more difficult than originally anticipated, and required considerable engineering ingenuity, to accomplish the desired result. In particular, difficulty was experienced in obtaining a flexible system with electrical heaters of suitable longevity at the highest test temperature. A second source of difficulty was associated with the need to obtain accurate performance data during actual operation. Early tests showed the necessity of protecting the numerous electrical leads used for voltage, resistance, and temperature measurements from the adverse high-temperature environments in the life-test chambers; it

became necessary in some instances to incorporate baffles and water-cooled load leads into the chamber.

Four separate life facilities were set aside for evaluation of TRECOM modules. These included complete parallel facilities for testing components in air and vacuum. The overall function of such testing facilities is indicated in Table 1. Photographs of the equipment are given in Figure 4 through Figure 6.

TABLE 1
SUMMARY OF LIFE TEST FACILITIES USED IN TRECOM PROGRAM

	Air	Vacuum
High-temperature storage facilities	5 air furnaces (Figure 4a)	4 vacuum furnaces (Figure 5)
Water-cooled SiGe thermocouple test stations	4 air test stations for modules (Figure 4b)	2 bell jar test station furnaces (Figure 6)

Although the major objective of the present study was to establish the performance characteristics of SiGe thermocouples in air, life tests in vacuum also played an important role in these studies. It was felt that operation data in oxygen-free environments would clearly delineate possible device limitations associated with high temperatures; for example, sublimation and long-term chemical changes, which might prove ultimate sources of device limitation. This would permit such effects to be distinguished from oxidation which might restrict temporarily maximum operating temperatures in air but which might be remedied by appropriate protective coating techniques.

The initial life test studies in this program were designed to test the stability of the SiGe material and bonds thereto during exposure to adverse high-temperature environments. Storage tests of SiGe material and associated thermocouple parts in the high-temperature air and vacuum furnaces permitted rapid screening of various construction techniques, permitting the more elaborate and time-consuming water-cooled thermocouple life-test stations to be reserved for devices which would have optimum prospects of stability.

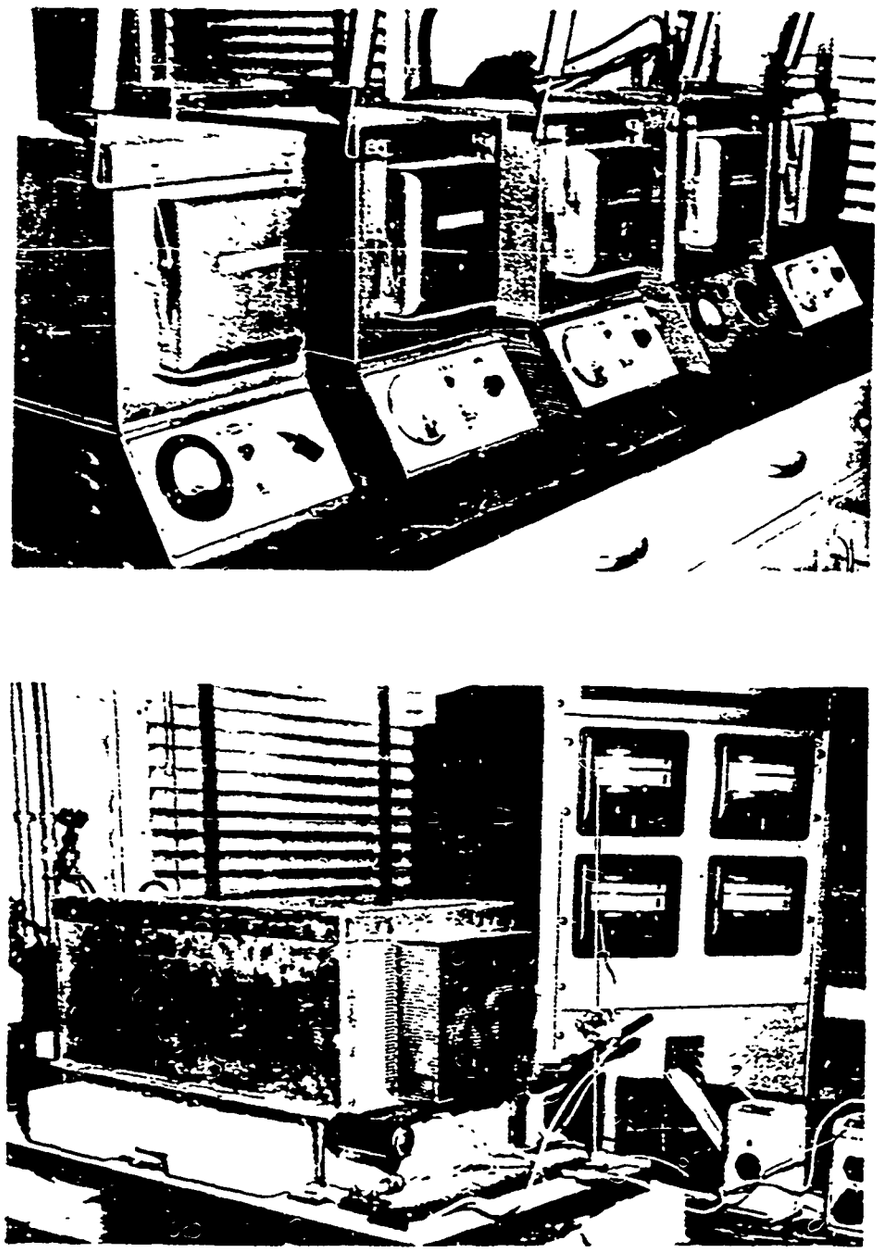

Figure 4. High-Temperature Facilities Used for TRECOM Life Tests in Air on Thermoelectric Modules and Materials.

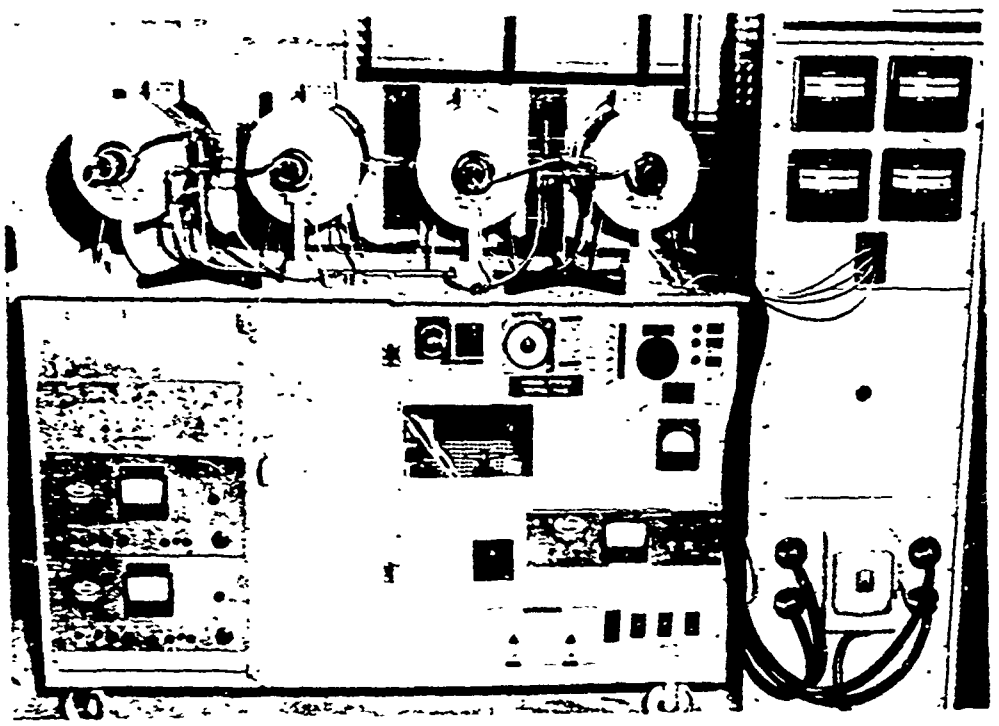

Figure 5. Four Vacuum Facilities for Material Storage at Elevated Temperatures.

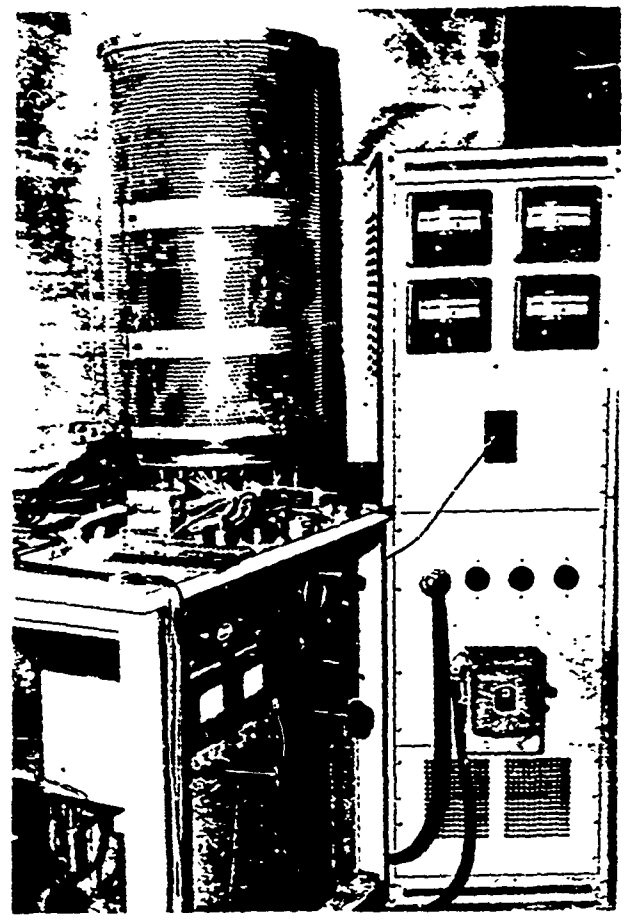

Figure 6. Typical Vacuum Bell Jar Life Test Facility Used for Life Tests on TRECOM Thermoelectric Modules at Elevated Temperatures.

ELECTRICAL STABILITY OF SiGe MATERIAL IN AIR AND VACUUM

A major objective of this initial phase of module development was to assess the stability of n-type and p-type SiGe alloy materials at different temperatures in air and vacuum. This type of data was considered of special importance, for any serious temperature limitations in the basic SiGe material itself would automatically fix the maximum operating temperature capabilities of SiGe devices. It was originally estimated at the start of this program that studies in the temperature range of 600°C to 850°C would prove adequate to verify material stability, and the test facilities were designed accordingly. The results of tests over this temperature range are described in this section. It may be noted, however, that since these data showed no evidence of material degradation at temperatures up to 850°C, the ultimate temperature limitations of SiGe alloys were clearly not approached during this test series. The life test data described in Section III for both 500- and 1000-hour operation of SiGe thermocouples in air at temperatures of 850°C, 950°C, 1000°C, and 1025°C also indicate essential stability of the SiGe material to temperatures in excess of 1050°C. The ultimate temperature limitations of SiGe devices are, therefore, still unknown but are undoubtedly in excess of 1100°C.

Experimental studies of the stability of the electrical properties of SiGe alloys were conducted by storing the material in the high-temperature air and vacuum furnaces (approximately 5×10^{-6} mm Hg pressure) shown in Figures 4a and 5 at temperatures between 600°C and 850°C. In all, 72 separate SiGe cylinders were exposed to various temperatures for 1000 hours. The SiGe specimens were machined cylinders of one square centimeter cross-sectional area (0.444-inch diameter) and 0.500 inch in length, to facilitate conversion of the measured element resistance to material resistivity values. The elements were periodically removed from the furnaces and measured for electrical characteristics at room temperature.

According to Equation 16, the figure-of-merit, Z, of a thermoelectric material is given by the expression:

$$Z = \left[\frac{S^2}{\rho}\right]\left[\frac{1}{K}\right] \qquad (16)$$

The thermoelectric property most adequately describing the electrical performance of a thermoelectric material thus is the ratio of the square of the Seebeck coefficient to the resistivity, S^2/ρ. Measurements of Seebeck coefficient, S,

and electrical resistivity, ρ, were, therefore, taken on conventional type test sets to generate curves of S and S^2/ρ as a function of high-temperature life.

Figures 7 through 10 summariz the results of room temperature electrical measurements taken on both n- and p-type SiGe material during exposure to high-temperature life. Each of the curves represents the average of measurements on three SiGe test cylinders for the air tests and six SiGe cylinders for the vacuum tests. Three of the six SiGe cylinders tested at each temperature condition in vacuum had tungsten metal contacts permanently bonded at each end to determine whether good electrical contact to the thermoelements was essential for accurate electrical property measurements. No essential difference was observed to result, thus indicating that the basic measurement techniques were satisfactory.

The results of the data obtained in these tests suggest the following generalizations:

1. SiGe thermoelectric alloy material shows no appreciable signs of degradation, either visually or electrically, as a result of exposure to either air or vacuum environments at temperatures up to 850°C.

2. Slight readjustment of material properties was noted, probably due to an effective high-temperature "annealing treatment" undergone by the SiGe material during these tests. The data suggest that the material efficiency perhaps improved slightly from the annealing treatment.

MODULE EVALUATION STUDIES

Module evaluation, encompassing studies of methods by which groups of thermocouples could be electrically interconnected and affixed to water-cooled heat sinks, received a substantial segment of the engineering effort in this investigation. Because severe thermal stresses can be generated when one side of a module is heated and the other side is cooled, the design must be carefully considered to ensure structural integrity under temperature-cycled conditions of operation.

The favorable mechanical properties of SiGe alloys permit this material to be used as a self-supporting, structural member of a device. Since the material is oxidation-resistant, no provision need be made for encapsulation or for protection of the thermoelectric material from direct exposure to the products of

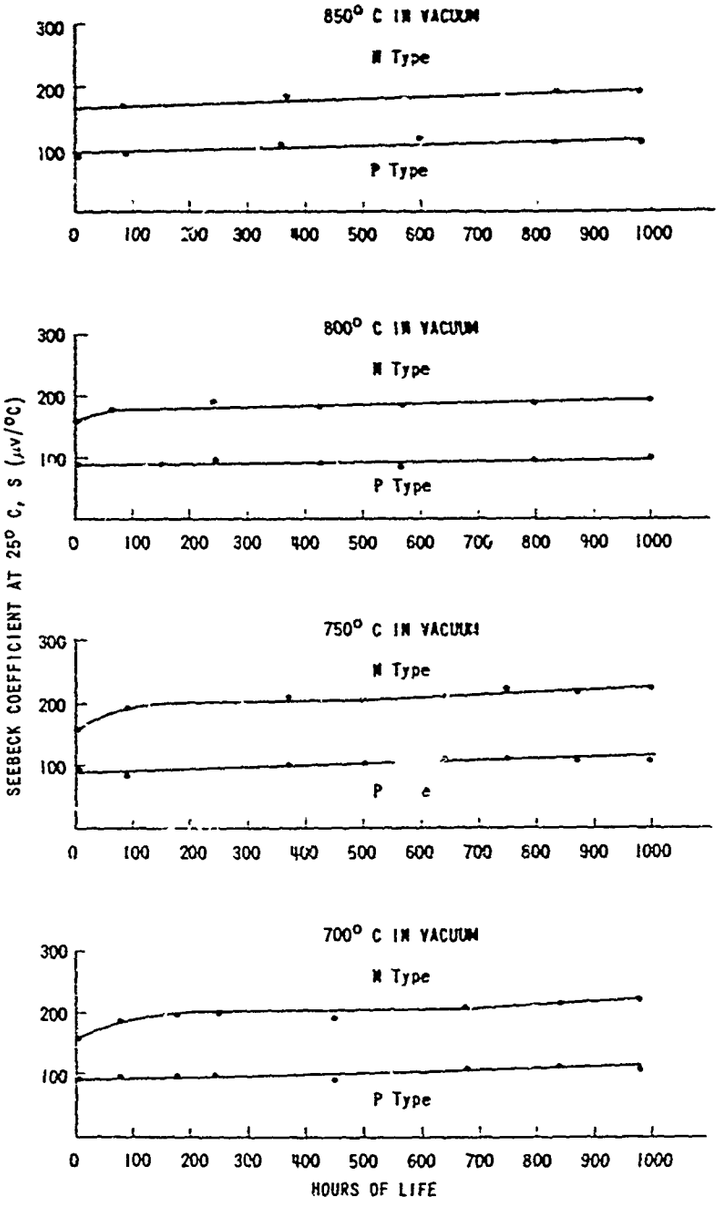

Figure 7. Seebeck Coefficient of SiGe Alloy During Life Tests in Vacuum.

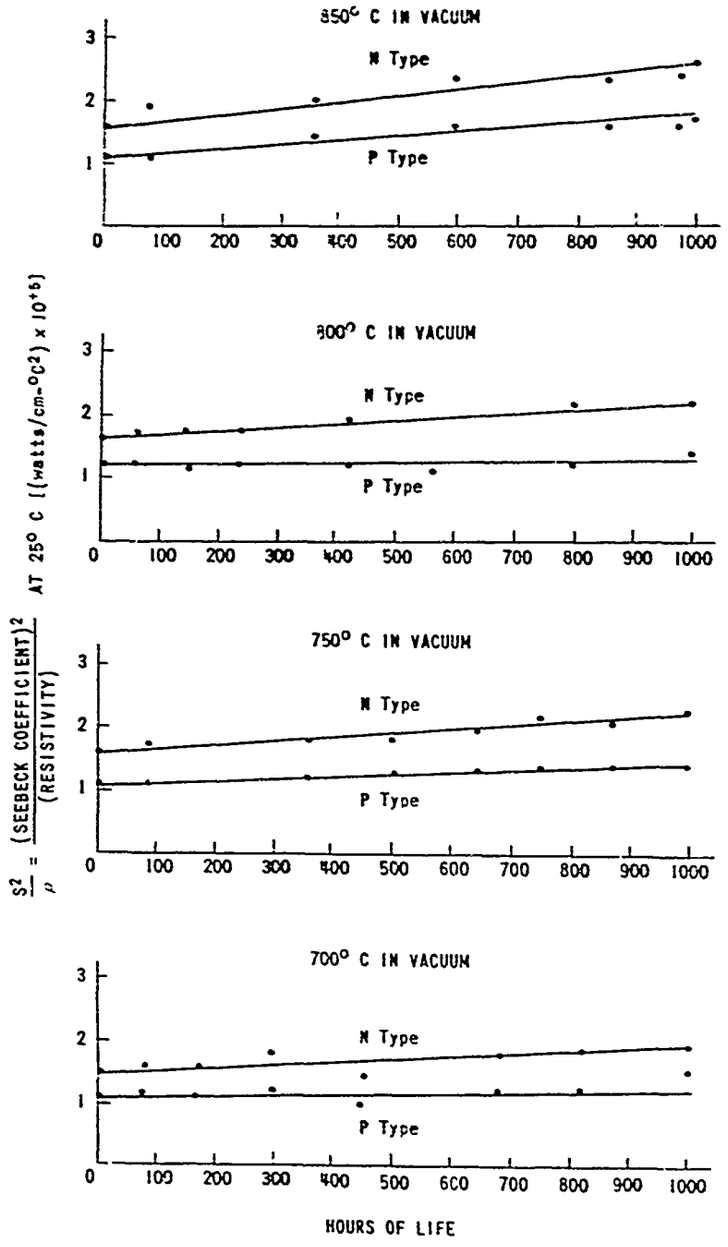

Figure 8. $S^2/$ Coefficient of SiGe Alloy During Life Tests in Vacuum.

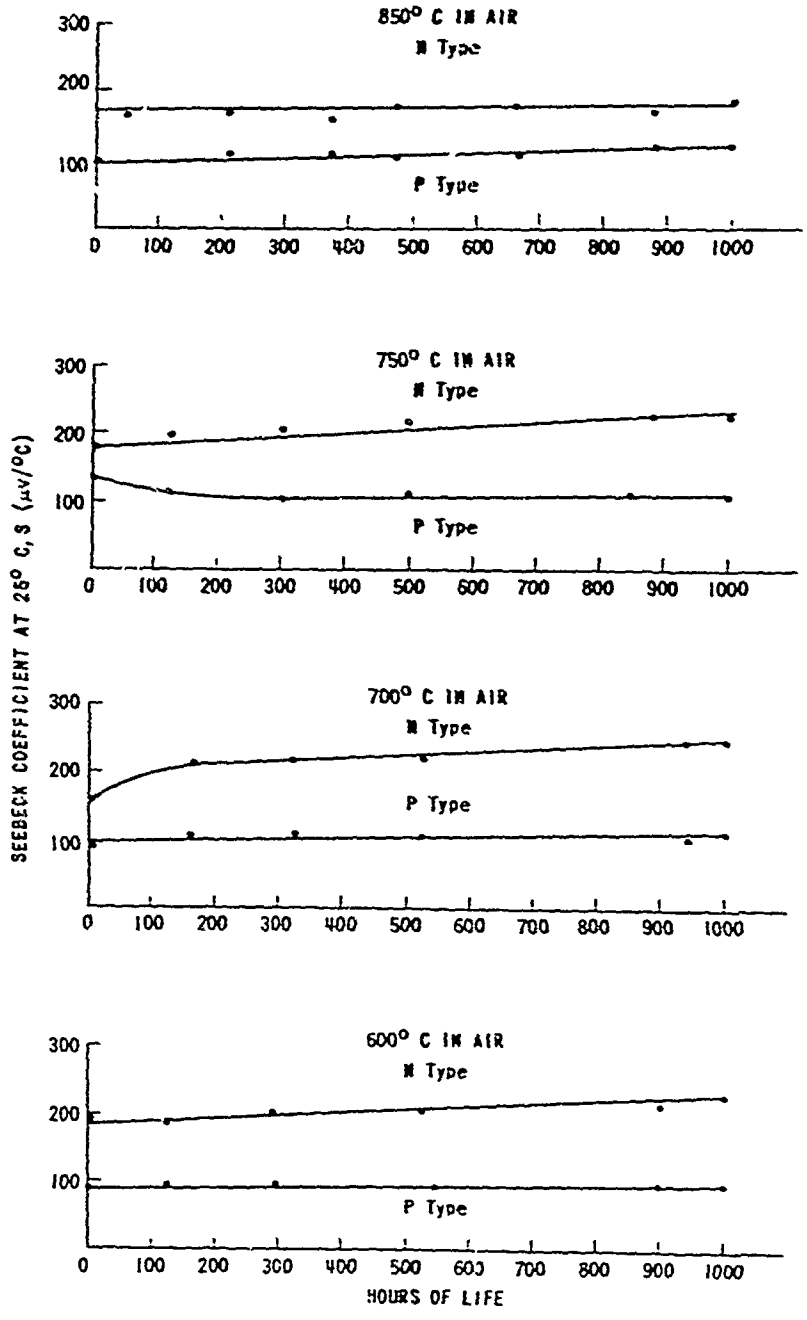

Figure 9. Seebeck Coefficient of SiGe Alloy During Life Tests in Air.

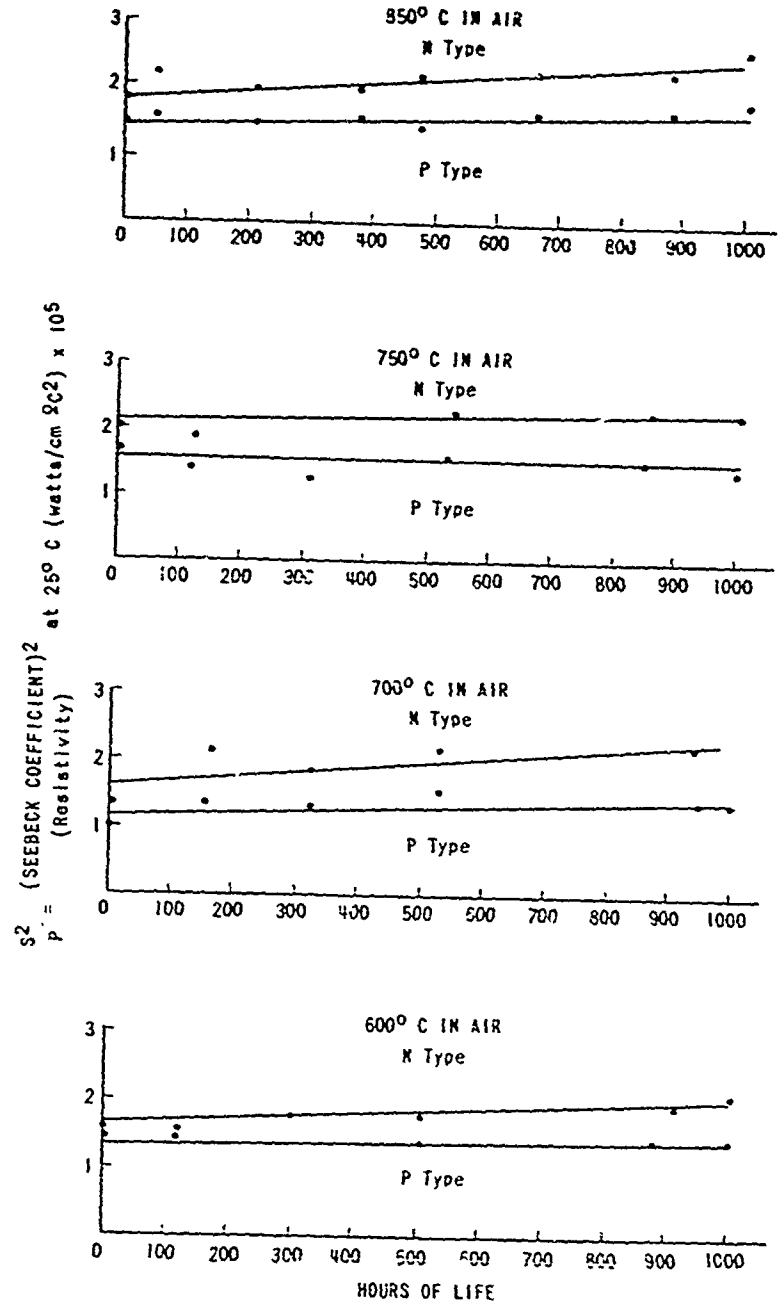

Figure 10. S^2/ρ Coefficient of SiGe Alloy During Life Tests in Air.

combustion liberated by a burner. The basic SiGe thermocouple configurations which were considered for TRECOM application took advantage of these desirable SiGe properties by having the hot junctions directly exposed to the source of thermal energy to take maximum advantage of the available heat. In the resulting rigid thermocouple constructions, the n and p legs were permanently bonded to a hot junction plate which also served as a heat acceptor.

The major objectives of this phase of the TRECOM program were:

1. To evaluate features of thermocouple construction necessary to permit a rigid thermocouple to be attached to a rigid water tube.

2. To evaluate means for electrically interconnecting such thermocouples when bonded to a common water tube.

In the past, thermoelectric power generators using telluride materials have required special provision to avoid thermoelement failures due to differential displacement stresses which result when one end of a thermocouple is heated and the other end of the thermocouple is cooled. Common means taken to avoid such stresses have included flexible connectors, pressure contacts, and nonrigid device structures; it may be noted that overall device performance levels normally suffer if such means are required, since nonproductive thermal paths and subsidiary hardware weight are increased. A major objective of this module development program was to demonstrate a suitable SiGe thermocouple configuration requiring no provision for differential expansion stress relief. This was successfully accomplished because of the low-expansion coefficient and high strength of SiGe alloys; and in the TRECOM design, thermocouples, permanently joined at the hot junction end, are rigidly mounted on a water tube.

If a thermocouple is rigidly bonded at both the hot and cold ends, the geometry must be such that differential displacements due to thermal expansion are small. The total differential displacement between the hot and cold ends of the legs in an operating thermocouple may be estimated from the equation:

$$\Delta\epsilon = \int (\alpha \cdot \Delta T) \, d \qquad (17)$$

where

α is the coefficient of expansion ($^{o}C^{-1}$)
d is the mean separation between n and p legs (inch)
ΔT is the temperature difference between hot and cold junctions (^{o}C)
$\Delta \epsilon$ is the differential displacement between the hot and cold ends of a thermocouple (inch).

Taking the coefficient of expansion of tungsten and/or SiGe to be $4.7 \times 10^{-6}\ ^{o}C^{-1}$, and assuming that a temperature differential of $970^{o}C$ exists across the thermoelements, according to Equation (17), the differential displacement between hot and cold junctions is 0.0045 inch per inch of separation between n and p legs.

Initial module studies were directed toward determining experimental values of mean distance between n and p legs, d in Equation (17), required to guarantee structural integrity of TRECOM thermocouples under temperature cycling. Experimental thermocouples were constructed having separations, d, of 0.6 inch, 0.45 inch, and 0.2 inch. Temperature-cycling tests on these devices showed that d values of 0.6 inch were unsatisfactory; d values of 0.45 inch were marginal; while couples with 0.2-inch separation between n and p legs withstood repeated cycling to hot junction temperatures of $1000^{o}C$ without failure. This dimension is practically achieved by constructing the TRECOM thermoelement arms of n and p half-cylinders each of 0.50-square centimeter cross-sectional area (see Figure 15). This half-cylinder construction feature has therefore been incorporated into all major life tests and in the sample module to assure thermocouple stability under temperature-cycled conditions of operation.

To take full advantage of the rigid half-cylinder thermocouple construction, attention was given to practical means for mounting and interconnecting individual thermocouples on a rigid water tube. Thermocouples mounted on such a water-cooled heat sink must not only be in good thermal contact with the sink, but also must be electrically insulated from the metal tube and suitably interconnected with other thermocouples to obtain the desired power-producing electrical circuit. This result is achieved in TRECOM modules by mounting each thermocouple on an "insulator stack" brazed to the water tube. A pattern of copper "cold strap connectors" between the various insulator stacks provides the means for interconnecting the individual thermocouples in any desired series or series-parallel electrical arrangement.

Previous RCA-sponsored development of insulator stack assembly techniques on other projects proved invaluable in developing a suitable stack for TRECOM modules. It may be noted that the problem of insulator stack design can be

quite complex, when it becomes necessary to join low-expansion coefficient SiGe to a high-expansion coefficient water pipe through an insulator of intermediate expansion coefficient. If materials of different thermal expansion coefficients are bonded together at high temperature, bi-metallic bending moments result upon cooling to room temperature. This will result in warped stack surfaces unless the various elements in the stack are suitably selected to produce overall bending moment compensation.

Figure 11 shows schematically the basic insulator stack configuration selected for TRECOM applications. The stack is a brazed assembly of half-cylinder discs, including a high-alumina ceramic wafer, copper electrical connectors, and a final tungsten end cap suitable for joining to SiGe thermocouples. Further details may be noted in Figure 16, which is a photograph of a sample six-thermocouple module.

The thermal loss between the cooling water and the thermocouple cold junction will consist of a film drop between the cooling water and the inside walls of the cooling tube, as well as thermal conductivity temperature drops across the members of the insulating stack. The thermal conductivity temperature difference terms for each member of the stack may be estimated by the relation:

$$\Delta T_i = \left[\frac{Q}{A}\right] \cdot \left[\frac{L}{K_i}\right] \qquad (18)$$

where

$\frac{Q}{A}$ is the thermal flux through the stack (watt/cm^2)

L is the thickness of the stack member (cm)

K_i is the thermal conductivity of the stack member (watt/cm-$^\circ$C).

Predicted and measured values for the temperature differential across the TRECOM insulator stack assembly are shown in Table 2, at a thermal flux density level, Q/A, of 20 watts/cm^2. The temperature differences computed from Equation 18 are based on the thermal conductivities of the major insulator stack members; possible sources of additional temperature differences associated with brazed joints are difficult to estimate but are probably not negligible.

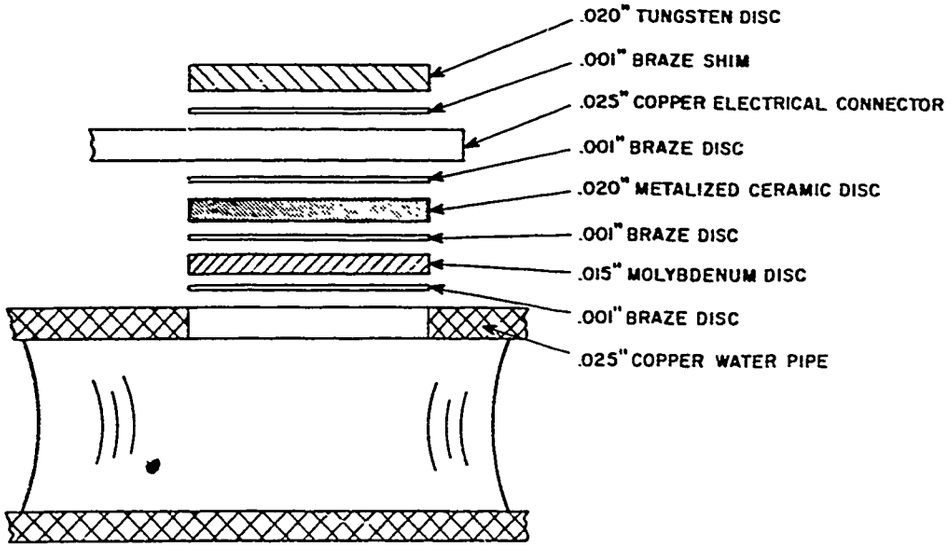

Figure 11. Composition of the Insulator Stack.

Figure 12 shows averaged measurements for the temperature drop across the TRECOM insulator stack as a function of SiGe thermocouple hot-junction temperature.

TABLE 2
COMPARISON OF CALCULATED PERFORMANCE
WITH EXPERIMENT FOR TRECOM INSULATOR STACK

Component	Thickness (inch)	Thermal Conductivity (watt/cm-^{o}C)	Temperature Drop (^{o}C) Calc.	Exper.
Water-to-tube film drop	-	-	8.1	-
Copper pipe	0.025	4.2	0.3	-
Molybdenum	0.015	1.4	0.5	-
Ceramic	0.020	0.2	5.0	-
Copper electric connector	0.025	4.2	0.3	-
Tungsten end cap	0.020	1.3	0.8	-
Tungsten shoe on thermoelement	0.020	1.3	0.8	-
		Total	13.8	22

Under the conditions of this test, the observed temperature drop across the insulator stack at a 1000^{o}C hot-junction temperature was 22^{o}C (corresponding to a thermal flux through the stack of 20.7 watts). The inlet water temperature for all measurements was 5^{o}C, and the flow rate was 0.57 gallon of water per minute through the rectangular copper water pipe (internal cross-section of 0.70 inch x 0.12 inch). The observed temperature drop, 22^{o}C, is somewhat higher than the computed temperature drop, 13.8^{o}C, but of the same order of magnitude. At a hot-junction temperature of 1000^{o}C, approximately 98 per cent of the available temperature difference was usefully maintained across the thermoelements.

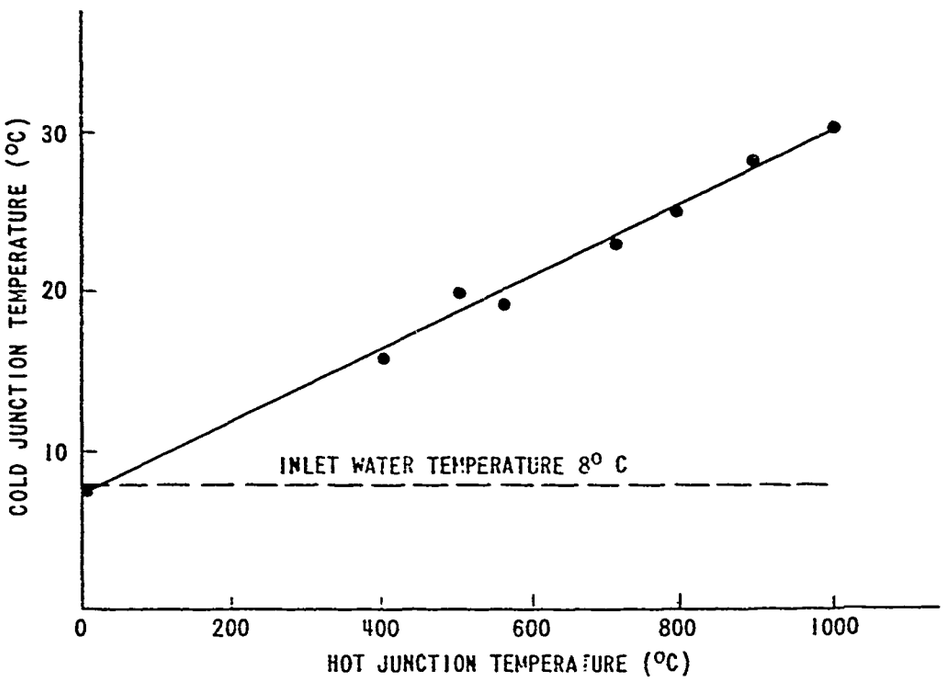

Figure 12. Thermal Drop Across the Insulator Stack.

TUNGSTEN HOT-JUNCTION THERMOCOUPLE CONSTRUCTION

Due to their low coefficients of thermal expansion, the RCA SiGe thermoelectric alloys are most satisfactorily bonded to themselves or to a comparable low-expansion material such as tungsten. Such thermal expansion matching is normally considered good bonding practice in joints which may be subjected to temperature-cycled conditions of operation. These two approaches to bonding were pursued in two parallel approaches toward thermocouple construction, namely, (1) the tungsten hot-junction construction, and (2) the all-SiGe construction.

The results of evaluation tests conducted on thermocouples of the tungsten hot-junction construction are summarized in the following paragraphs. Although these initial tests indicated that this basic structure was quite free from sources of efficiency loss (at least 95 per cent of theoretical material efficiency recovered), it was less favorable in other respects. The increased moment of inertia associated with a heavy tungsten plate (specific gravity = 19.6) cantilevered from SiGe legs adversely affected shock resistance of the thermocouple structure as well as adding substantially to the weight. More seriously, the maximum operating temperatures in air were limited by severe oxidation of the tungsten hot junction parts at temperatures in excess of 750°C. These restrictions ultimately lead to the choice of the all-SiGe construction for TRECOM requirements.

Tungsten is among the most refractory of the known metals, but it oxidizes catastrophically in air at temperatures in excess of 600°C to a yellow powder (WO_3). Although initial tests described previously had indicated that the RCA SiGe alloys were stable in air to temperatures in excess of 600°C, it was clear that tungsten metal parts at the hot junction would require protection to assure long-term thermocouple operation in air, if a tungsten hot-junction thermocouple construction were to be employed.

Because of anticipated tungsten oxidation difficulties, an extensive literature search for protective coatings was made at the start of this contract; this literature survey is summarized in the Appendix. The protective systems reviewed include mechanical cladding, electroplating, high-temperature plasma spraying, ceramic enamels, sealing glasses, hot dipping, vapor deposition, and pack cementation. Unfortunately, the results of this literature search were less promising than might have been anticipated. Although it has been the subject of intensive investigation, the problem of developing suitable protective coatings for tungsten in high-temperature air operation does not appear to have been adequately resolved by present-day technology. Complete elimination of thin spots, pin-hole defects, and adequate coverage of recessed corners present challenging technical problems. Many of the more promising protective systems

reported in the literature are not compatible with tungsten bonded to SiGe. For example, protective coatings with application temperatures in excess of the melting point of SiGe could not be used.

Analysis of the many possible protective coating systems for tungsten suggested that two basic types offered best prospects for the present application, namely, electroplating and ceramic enamelling. A total of 75 different combinations of electroplated protective coatings for tungsten were investigated and subjected to high-temperature storage tests in air furnaces. The most favorable type of electroplated protective coating was found to be an electroplated and sintered composite: tungsten, chromium, rhodium, and nickel. Because this system has a graded thermal expansion coefficient structure which minimizes thermal expansion mismatch stresses, adherence to tungsten is quite good. To obtain optimum protection for the tungsten substrates, it was determined that the chromium and rhodium layers should be electrodeposited under "crack-free" conditions. This required the use of carefully controlled electroplating solutions as well as careful attention to bath temperatures and current densities during application. Although tungsten test specimens coated in this manner with successive layers of chromium, rhodium and nickel satisfactorily withstood long-term storage tests in air at 700°C and 750°C, results were somewhat less favorable on actual thermocouples with tungsten-to-SiGe bonds. The electroplated coatings did not adhere satisfactorily to SiGe. Consequently, difficulty was experienced in preventing oxidation of the tungsten at the tungsten-to-SiGe joint. To remedy this defect, the joint area could be further covered with the enamel coating described in the next paragraph. This combination, based on air storage tests, would provide satisfactory oxidation protection of the tungsten hot-junction parts up to 700°C and perhaps to 750°C.

Ceramic enamels provided a parallel approach to protective coatings for tungsten which were intensively surveyed during the initial phase of this TRECOM study. Although ceramic enamels offer many advantages with respect to ease of coating and a well-developed technology, the upper operating temperature capability of these coatings is limited by the maximum temperature at which the coatings may be fired on. As a general rule, the application temperature should be at least 500°C higher than the proposed temperature of operation in order to ensure that the coating will be refractory under actual use. For SiGe devices in which the tungsten parts are protected with ceramic enamels, this restriction tends to limit maximum operating temperatures to the range 750° to 800°C. Of the ceramic enamels investigated during this phase, the most satisfactory was a slip formulated of powdered Corning No. 3320 glass frit and a tetra-boron silicide filler. The resulting enamel, when fired on in an air-free atmosphere, resulted in a good thermal expansion match to both tungsten

and SiGe and, based on air furnace storage tests, provided substantial device protection at temperatures up to 750°C. Some difficulty occurred due to spots and pin holes in the coating, especially at the edges. The most satisfactory protective coatings resulted when ceramic enamels were applied over the electroplated coatings described in the previous paragraphs. This system produced two lines of defense against air attack and at 700°C appeared to provide long-term protection at the tungsten-to-SiGe joint which was lacking in the electroplated coatings alone.

In order to evaluate the protective coatings and the tungsten hot-junction construction, a total of 112 thermocouples with tungsten hot junctions were made up for use on this contract. These thermocouples were expended according to a planned schedule for oxidation studies, strength tests, and life tests. Figure 13 shows details of the basic construction employed. The thermocouples consist of cylindrical n and p legs of 1 square-centimeter cross-sectional area (0.444-inch diameter) and of 0.500 inch in length. The two thermoelements are bonded to a 0.040-inch rectangular tungsten plate forming the hot junction which serves the dual purpose of a heat acceptor and electrical junction between n and p arms. The cold-junction ends of the thermocouple legs are terminated with tungsten metal "shoes" suitable for brazing to the insulator stack discussed in previous sections.

During the initial survey period, samples of these thermocouples were life-tested in vacuum to verify the electrical and mechanical performance of the basic tungsten hot-junction construction at high temperature. The test thermocouples were operated under water-cooled conditions in the bell jar vacuum life test stations shown in Figure 6 at a pressure of approximately 5×10^{-6} mm Hg at temperatures of 650°C, 675°C, and 700°C respectively. The degree of stability of the couples was determined at the various operating temperatures by measuring the resistance R, and open circuit voltage E_{oc}, at various time intervals for a total period of 800 hours. During these tests the couples were water-cooled at the cold junction and heated at the hot junction by means of a tungsten heating coil.

Figure 14 summarizes the results of the vacuum life tests performed on thermocouples of the tungsten hot-junction construction. Measurements of open-circuit voltage and power into a matched load, $E^2/4R$, indicate essentially stable performance up to 700°C in oxygen-free environments. The life data, in combination with previously described air storage life tests of protected tungsten hot-junction parts, suggest that satisfactory long-term operation with this construction could be achieved up to maximum hot-junction temperatures in the range 700°C to 750°C. The data also indicate, however, that at a higher

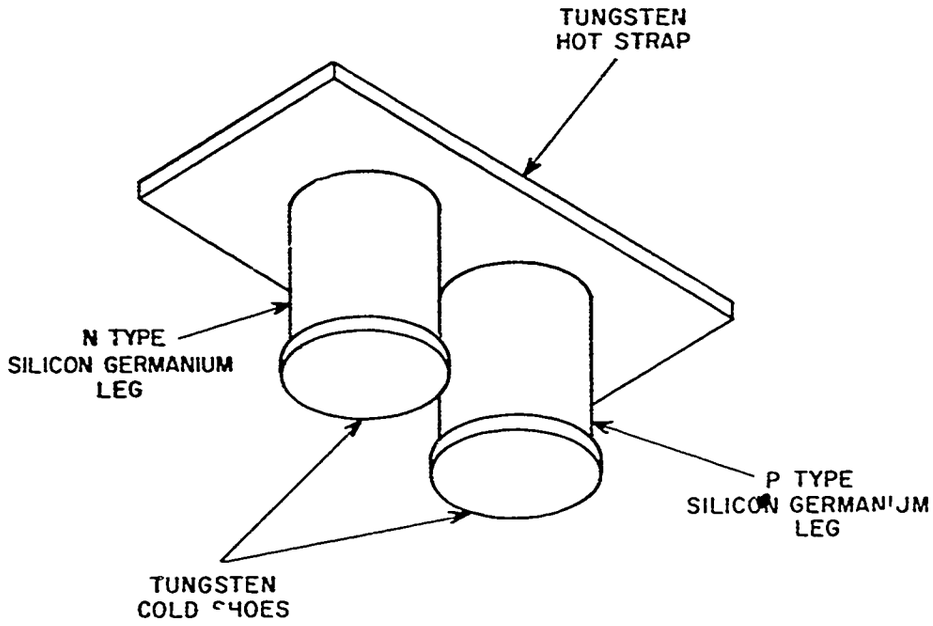

Figure 13. The Tungsten Hot Strap Thermocouple.

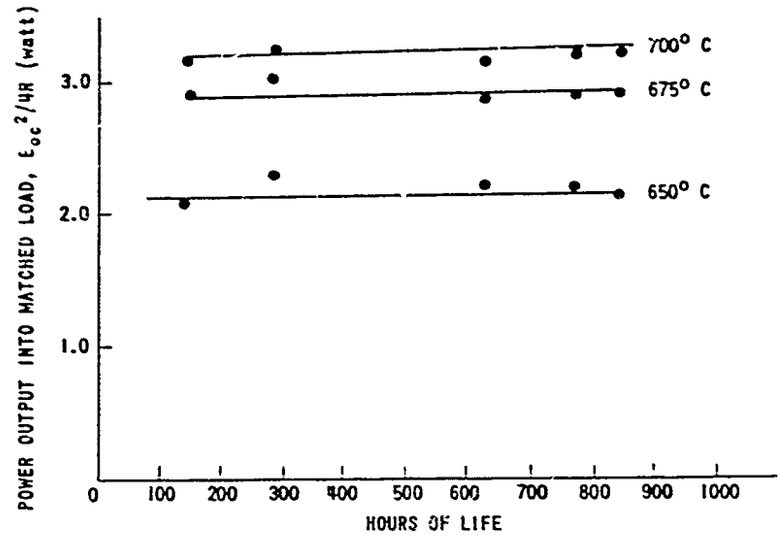

(a)

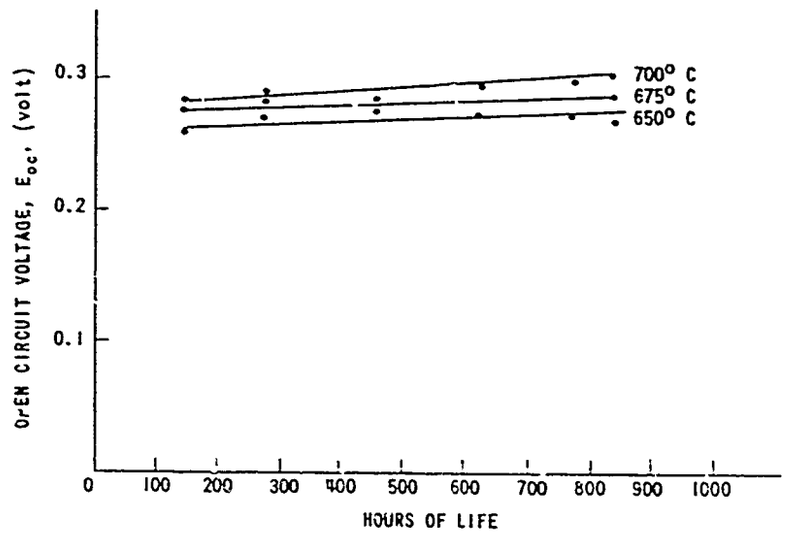

(b)

Figure 14. Vacuum Life Test Data on Tungsten Hot Strap Thermocouple.

temperatures, stringent oxidation requirements for the tungsten parts would seriously limit life. Such performance characteristics are less favorable than those of thermocouples with the all-SiGe construction in which oxidation problems are automatically resolved. The decision was made, therefore, to terminate further evaluation effort on tungsten hot-junction thermocouple construction, and to concentrate available effort on the more promising all-SiGe construction.

ALL-SiGe THERMOCOUPLE CONSTRUCTION

The all-SiGe thermocouple construction provided a second RCA-developed approach to thermocouple design which was evaluated in detail for TRECOM applications. Although this markedly different construction technique results in sources of power loss* which do not exist in thermocouples of the tungsten hot-junction design, it was believed capable of operating at higher hot-junction temperatures so that overall net efficiency gains might be achieved. For example, stringent oxidation requirements restrict, at present, tungsten hot-junction thermocouples to temperatures in the range of 700°C to 750°C; equivalent efficiency performance is obtained, however, by thermocouples of the all-SiGe construction at hot-junction temperature levels approximately 50°C to 75°C higher. The objective of initial evaluation tests was, therefore, to obtain projections of the maximum temperature capability of thermocouples of the all-SiGe design. Since the experimentally determined operating temperatures were in excess of 850°C, this design was judged to have superior performance characteristics and was ultimately selected for TRECOM applications.

The overall appearance of the all-SiGe thermocouple is shown in Figure 15. It may be noted that the entire hot-junction area of the thermocouple is constructed of active thermoelectric material and the n and p arms are bonded directly to each other instead of to an intermediate tungsten hot-junction plate. The hot-junction end of the all-SiGe thermocouple is a rectangular plate composed of n and p material. This rectangular shape permits close packing of groups of thermocouples and provides a convenient heat accepting area which may be exposed directly to a fossil fuel heat source. The cold junctions of the all-SiGe thermocouple are terminated in thin tungsten metal shoes which may be bonded to a water-cooled heat sink by conventional metallurgical means. Because the cold-junction operating temperatures are low (i.e., well below 500°C), oxidation protection for the tungsten cold shoes is not required. The n and p arms of all-SiGe thermocouple shown in Figure 15 are "half-cylinders", each of approximately 0.45 square-centimeter cross-sectional area. As shown by

* See Section III for analogue performance analysis.

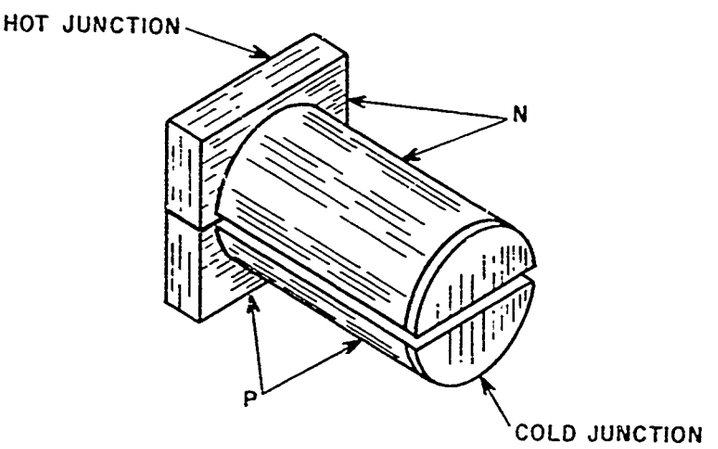

Figure 15. The Al-SiGe Thermocouple.

experiments conducted during module evaluation, the half-cylinder configuration results in a mean separation between the n and p arms which is satisfactory for temperature-cycled conditions of operation.

Two major technical requirements for a high-temperature thermocouple are automatically resolved with the all-SiGe thermocouple construction. Firstly, a close thermal expansion match between all components of a thermocouple exposed to high temperatures is normally necessary to avoid thermal stresses. This condition is clearly met in a highly favorable manner if thermocouples employ only the same basic SiGe alloy materials throughout. Secondly, SiGe alloys are oxidation-resistant and unaffected by exposure to high-temperature air environments. Thermocouple oxidation problems (which restricted the maximum hot-junction temperature capability of thermocouples with the tungsten hot-junction construction) are essentially eliminated by the use of oxidation-resistant SiGe throughout. The maximum hot-junction temperature capabilities of all-SiGe devices are, therefore, defined only by temperature limitations of SiGe alloys themselves.

During the initial survey period, materials tests were conducted to permit estimates of the long-term performance of all-SiGe thermocouples up to hot-junction temperatures of 850°C. Tests of special pertinence were the previously described vacuum and air storage tests of n- and p-type SiGe alloys which indicated no degradation of the basic thermoelectric material at temperatures up to 850°C. In addition, air storage tests were performed at 850°C to evaluate the stability of the RCA-developed bond between the n and p arms of the all-SiGe thermocouple. Resistance measurements at room temperature indicated low p-n junction resistances (of the order of 50 micro-ohms per square centimeter) which remained stable during prolonged storage at 850°C in air.

Based on such material survey evaluations, it was concluded that operation of the thermocouples in air at temperatures well in excess of 850°C would be satisfactorily demonstrated. The projected net performance gains from this higher temperature capability result in superior efficiency performance for thermocouples of the all-SiGe construction. This construction was, therefore, selected for TRECOM applications. Life performance characteristics of such thermocouples at hot junction temperatures up to 1025°C are given in Section III.

SECTION III

PERFORMANCE OF TRECOM MODULES

INTRODUCTION

During the initial survey phase of the TRECOM program, evaluations were made of alternative RCA-developed approaches towards module construction to establish constructional features which would be most applicable to TRECOM requirements. These studies led to the selection of modules employing thermocouples of the all-SiGe construction which were mounted rigidly on individual insulator stacks brazed to a common water tube.

During the present phase of this program, life test measurements were made upon sample modules of this construction to determine accurate performance characteristics and to establish operating temperature limits for satisfactory life. These experimental results are described in this section, and made use of in Section IV in the design studies for a 30-kilowatt silent-boat power source.

Life tests on TRECOM-type modules performed in air, over the temperature range 850°C to 1025°C for periods of 500 and 1000 hours, show no signs of degradation and suggest 1000°C as a suitable operating temperature. At this temperature, conversion efficiencies of approximately 10 per cent were achieved. To RCA knowledge, this represents the highest long-term efficiencies yet obtained with thermoelectric devices.

DESCRIPTION OF FINAL TRECOM MODULES

Figure 16 shows a photograph of a sample module developed for TRECOM applications. The module contains six thermocouples connected electrically in series, and produces approximately 13.9 watts of electrical output at 10 amperes when operated at 1020°C into a load matched for optimum efficiency. Based on measurements of sample thermocouples, the conversion efficiency of a module, defined as the ratio of electrical power output to the heat input to the thermocouples, is estimated as 10.0 per cent.

In a working generator, thermocouple modules similar to those shown in Figure 16 would be grouped together so that the hot-junction surfaces would form an enclosing chamber for a fossil fuel burner. The hot-junction surfaces are

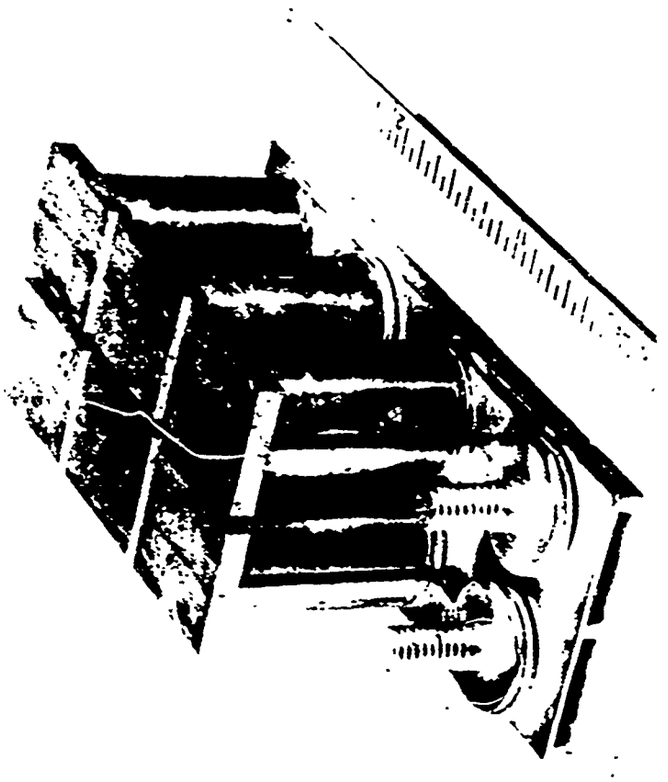

Figure 16. Six-Thermocouple Module Incorporating Optimum Design Features for Maximum Efficiency and Extended Life in High-Temperature Air Operation.

operated at 1000°C and are directly exposed to the burner to provide efficient heat transfer to the active thermoelectric material. Inlet cooling water (at 15°C) flowing through the water cooling tube reduces the cold-junction temperature to approximately 37°C (see Table 1) so that 97 per cent of the available temperature difference is developed across the thermoelements.

The overall height of the thermocouples (including insulator stack assembly) above the water-cooling tube is 1.00 inch. This figure includes an overall thermocouple height of 0.90 inch and an insulator stack assembly height of 0.10 inch. These thermocouple dimensions have been selected as a suitable compromise between optimum efficiency, low weight ratios, and thermal transfer requirements. Further dimensional details of the sample module may be noted in Figure 17.

Typical weights of the sample module are 8.9 grams per all-SiGe thermocouple (including tungsten cold-junction shoes). The six thermocouples are mounted in an area approximately 1 inch by 2 inches to provide a packing density, based on the cross-sectional area of the thermocouple arms, of approximately 50 per cent. Typical weights of the water-cooling tube and insulator stack, based on the area covered by the thermocouples, are 5.0 grams per thermocouple, so that the total basic module weight per thermocouple is 13.9 grams. At 1000°C hot-junction temperature (2.2 watts per thermocouple), the basic weight per thermocouple is 0.158 watt per gram. This figure corresponds to 71.7 watts per pound or 13.9 pounds per kilowatt. Somewhat improved weight performance could be obtained by using shorter thermocouples if compactness, and not maximum efficiency, were the major criterion of a generator.

The water-cooling tube in the present module is constructed of gold-plated copper and is suitable for fresh-water cooling. Initial engineering evaluations of sea water as a cooling medium indicate that sea water is a feasible alternative to fresh-water cooling. The basic weights of the water-cooling tube employed in the sample module were selected with this alternative in mind. It will, however, be necessary for sea-water applications to construct water tubes and other parts of a generator that come in contact with sea water from special alloys. Monel, Inconel, and Ni-Resist are among the alloys most usefully resistant to corrosion by sea water.* Somewhat improved water-cooling tube weight ratios over those employed in the sample module could be achieved if only fresh-water applications were envisaged. Lower density alloys could then be employed to reduce the weight of the water-cooling tube.

---

*J.A. Lee, "Materials of Construction for Chemical Process Industries", McGraw-Hill, New York, 1950, p. 326.

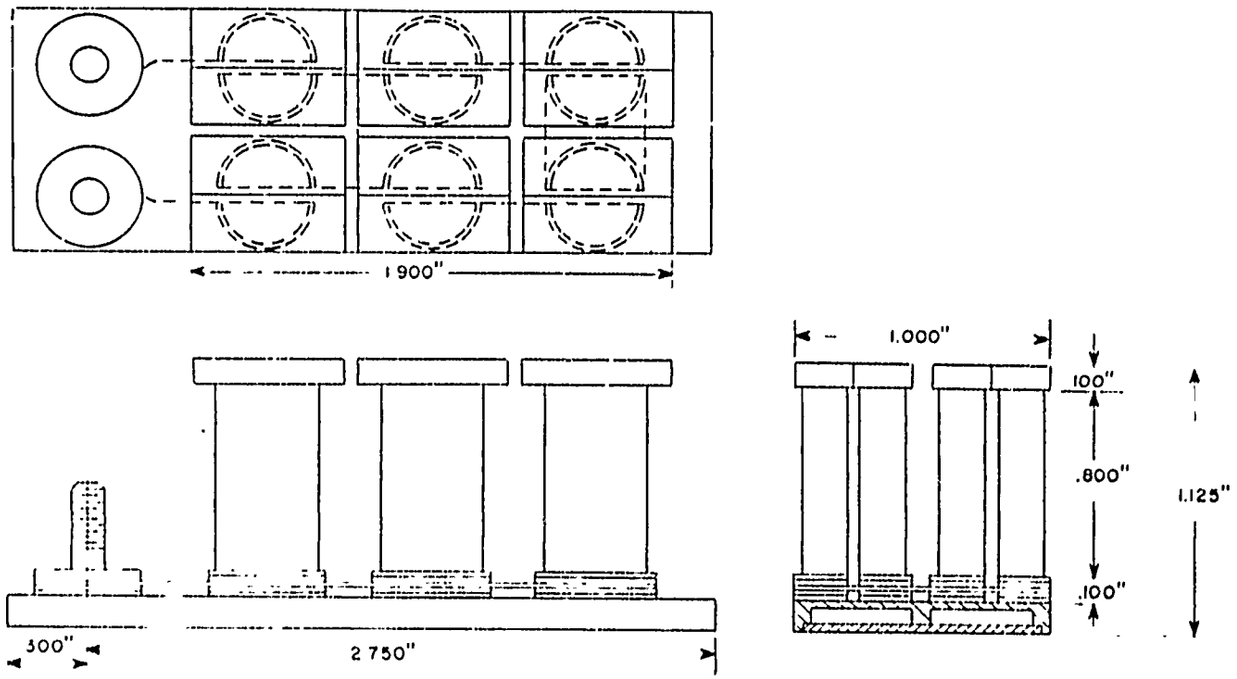

Figure 17. Engineering Drawing of the TRECOM Final Module.

All thermoelectric modules whose life performance is reported in subsequent paragraphs closely resembled that shown in Figure 16. The same basic all-SiGe thermocouple configuration and insulator stack assembly was used in all tests, although minor variations were adopted for convenience. Individual thermocouples were, for example, more widely spaced to allow room for necessary voltage, resistance, and temperature probes. Life tests and temperature cycling tests were performed on thermocouples with somewhat shorter arms (0.6 inch overall height) since final optimization of dimensions could not be established until life performance was known. Because the life test thermocouples operated under higher temperature gradients, the actual life test conditions are considered to demonstrate satisfactory performance under more severe conditions than would be encountered in TRECOM applications. Shock and vibration tests as well as efficiency performance measurements were conducted near the end of the testing period when the dimensions of TRECOM thermocouples had been established and were, therefore, conducted on samples identical with those in Figure 16.

LIFE TESTS OF ALL-SiGe THERMOCOUPLES

Life tests of 500 to 1000 hours were run on modules of all-SiGe construction of four to six couples at temperatures of 850°C, 950°C, and 1025°C in air, and at 825°C in vacuum. Several problems were encountered in maintaining load and measuring probes at these temperatures, but these problems were largely overcome by the end of the life test period. Although these equipment problems resulted in some erratic data points during the life tests, there was no measurable degradation in any of the modules. During the test period, all modules were operated into a matched load except for the time necessary to take open-circuit readings. Closed-circuit output voltage was continuously monitored with recorders.

The primary objective of the module life tests was to determine if the modules would be stable at high temperatures in regard to the voltage output and electrical resistance of the thermoelectric material and the electrical resistance of the joints. Also of interest was the ability of the modules to withstand the mechanical stresses induced by alternate expansion and contraction of the parts during heating and cooling. A secondary objective of the life tests was to compare the performance of couples having different doping agents, and couples having different proportions of SiGe.

Life tests were performed in the four furnaces constructed for testing modules in air (Figure 4b). These units consisted of an insulated chamber through which

a "Globar" heating element was passed. The hot junction plates of the all-SiGe thermocouples were adjusted to a distance of approximately one-half inch from the "Globar" elements and heated directly by radiation. The hinged aluminum cover supporting the silicon carbide "Globar" heating element allowed the heater to be moved out of the way for inspection of the module without disturbing the module or its leads.

Temperature of the hot shoes of the modules in the air furnaces was measured by inserting a thermocouple of 12-mil chromel-alumel wires into a hole sand-blasted into the side of the shoe. The thermocouple wires were covered with ceramic tubing and led to a terminal strip on the asbestos base plate of the furnace. At the higher operating temperatures, difficulty was experienced with the thermocouple lead wires failing after several hundred hours of operation. This problem was largely overcome by placing ceramic heat shields over the thermocouple wires so that they were not subjected to the direct radiation of the heater.

Voltage measuring wires were brought out to the terminal strip from each end of the module and from the junctions of the cold straps between each couple. Here, again, problems were encountered with oxidation of the wires. Ceramic heat shields plus use of stainless steel wire were used to minimize this problem. Heavy load leads were brought out from each end of the module to an external load. The modules were operated into a fixed load resistance approximately equal to the hot resistance of the module. After copper and nickel load leads were found to oxidize too rapidly, water-cooled copper load leads were used with satisfactory results. The temperature of the air furnaces was measured by a heavy chromel-alumel thermocouple mounted in the rear wall of the furnace. The output of this thermocouple was used to control the temperature of the furnace by means of a proportional controller.

The furnaces used for testing modules in vacuum were constructed inside a bell jar mounted on a Veeco VS400 vacuum system. The module was mounted in a horizontal position inside a water-cooled copper heat shield used to prevent excessive radiated heat from overheating the glass bell jar. Aluminum foil reflectors were also used inside the bell jar to help keep the glass cool. The module was supported by the heat shield, which in turn was supported by two vertical support rods -- one at each end of the module. The heater for the vacuum modules consisted of tungsten wire wound on a ceramic rod. Above the heater was mounted a reflector to direct the radiation down at the module. The entire heater assembly was supported above the module by the same vertical support rods used to support the module and heat shield. The position of the heater assembly was adjusted to bring the heater about one-half inch above the hot shoes of the module.

Thermocouples were mounted in holes sandblasted in the side of the hot shoes as was done in the modules operated in air. Chromel-alumel thermocouples were welded to the cold shoes of the module. Wires for voltage and resistance measurement were soldered to each cold strap. All thermocouple and voltage measurement wires were led through a shielded slot in the bottom of the heat shield to a connector located on the outside of the heat shield. A cable led from this connector through a vacuum-tight fitting in the base plate of the bell jar to a terminal board located on the outside of the vacuum system. This plug-in arrangement allowed the thermocouple and voltage measurement leads to be attached with the module and heat shield assembly on the bench. Heavy copper leads were led from each end of the module through vacuum-tight fittings to an external load resistance. Temperature of the vacuum furnace was controlled by a proportional controller as in the case of the air furnaces, except that in the vacuum system the control couple was placed in a hole in the side of one of the module hot shoes.

In both the vacuum and air life test facilities, temperatures (as indicated by hot- and cold-junction thermocouples) were read using a Minneapolis Honeywell Regulator Company Potentiometer, Model No. 2715. Although this instrument is accurate to $\pm$ 3°C, considerable difficulty was experienced with deterioration of the thermocouple wires. In general, with the furnaces operated at a constant temperature controller setting, the output voltage of the silicon-germanium couples is considerably more constant than that of the chromel-alumel thermocouples.

During the course of the life test studies, resistance measurements of thermocouples, modules and loads were independently checked by several independent "four probe" a-c resistance test sets whose accuracy had been established by comparisons with primary resistance standards. Consistent results were obtained at all times. For routine measurements, an a-c voltmeter-ammeter proved satisfactory. A 60-cps current of 1 ampere was passed through the sample to be measured, and the a-c voltage developed across the sample was measured using a Ballantine Laboratories RMS VTVM, Model 320. The 1.0-ampere current was monitored using an a-c ammeter calibrated accurately at the 1.0-ampere point. The 1.0-ampere current was large enough so that little trouble was experienced from a-c currents induced from the a-c heater supply. As an added precaution against this source of error, the leads were reversed after each reading and a second reading taken. In those cases where a small difference existed between the two readings, the average of the two was recorded as the true reading. The accuracy of resistance measurements is estimated to be $\pm$ 2 per cent. The voltage measurements of couples were made using a Minneapolis Honeywell Regulator Company Potentiometer, Model

2731, or a John Fluke Company Model 301 differential voltmeter. Accuracy of these measurements is estimated to be within ± 0.5 per cent.

Life test results are plotted by module in Figure 18 through Figure 22 for tests performed on all-SiGe thermocouples in both air and vacuum. For each module, the closed-circuit voltage developed across a fixed load resistance by the entire module has been plotted. This represents a direct measure of actual power output; and since the voltage measurements are more accurate than the resistance measurements, the closed-circuit voltage is considered to be the best indication of the overall stability of the module, both in terms of developed voltage and internal resistance. On the same page with total module closed-circuit voltage is plotted $E_{oc}^2/4R$ (Equation 10), where E_{oc} is the open-circuit voltage of each couple and R is the resistance of each couple; $E_{oc}^2/4R$ represents the power which each couple could deliver into a matched load. Careful comparison of power estimates made by $E_{oc}^2/4R$ measurements and closed-circuit resistance, using standard open- and closed-circuit formulae for thermocouples, has demonstrated that the two estimates of power are identical within measurement accuracy for all-SiGe thermocouples. Since the average temperature of all furnaces was closely controlled by proportional controllers, all data have been plotted as recorded with no corrections for temperature variation. The temperature reported for each life test refers to average temperature over each life test module. Because the individual thermocouples on a module were not separately heated, there was normally an appreciable spread (± 25°C) in individual all-SiGe hot-junction temperatures along a module. For example, in the 1025°C life test series in air, some of the thermocouples were operated at 1050°C, so that, in effect, stable performance at 1050°C was also demonstrated by this test series. Such temperature variation effects were especially pronounced in the vacuum life tests (± 50°C at 825°C) because of the absence of convective heat transfer which undoubtedly caused an appreciable smoothing of the temperature distribution in the air life test series. It may be noted that if the raw data on individual thermocouples had been normalized to take this temperature distribution into account, much of the spread in power output levels between different thermocouples would have been eliminated.

The life test data in Figure 18 through Figure 22, as noted previously, refer to thermocouples of 0.6-inch overall height instead of the 0.90-inch overall height specified in the TRECOM module and generator computation. Because of the shorter thermocouple length, the power output levels of the life test thermocouples are higher than those specified elsewhere in this report for thermocouples of the TRECOM configuration. The objective of these life test series was to explore the temperature stability of SiGe alloy materials during high-temperature operation, so that the individual thermocouples tested were not all

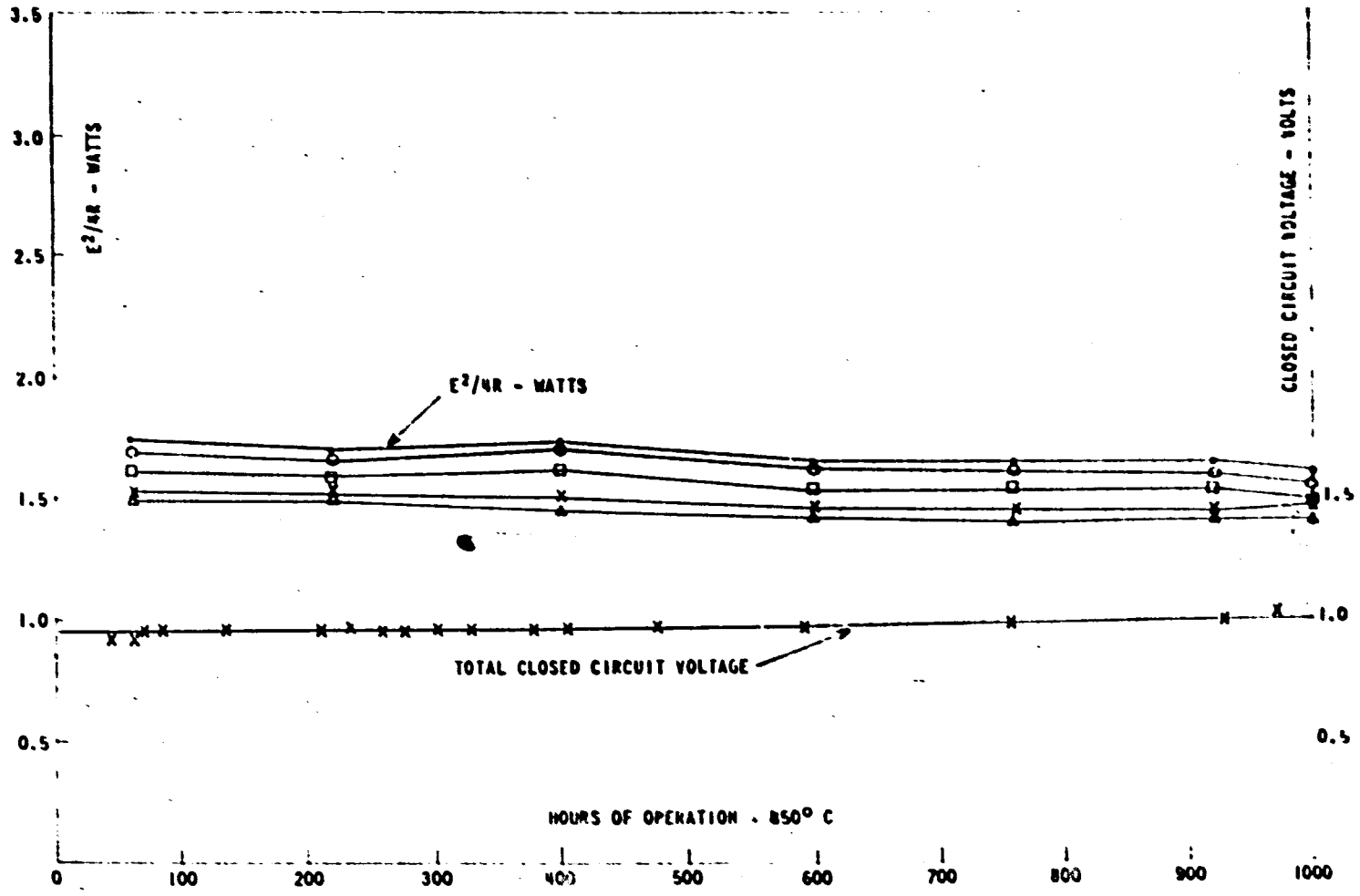

Figure 18. All-SiGe Thermocouple Life Test Performance in Air at 850° C.

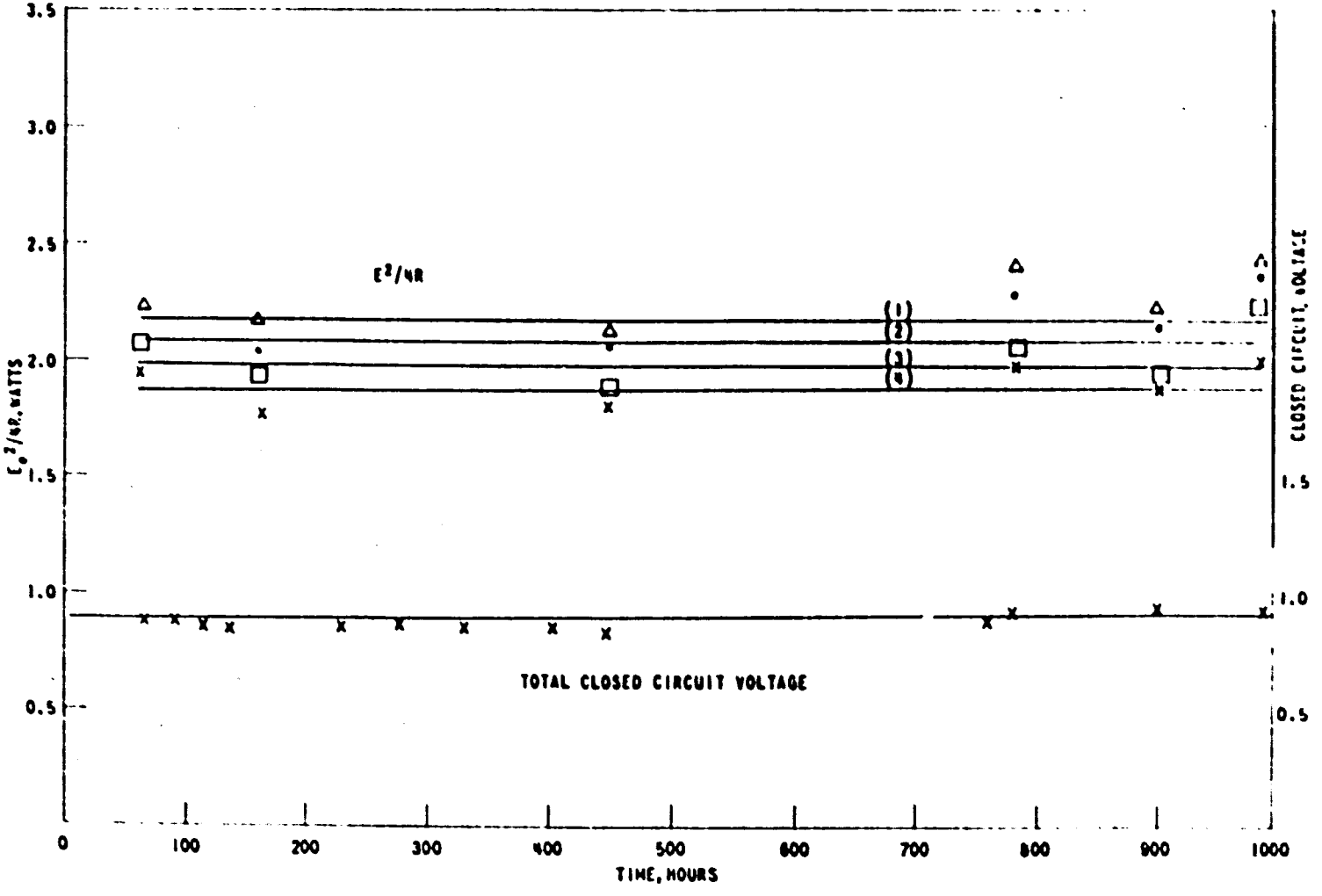

Figure 19. All-SiGe Thermocouple Life Test Performance in Air at 950° C.

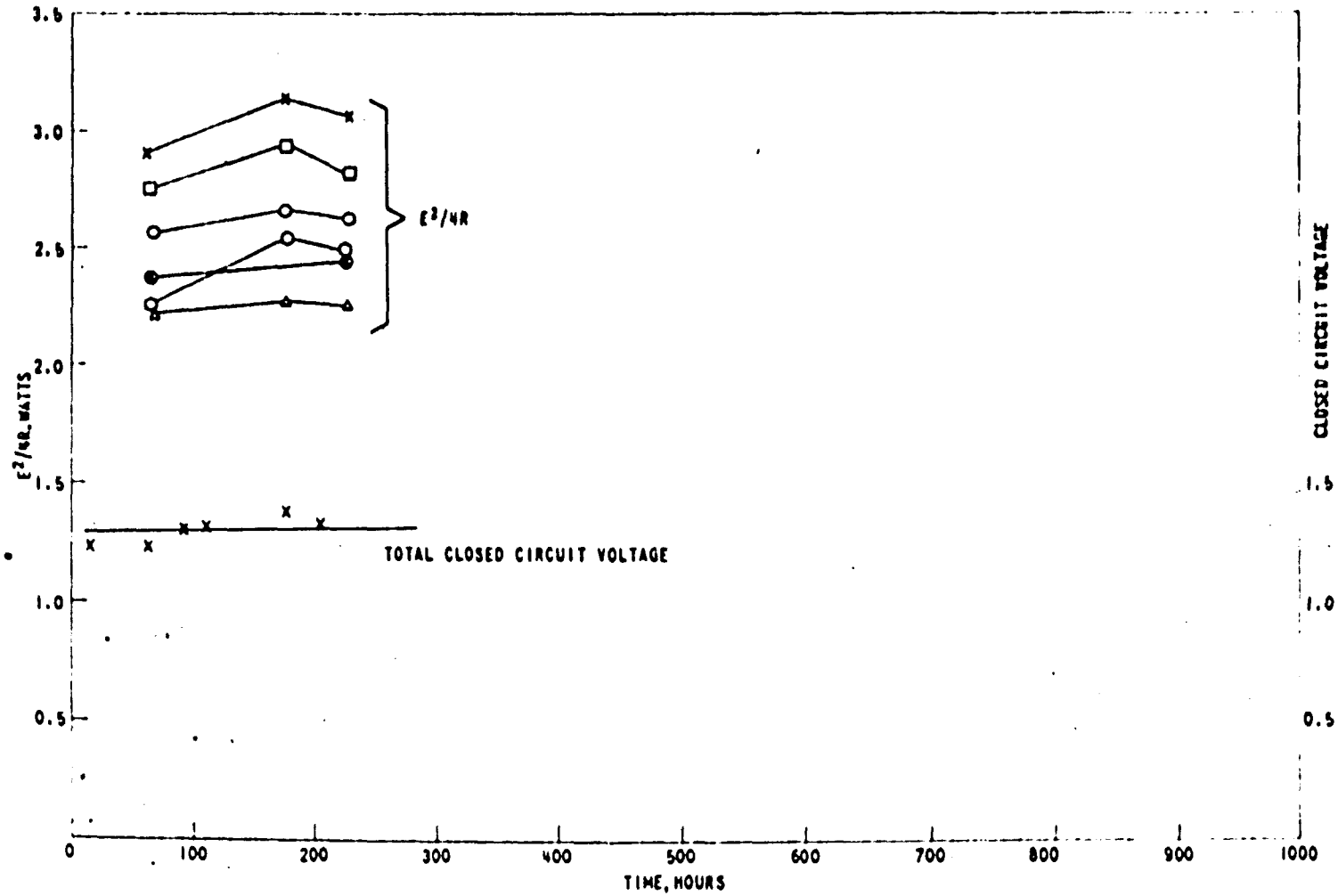

Figure 20. All-SiGe Thermocouple Life Test Performance in Air at 1000° C.

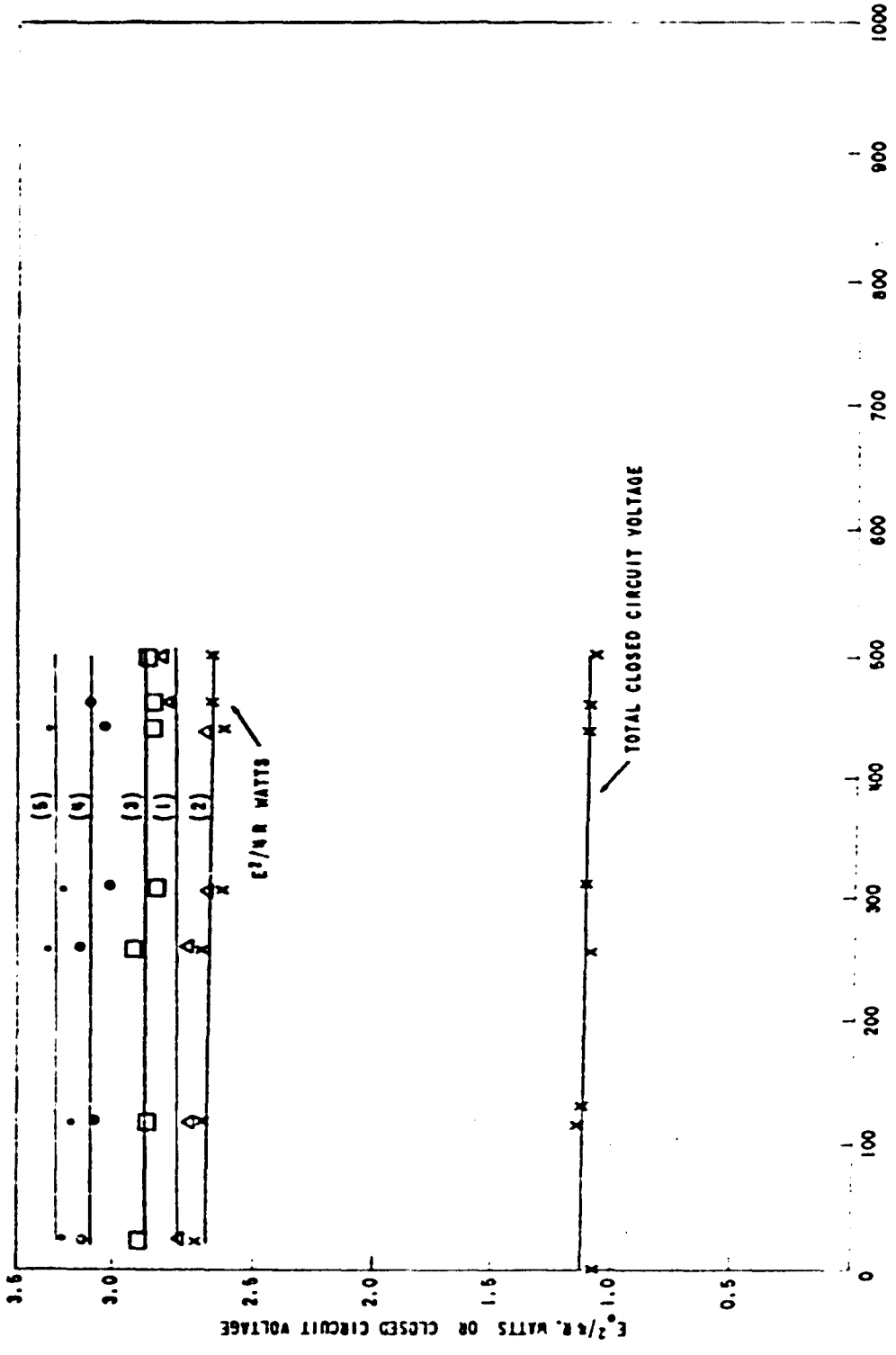

Figure 21. All-SiGe Thermocouple Life Test Performance in Air at 1025° C.

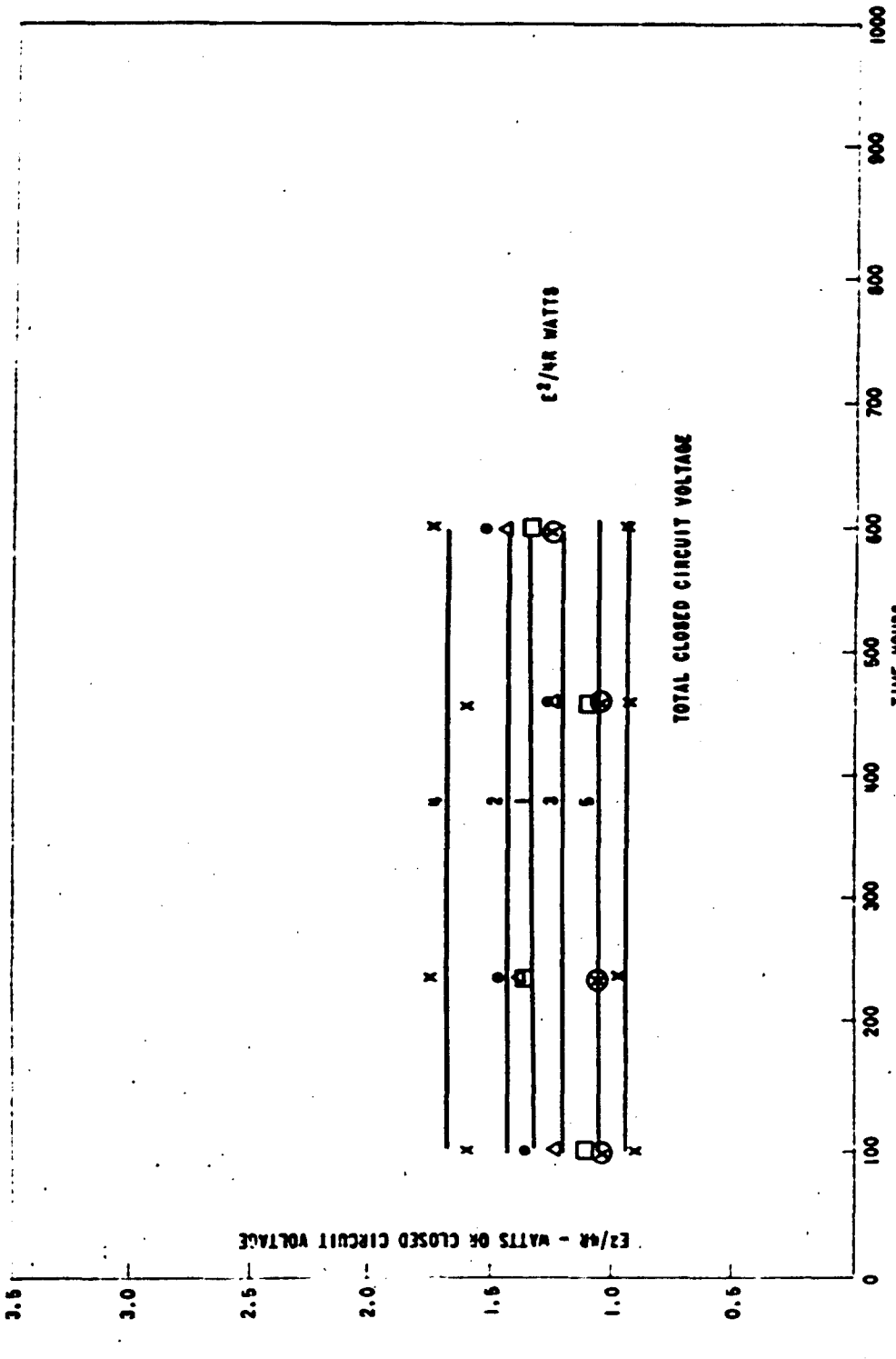

Figure 22. All-SiGe Thermocouple Life Test Performance in Vacuum at 825° C.

identical but cover a range of construction techniques, SiGe alloy compositi s, and doping levels. No appreciable degradation was noted in any of the life ' sts with any of the basic RCA alloys tested (2113, 2213, 2130, and 2230), so that selection of alloys for the TRECOM modules could be based upon known values of figure-of-merit. As anticipated, alloys in the 2200 series showed somewhat higher output than those in the 2100 series when hot-junction temperatures were normalized to the same level. The highest electrical outputs were obtained with alloy 2230; but since this alloy has a higher thermal conductivity than alloy 2213A, the conversion efficiencies do not differ appreciably. Alloy 2213A has been selected for use in TRECOM applications.

On the basis of the life tests shown in Figures 18 through 22, each of which were temperature-cycled several times, the following conclusions may be drawn:

1. The all-SiGe thermocouple is satisfactory for unprotected operation in air at temperatures up to 1025°C. Since some of the thermocouples in the 1025°C test series were, in fact, operated at temperatures of 1050°C without degradation, use of a 1000°C design temperature would appear to be a conservative value for use in generator designs.

2. No thermocouple failures occurred in any of the tests conducted. Although insufficient numbers of thermocouples were run to establish reliability statistics, the reliability of SiGe devices should be high.

3 The all-SiGe thermocouple may be temperature-cycled without degradation.

SHOCK AND VIBRATION TESTING OF ALL-SiGe THERMOCOUPLES

Shock and vibration tests were made on sample thermocouples of all-SiGe construction to evaluate their suitability in practical devices. The alloy 2213A thermocouples survived 60-g. vibration and 100-g. shock. These levels are substantially in excess of normal military specifications for electronic devices.

The shock and vibration tests were made by mounting the couples to be tested on a one-inch-square brass block, which in turn was bolted to the shaker or drop machine. Mounting holes were tapped in three perpendicular faces of the brass block so that the couples could be tested in each of three mutually perpendicular planes. The thermocouples were mounted on the standard insulator stacks, brazed to one face of the block in accordance with standard module

assembly technique to simulate performance in modules. Very flexible voltage and current leads were soldered in the insulator stacks so that couple resistance could be monitored during the vibration runs.

Vibration tests were made on a Ling 227 shaker system, and shock tests were made using a Barry Controls Corp. Drop Machine, Model 16750. All tests were made in each of three perpendicular planes. Shock tests were made using a half-sine pulse of six milliseconds duration, with three blows delivered in each test axis. Vibration tests were made using a 25-minute sweep from 20-3000 cps. Displacement at the lower frequencies was limited to one-half inch to stay within the ratings of the 227 shaker.

The tests were performed in the following sequence in each of three perpendicular planes:

1. Vibration at 20 g.
2. Shock at 25 g.
3. Vibration at 30 g.
4. Vibration at 50 g.
5. Shock at 50 g.
6. Vibration at 60 g.
7. Shock at 100 g.

The 60-g. vibration test represents the highest level which can be obtained from the 227 shaker with the weight of the fixtures used.

Each test couple was examined for cracks under the microscope before and after each test run. The electrical resistance of each couple was also measured before and after each run. During vibration runs, the couple resistance was continuously monitored.

The all-SiGe thermocouples employed in TRECOM modules developed no cracks and showed no significant change in resistance during the entire test sequence. Apparently the all-SiGe construction is sufficiently rugged so that the maximum capabilities of the equipment available for shock and vibration tests do not permit testing to destruction. On the basis of the levels reached without failure, it may be concluded that there is no significant strength problem in the all-SiGe construction.

ANALOGUE EFFICIENCY ANALYSIS OF ALL-SiGe THERMOCOUPLE

The all-SiGe constructed thermocouple has many desirable mechanical features, such as ruggedness and the ability to operate in high-temperature air environments, but, it is believed, functions at a somewhat reduced efficiency for any given hot-junction temperature. Sources of efficiency loss, however, are more than offset by net efficiency gains which result from a higher operating temperature capability, as demonstrated by direct efficiency measurements. In order to estimate the efficiency losses associated with this structure and to optimize thermocouple geometry, an analog study of its performance was made. On the basis of this analog analysis, which appears to be confirmed by direct efficiency measurements, it has been concluded that 90 per cent of the theoretical SiGe material performance can be conveniently recovered with practical devices.

An intuitive picture of the efficiency performance can be obtained by consideration of Figure 23, in which the construction of an "ideal" thermocouple and an all-SiGe thermocouple are compared. Gehlhoff* has shown that such an ideal thermocouple (with properties independent of temperature, which is assumed throughout all discussions in this section) will deliver the maximum performance possible from a thermoelectric material. By comparing the electrical output of an all-SiGe thermocouple to that of a thermally equivalent ideal thermocouple, it is possible to estimate the efficiency of devices with the all-SiGe thermocouple construction.

Two major factors modify the performance of thermocouples of the all-SiGe construction relative to those with the ideal construction. First, a temperature gradient exists across the junction between the p and n arms of the all-SiGe thermocouple, so that the characteristic hot-junction temperature will not correspond to the maximum junction temperature but, instead, will more nearly approximate the average temperature of the junction. As a result, the output voltage of an all-SiGe thermocouple will be somewhat lower than that of an ideal SiGe thermocouple. To minimize this effect, the thickness of the p-n junction should be made as thin as possible to maintain the junction at the highest possible temperature. The second factor relates to the electrical current between the p-n arms which must also flow through the hot-junction bridge. The thickness of the p-n junction cannot be profitably reduced beyond a certain point or else the resulting constriction in electrical path will cause the total resistance of the thermocouple to become excessive. For any particular arm cross-section, the relative dimensions of the hot strap may be adjusted to obtain optimum volt-

*P.O. Gehlhoff, E. Justi, and M. Kohler, "Abh. Braunsch. Wiss. Gesell.", Vol. 2, 1950, p. 149

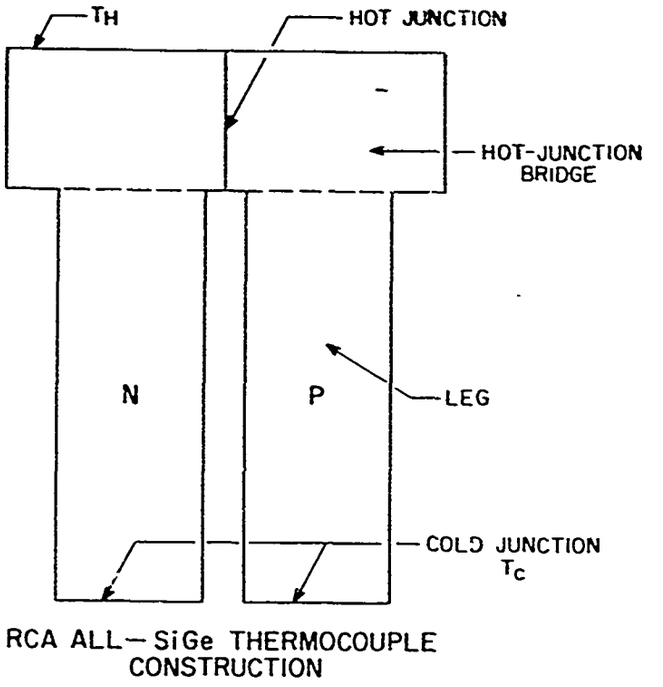

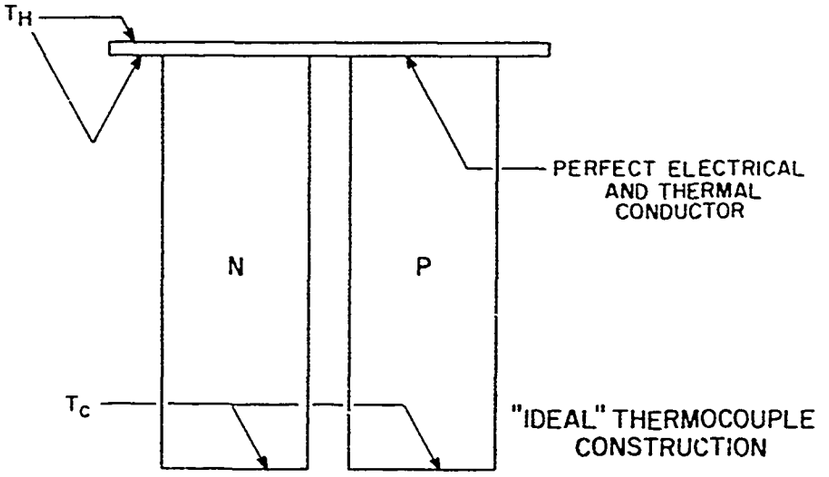

Figure 23. Comparison Between All-SiGe Thermocouple and Ideal SiGe Thermocouple.

age and resistance characteristics.

Because of the non-simple geometry employed in the all-SiGe constructed thermocouple, the temperature-dependent properties of SiGe alloys, and the complex nature of the thermoelectric gene ·.tor equations, a direct analytical solution has not been attempted. Instead, analog solutions based on potential plots of two-dimensional models were used to obtain estimates of efficiency and also to optimize thermocouple configurations experimentally. Potential field plots provide an exact and accurate analogue method for the solution of those problems relating to heat and electrical flow governed by the Laplace equation. These conditions are essentially fulfilled for thermocouples under open-circuit conditions. The models used in the two-dimensional potential field plot studies were about two feet in length (30 times actual size) to effect better accuracy in the data. Standard commercial potential plotting resistance paper was used for the model and equipotential lines were located on the models using standard commercial null-detecting equipment.

Approximately 100 two-dimensional models of four basic potential field plots were employed to generate data necessary for performance estimates. The first two types, shown in Figure 24, are typical of those plots used to furnish information concerning the temperature and resistance distributions in thermocouples.

The purpose of the third series of potential field plots, shown in Figure 25, was to locate the effective Seebeck temperature point. By assumption, this occurs at the point of mean (50 per cent) electrical current flow through the p-n junction. The models used for this study were similar to that employed to obtain resistance data, but boundary conditions were appropriately modified to satisfy orthogonality relationships between voltage and current, and so generate the appropriate field plots. For thin hot-junction bridges, the effective Seebeck point occurs at the approximate midpoint of the bridge. However, for thicker bridges this midpoint approximation is not the same, since the path of least resistance of the current flow will not be appreciably altered by increasing the bridge thickness beyond the optimum thickness.

The model analysis indicated that the resistance loss through the hot-junction bridge could be reduced by allowing it to overhang the legs, thus providing a larger cross-section for current flow. The model and resultant data of the fourth series of potential field plots to evaluate overhang are shown in Figure 26. The purpose of these studies was to determine (1) the resistance through the hot-junction bridge as a function of hot-junction bridge overhang, and (2) the influence of hot-junction bridge overhang upon effective Seebeck tempera-

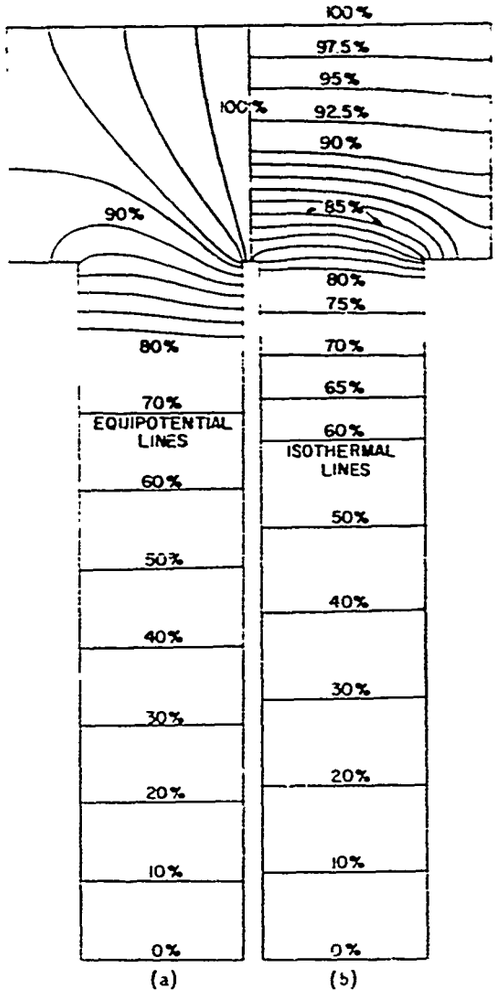

Figure 24. Typical Field Plots Used in Analogue Efficiency Analysis of All-SiGe Thermocouple.

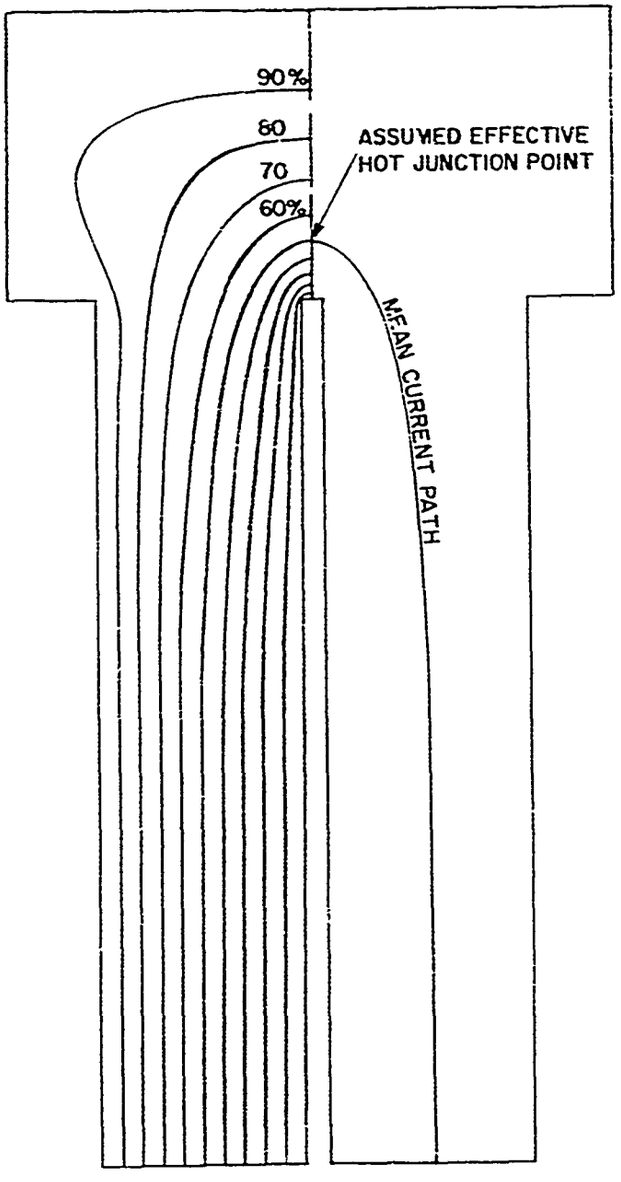

Figure 25. Typical Field Plot Used in Analogue Efficiency Analysis Showing Distribution of Current Flow.

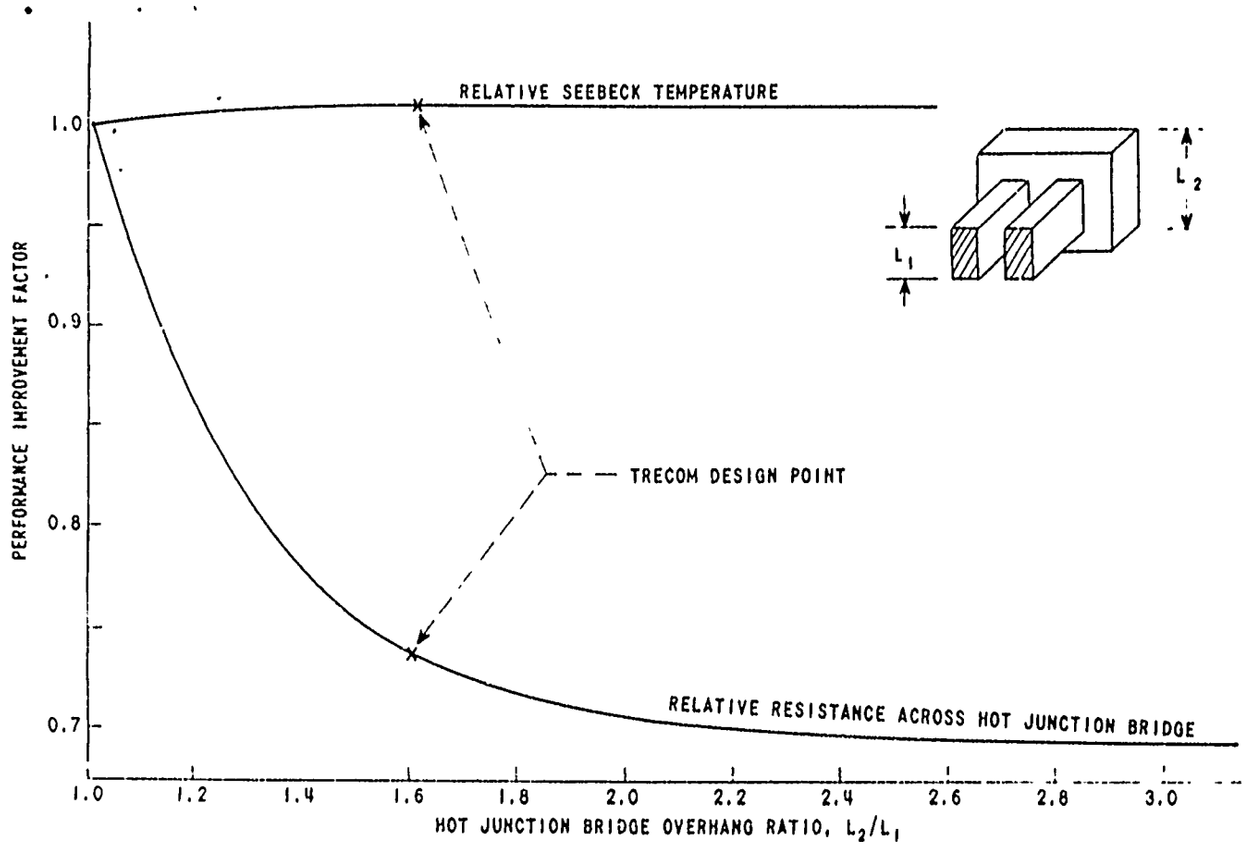

Figure 26. Effect of Hot Junction Plate Overhang in All-SiGe Thermocouple.

ture. As seen in Figure 26, the resistance of the hot-junction bridge for the all-SiGe thermocouple is substantially reduced by a factor of 0.26. For thermocouples of the TRECOM dimensions, this produces a performance increase of 3 per cent over a bridge with no overhang. Overhang also results in improved voltage output, since the average hot-junction temperature is also increased as a result of increased area of the thermal path at the hot end of the all-SiGe thermocouple.

It is to be noted that, after a point, further increase in bridge width (and hence weight) does not produce a corresponding increase in Seebeck temperature nor a decrease in resistance. This point of diminishing returns for the TRECOM design was approximately 1.61.

Figure 27 summarizes the results of the model analyses and indicates the power-generating performance of the all-SiGe thermocouple of optimized dimensions relative to an ideal thermocouple having the same thermal input. It may be noted that relative efficiency of the all-SiGe construction increases with leg length, approaching that of the ideal SiGe construction as a limit with infinite leg length. The power per unit weight, as in all thermocouples, decreases with increased leg length, so that where compactness is a prime requisite and efficiency is not critical, shorter leg lengths should be considered. Figure 27 indicates the design point employed in TRECOM thermocouples. When due allowance is made for additional joint resistances, lead resistances, etc., it is anticipated that 90 per cent of maximum SiGe performance is obtained. To achieve this value, the basic dimensions of the TRECOM all-SiGe thermocouple are: leg length, 0.80 inch; hot-junction bridge thickness, 0.10 inch; and hot-junction bridge width, 0.60 inch. Direct efficiency measurements, described in the following section, appear to be in general agreement with analytical estimates.

EFFICIENCY PERFORMANCE OF ALL-SiGe THERMOCOUPLE

Direct measurements were performed during the TRECOM module evaluation program to supplement analytical estimates of the efficiency performance of all-SiGe thermocouples of the TRECOM geometry. Because it was recognized that sophisticated experimental techniques may be required for reliable efficiency estimates, evidence from three independent sources has been considered. Each of these sources is in good agreement and indicates that, at hot-junction temperatures near 1000°C, conversion efficiencies of 10 per cent are attained.

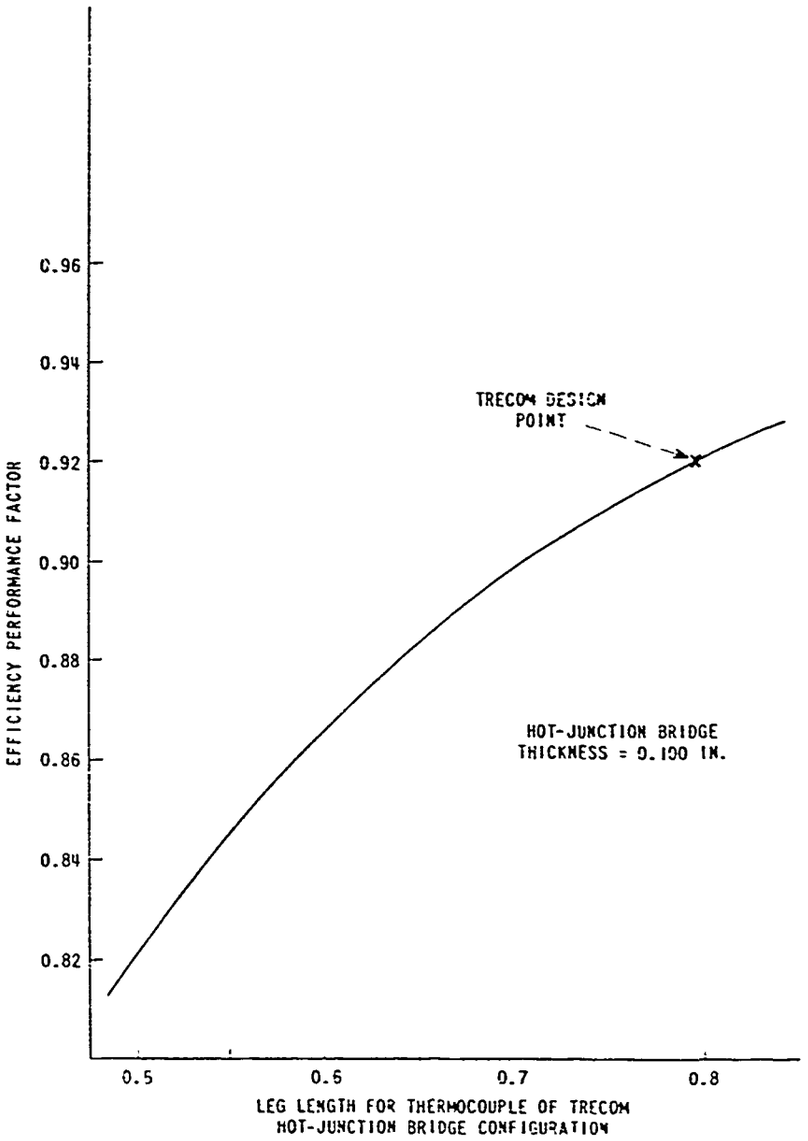

Figure 27. Efficiency Performance of All-SiGe Thermocouple Relative to Ideal SiGe Thermocouple.

The major experimental difficulty in direct efficiency determinations of thermoelectric devices arises from the fact that heterogeneous measurements of electrical and thermal power levels are required. While direct-current electrical measurements can be made to a high degree of accuracy (± 1.0 per cent) with commercially available equipment, thermal measurements are less amenable to routine laboratory measurements. Errors in thermal power measurements may arise due to heat losses or gains in the system under study, unless extreme experimental precautions are taken. The reliability of any efficiency determination, therefore, depends in large measure on the accuracy of basic thermal measurements (or equivalently, thermal conductivity measurements). The most reliable efficiency measurements, therefore, are considered to result upon combining direct measurements of electrical performance with computations of thermal input, based on known thermal conductivity values of the SiGe material.

The three methods by which the efficiency of the all-SiGe thermocouple has been estimated may be summarized as follows:

1. Measured Electrical Output, Computed Thermal Input

   Direct electrical output measurement may be combined with computed thermal input. The most reliable estimates of the thermal input terms are considered to result by combining electrical measurements with the thermal conductivity values for the n and p SiGe material given in Figure 3. This procedure references efficiency measurements to thermal conductivity values determined at the RCA David Sarnoff Research Center, Princeton, New Jersey, by Dr. Abeles and coworkers using the thermal diffusivity technique*. Thermal diffusivity measurements are generally accepted as providing the most accurate (± 3 per cent) determinations of thermal conductivity at high temperatures, since extraneous heat losses do not significantly affect the results.

   The basic principles of the thermal diffusivity method of thermal conductivity measurements were recognized by Angstrom in 1863 and the basic technique is widely used at the present time for accurate high temperature measurements.

---

* B. Abeles, D.S. Beers, G.D. Cody, and J.P. Dismukes, "Thermal Conductivity of Ge-Si Alloys at High Temperatures", PHYSICAL REVIEW, Volume 125, January 1, 1962, pp 44-46.

In thermal diffusivity measurements, a cam-driven variable transformer is employed to generate a temperature perturbation at one end of a test specimen which has an ambient, "background" temperature controlled independently by a separate fixed-input heater. The resulting sinusoidal thermal wave which travels down the test specimen is analyzed by means of probes and thermocouples located at various points along its length. Thermal conductivity values are computed from direct measurements of the velocity and the attenuation experienced by the sinusoidal heat wave as it propagates down a specimen. The major advantage of the thermal diffusivity measurement technique is that thermal losses by radiation (which limit the accuracy of static high-temperature thermal conductivity measurements) effectively "cancel out" of the equations in this dynamic method of thermal conductivity measurement. Since heat capacity measurements may be made to a high order of accuracy by conventional techniques, the thermal diffusivity method provides a highly sophisticated and reliable method of thermal conductivity measurement.

According to Figure 4, an appropriate mean value for the thermal conductivity of the SiGe alloys employed in TRECOM application is 0.0425 watt/cm-^{o}C over the range 37^{o}C to 1000^{o}C. This figure has been employed in computations of thermal input summarized in Table 1.

2. Measured Electrical Output, Measured Thermal Input

Figure 28 shows schematic details of an apparatus employed to obtain direct estimates of the conversion efficiency of thermocouples of the all-SiGe construction. Although efficiency estimates obtained with this equipment are considered to be less reliable than those of method 1, they are, nonetheless, of interest in that they are based entirely upon independent measurements of operating thermocouples. It is believed that values obtained by this method are accurate $\pm$ 10 per cent.

As may be noted in Figure 28, the thermocouple under test is soldered onto water-cooled, pure nickel blocks of the same cross-section as the arms of the thermocouple under test to permit simultaneous measurements of electrical and thermal performance. Estimates of the heat flux through an operating thermocouple are based on the temperature difference observed across nickel blocks, which are of known thermal conductivity. For this "comparison method" to be effective, however, it is necessary that heat losses from the body of an operating thermo-

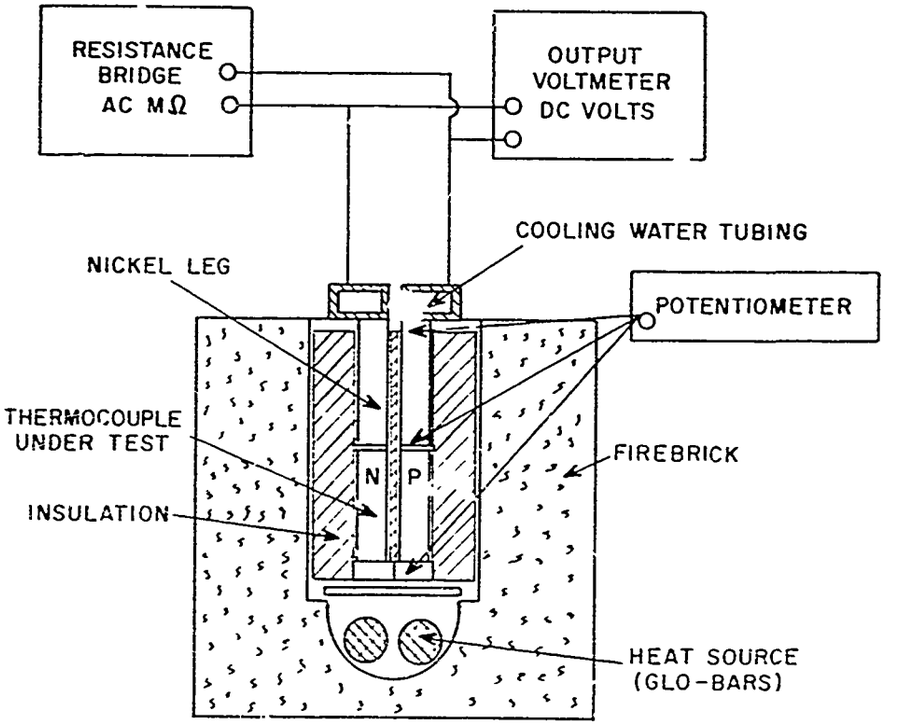

Figure 28. Test Equipment Arrangement for Thermocouple Efficiency Measurement.

couple be minimized. This condition is approximately achieved for operating thermocouples by surrounding them with insulation to which heat is also supplied. Because of the uncertain heat balance in this system, the absolute accuracy of thermal measurements is estimated as ± 10 per cent. Direct comparisons show thermal inputs estimated by this method were, in general, 5 per cent more pessimistic than those obtained by method 1.

3. Computed Performance

A third method of estimating the efficiency performance of the all-SiGe thermocouple is to apply the results of the analogue efficiency analysis and to compute the performance from the known thermoelectric properties of the SiGe alloys employed (Figure 3). According to this analysis, 92 per cent of theoretical materials efficiency is recovered by thermocouples of the type employed in the TRECOM modules. Comparisons of this estimate with more direct efficiency estimates provide a direct test of the analogue analysis.

Table 3 summarizes the results of the three methods of efficiency analysis based on a hot-junction temperature of 1000°C (1832°F). Assuming an inlet cooling water temperature of 15°C (59°F), according to Table 2, the cold-junction temperature will be 22°C higher, resulting in a cold-junction temperature of 37°C (99°F).

Computations of efficiency have been based, in the standard manner, upon the determination of an effective thermocouple figure-of-merit:

$$Z_{eff} = \frac{S^2}{\rho K} = \frac{\left[\frac{E_{oc}}{T_H - T_C}\right]^2}{R \cdot \left[\frac{Q_c}{T_H - T_C}\right]} \qquad (8a)$$

where

Z_{eff} is the effective thermocouple figure-of-merit ($^{o}C^{-1}$)
E_{oc} is the open-circuit voltage
T_H is the hot-junction temperature (1000°C)
T_C is the cold-junction temperature (37°C)
R is the open-circuit resistance of the operating thermocouple (ohm)
Q_c is the heat conducted through the thermocouple (watt)

The efficiency is then determined from Equation 15:

$$\epsilon_{max} = \left[\frac{T_H - T_C}{T_H}\right] \cdot \left[\frac{M - 1}{M + T_C/T_H}\right] \qquad (15)$$

in which

$$M = (1 + Z_{eff}\, T_{avg})^{1/2} \qquad (14)$$

where

$$T_{avg} = \frac{T_H + T_C}{2} \qquad (12)$$

It will be noted from Table 3 that the performance of the all-SiGe thermocouple is less than that which is theoretically available from the SiGe thermoelectric material itself, as was indicated in the analogue analysis of performance. Based on method 1, which is considered to provide the most reliable estimate of efficiency, it is concluded that the efficiency of the all-SiGe thermocouple is 9.8 per cent at a hot-junction temperature of 1000°C.

TABLE 3

EFFICIENCY ESTIMATES OF THE TRECOM ALL-SiGe THERMOCOUPLE
AT A HOT-JUNCTION TEMPERATURE OF 1000°C
BY THREE DIFFERENT METHODS (SEE TEXT)

		Method 1	Method 2	Method 3	Theoretical Matl. Perform.
T_H	(°C)	1000°C	1000°C	1000°C	1000°C
T_C	(°C)	37°C	37°C	37°C	37°C
E_{oc}	(volt)	0.410	0.410	0.415*	0.439*
R	(milliohm)	18.6	18.6	18.9*	19.2*
Q_c	(watt)	17.3*	17.9	17.3*	17.3*
Z_{eff}	($°C^{-1} \times 10^3$)	0.542	0.524	0.547	0.603
ϵ_{max}**	(per cent)	9.80	9.54	9.84	10.7
Power Output	(watts)	2.24	2.24	2.25	2.48

* Computed values

** At optimum load (Equation 13)

The efficiency of the all-SiGe thermocouple is essentially a linear function of hot-junction temperature. In excellent approximation, the efficiency increases 1 per cent for each 100°C increase in hot-junction temperature. Thus, according to Table 3, 10.0 per cent conversion efficiency is obtained at 1020°C. This temperature is within the temperature range of the TRECOM tests. Therefore, it may be concluded that, according to the most reliable data available, long-term thermocouple efficiencies of 10.0 per cent have been demonstrated with SiGe devices operating in air at 1020°C. To RCA's knowledge, this represents the highest stable efficiency yet obtained from a single thermoelectric material.

SECTION IV

30-KW THERMOELECTRIC CONVERTER DESIGN STUDY*

INTRODUCTION

The power conversion equations for a 30-KW thermoelectric converter employing SiGe elements have been solved under a wide range of values for hot-junction temperature. Assuming the use of a regenerated fossil fuel burner, an optimizing curve has been plotted which shows that an extremely useful configuration for a thermoelectric converter is one employing all-SiGe thermocouples 0.90 inch long and a hot-junction temperature of 1000°C. The solution of the basic equations indicate that it is probable that a 30-KW thermoelectric converter can be designed to occupy approximately 12 cubic feet and weigh about 1000 pounds. Such a generator would be capable of supplying power to an electric motor to provide a power source for a silent-boat design. The weight of the motor and associated gearing equipment would amount to a further 1500 pounds, resulting in a total system weight of 2500 pounds.

THERMOCOUPLE GEOMETRY

In order to determine size and performance characteristics of a 30-KW silent-boat power source, computations have been based on thermocouples of the all-SiGe construction whose life performance has been documented in previous sections of this report. Although generator optimizations employing other criteria than maximum thermocouple efficiency might also be usefully pursued, the lack of an analytical expression describing the performance of couples in this configuration makes this procedure very cumbersome and is outside the scope of this contract. The couple illustrated in Figure 15 is taken to represent an optimum couple within the present state of the art.

The performance of such a couple has been measured to be 96 per cent of the calculated performance of a couple having elements 0.90 inch long. With these experimentally determined facts as a basis, it is possible to further explore the performance of an overall system as a function of the temperature at the hot junction. It is clear that there will be an optimum operating temperature since combustion efficiency will decrease with temperature while

* Prepared by Applied Research, Defense Electronic Products, Camden, N.J.

converter efficiency increases. At some temperature, a maximum overall efficiency will occur.

HEAT TRANSFER REQUIREMENTS FOR A RADIANT HEAT SOURCE

The couple configuration considered in this section allows little flexibility in the design of the heat transfer surfaces of both the burner and hot junctions if close packing is employed. The use of extended surfaces is precluded by weight and volume requirements, and packing density cannot exceed 58 per cent. The thermal requirements associated with a given hot-junction temperature fix a heat absorption rate at the hot junctions which in turn determines the heat source temperature. As the temperature level rises, the mode of heat transfer becomes increasingly more radiative and less convective; as an example, consider the case of the hot junctions operating at 1275°K or 1002°C. The power per unit area at a hot junction of 1275°K and cold junction at 375°K is 2.3 watts/cm^2. Taking the thermoelectric conversion efficiency at .10, the heat flux rate at the hot junction must be 23 watts per all-SiGe thermocouple. Since the packing density is .58, the heat flux rate at the hot surface is 42,300 BTU/hr-ft^2.

It is possible to determine the temperature of a heat source using both radiative and convective heat transfer. Using a source temperature of 2820 °R (1294°C) and absorber temperature of 2300°R (1002°C), a typical estimate of the radiative heat transfer can be calculated from the expression

$$Q_R = \sigma \epsilon_R \cdot \epsilon_A \left[\frac{A_1}{A_2}\right]\left[T_R'^4 - T_A'^4\right] \qquad (19)$$

where

- σ is the Stefan Boltzmann Constant ($.171 \times 10^{-8}$)
- ϵ_R is the emissivity of radiator (0.95)
- ϵ_A is the emissivity of absorber (0.95)
- A_1/A_2 is the radiator-absorber area ratio (0.675)
- T_R is the radiator temperature (°R)
- T_A is the absorber temperature (°R)

Substituting numerical values in Equation 19:

$$Q_R = 0.171 \times 10^{-8} \times 0.95 \times 0.95 \times 0.675 \left[(2820)^4 - (2300)^4\right]$$

$$Q_R = 0.104\ (635000 - 279000)$$

$$Q_R = 37100\ \text{BTU/hr-ft}^2$$

The convective heat transfer rate which occurs is described by the expression

$$Q_C = h A \Delta T \qquad (20)$$

where

h is the film heat transfer coefficient (10 BTU/hr-ft^2 - $^\circ$R).

It is customary in heat computations to take the radiator temperature as the average gas temperature in the convective process. Thus

$$Q_C = 10 \times 1 \times (2820 - 2300)$$

$$Q_C = 5200\ \text{BTU/hr-ft}^2$$

The total heat transfer rate (Q_t) is $Q_R + Q_C$. Therefore

$$Q_t = 37100 + 5200$$

$$Q_t = 43200\ \text{BTU/hr-ft}^2$$

This fixes 2820°R (1294°C) as the minimum heat source temperature for hot junctions at 1275°K (1002°C), since emissivity coefficients of 0.95 are unlikely to be exceeded. It is interesting to note that .86 of the heat transfer (37100/43200) is by radiation and that convective heat transfer is no. appreciable at these temperatures. Figure 29 shows the heat source temperature appropriate to a range of hot-junction temperatures.

BURNER AVAILABILITY

Evaluations of burners suitable for a thermoelectric heat source indicated that a radiative type burner, operating at a minimum source temperature of 2360°F

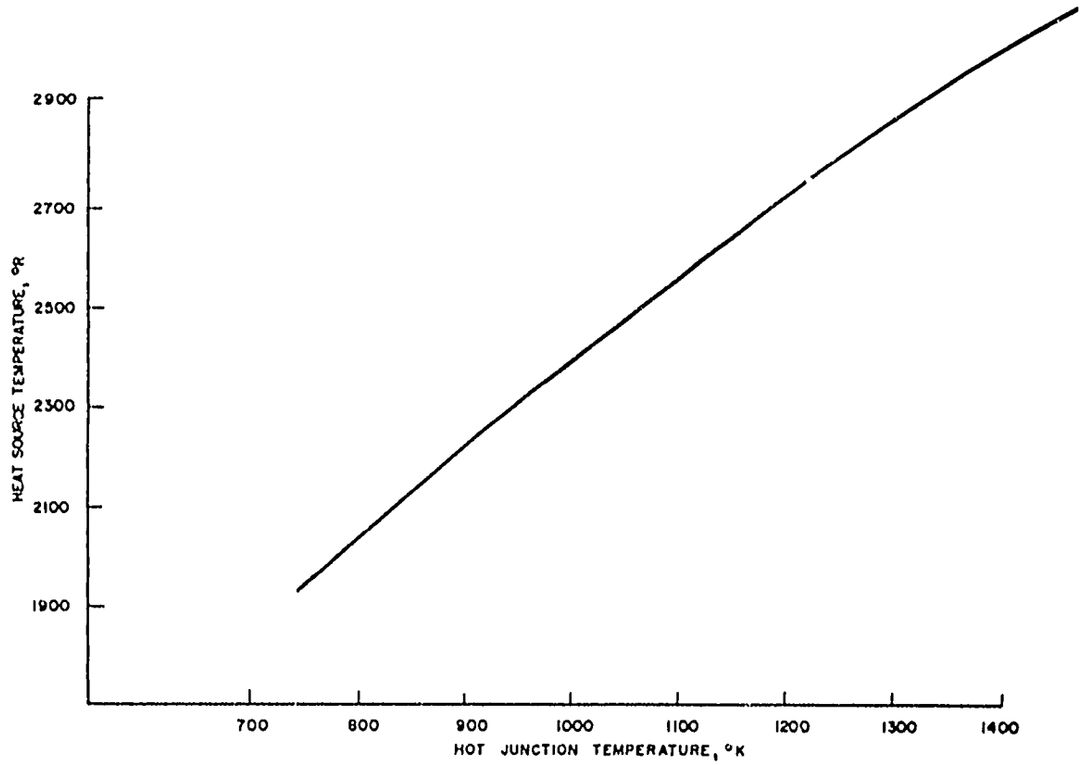

Figure 29. Heat Source Temperature as a Function of Hot Junction Temperature.

(1294°C), was required. More specifically, the burner must be capable of supplying 42300 BTU/hr-ft^2 to a surface at 1840°F (1002°C). RCA has been in contact with specialists in these fields, and the general consensus is that efficient devices releasing heat at this rate are entirely feasible. In certain of these contacts, the vendors indicate that laboratory models of burners were available for immediate delivery, and would be capable of operating on diesel oil or other suitable fossil fuel. It is anticipated, however, that further development activity would be required to establish the efficiency and the life performance of such burners, as well as to integrate commercially available units into a compact thermoelectric device.

BURNER EFFICIENCY WITHOUT REGENERATION

Increases in the thermoelectric converter efficiency accompanied by increased hot-junction temperature must be carefully weighed against burner efficiency. Unless provisions are made to utilize the energy in exhaust gases through regeneration, burner efficiency will decrease rapidly with increased hot-junction temperature, since exhaust gas temperature must increase with hot-junction temperature. At lower temperatures where the convective heat transfer is an appreciable portion of the total, the exhaust gases are much cooler than the radiator temperature. However, at the higher temperatures the exhaust gases leave at very close to the radiator temperature. Figure 30 indicates the magnitude of these effects and gives combustion efficiency as a function of exhaust gas temperature for burning octane (C_8H_{18}) with 10 per cent excess air. Figure 31 presents these combustion efficiency data as a function of hot-junction temperature of thermoelements such as used in the RCA design. Burner efficiencies comparable to those shown in Figure 31 can be closely approached in actual devices without regeneration. Improved burner efficiency results if regeneration is employed.

REGENERATION DESIGN

The Carnot Theorem states that all heat engines have an upper limit to their thermal efficiency given by the expression

$$\eta = \frac{T_H - T_C}{T_H} \qquad (21)$$

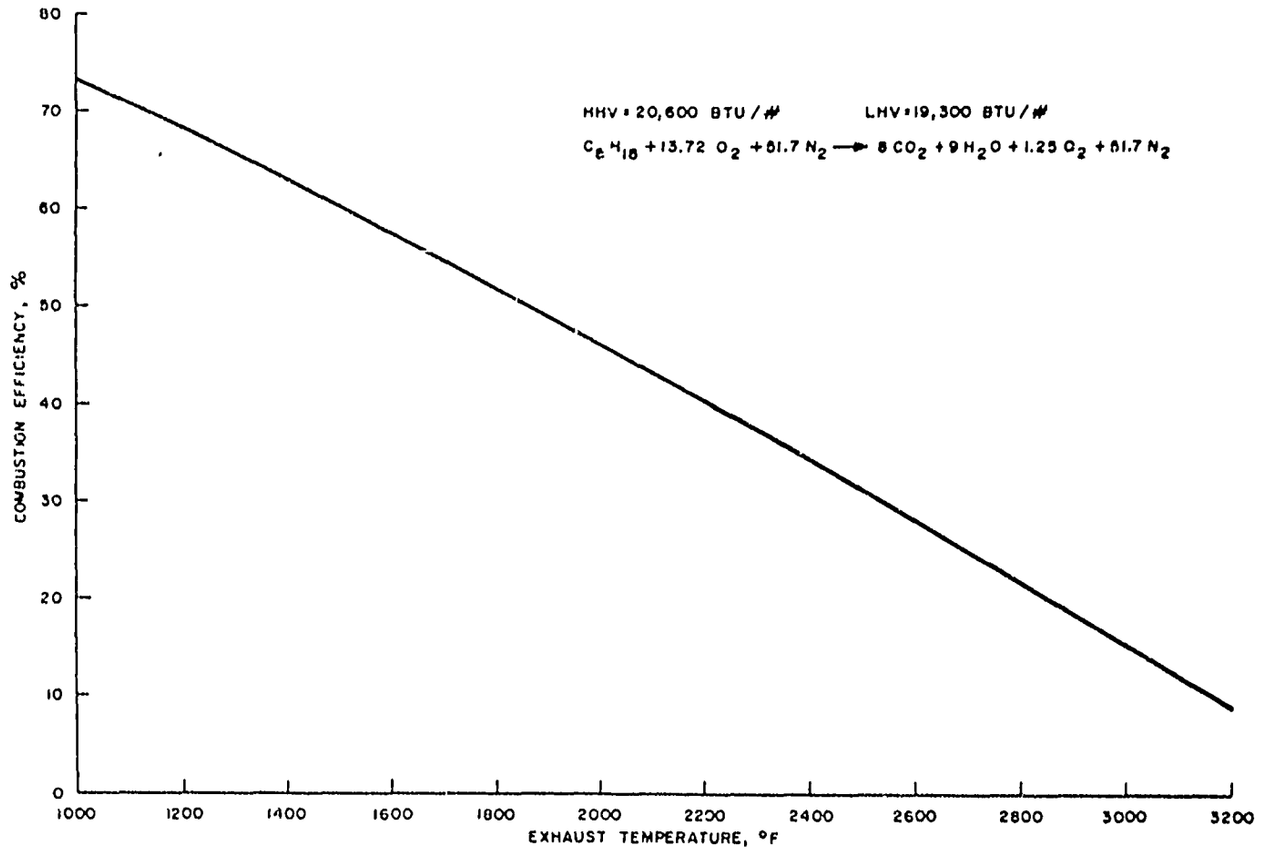

Figure 30. Combustion of C_8H_{18} with Ten Per Cent Excess Air.

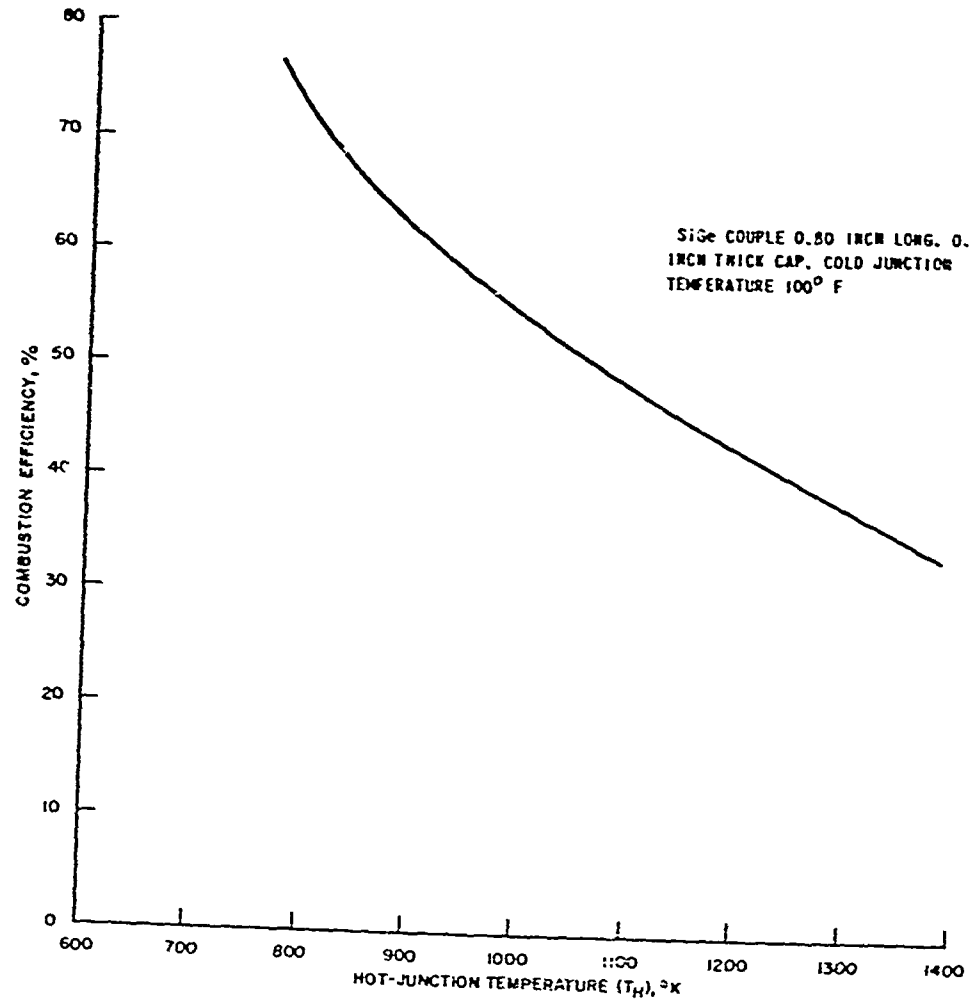

Figure 31. Combustion Efficiency as a Function of Hot Junction Temperature.

where

η_i is the Carnot efficiency.

T_H, T_C are the highest and the lowest temperature in the system, respectively.

Consider the thermodynamic system formed by the hot gases at T_H from the combustion chamber and the hot junctions of the thermoelectric modules at T_C. For this system, the hot-junction temperature sets the temperature at which energy becomes unavailable. In fact, because both the extended surface area and the film coefficient have finite values, the threshold temperature for availability of energy is above the hot-junction temperature. As indicated in Figure 31, this effect causes increases in the thermoelectric efficiency resulting from increased hot-junction temperature to be largely offset by reduced burner efficiency.

Significant improvements in burner efficiency may be gained, however, by use of a regenerator or economizer. Such a device recovers a part of the energy in the exhaust gases by heating the incoming air to some temperature between the ambient temperature and the hot gas temperature. The air is finally heated to T_H by chemical reaction with the fuel. An ideal regenerator would heat the incoming air to the temperature of the exhaust gases and the reaction of the fuel would only have to supply the energy absorbed through the thermopiles. The less ideal a regenerator becomes, the more chemical energy is required to heat the incoming air, thereby making the process less efficient.

It is clear that the use of regenerator should cause the thermoelectric generator system to increase its performance so as to approach thermocouple efficiency as a limit. There are several factors which preclude the possibility of an ideal regenerator. The first is the frictional losses which occur when air is moved through a heat exchanger. These losses must be made up using a fan which will draw on the electrical power being generated so that regeneration will occur only as long as the increased thermal performance exceeds the power required of the fan. The second precluding factor arises because the increased requirement for heat transfer area causes the preheated air temperature to approach that of the exhaust gas (diminishing ΔT). To approach the ideal generator performance, the heat transfer area becomes unacceptably large.

Figure 32 shows a regenerator which occupies the space above each burner; it is 4 inches by 4 inches in cross-section and can be made as tall as is

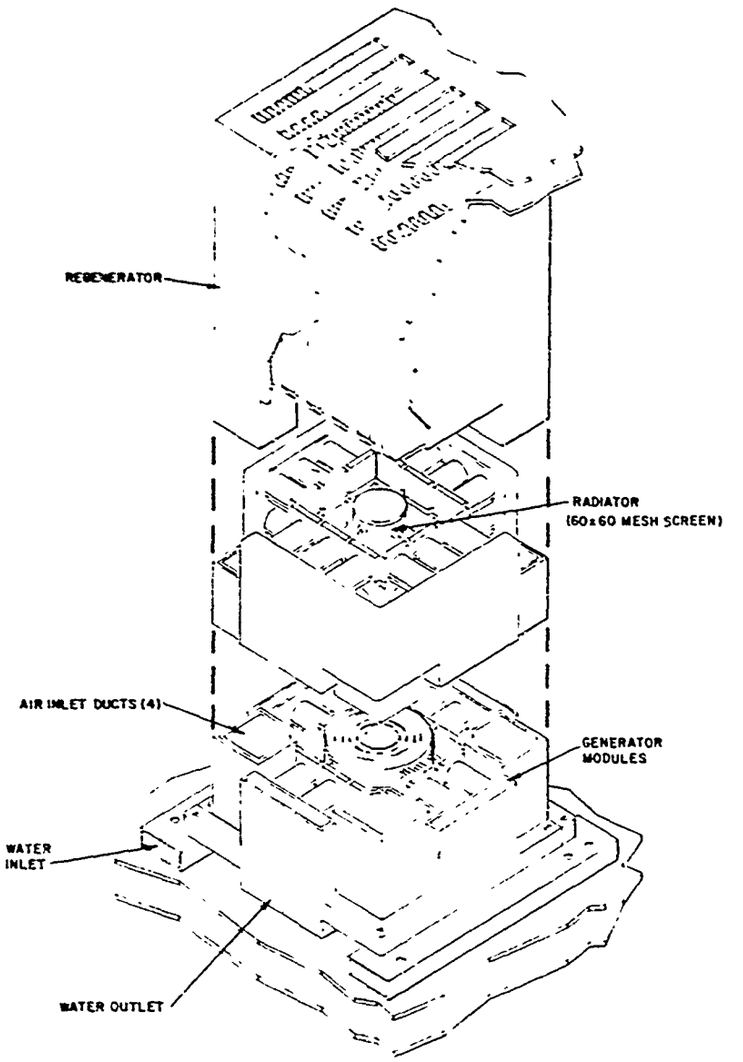

Figure 32. Typical Exploded View of Overall Assembly.

necessary. It is constructed of stainless steel fins 0.009 inch thick and 0.310 inch high; there are 12.5 fins per inch. The regenerator is a counterflow heat exchanger with thirteen parallel flow passages, seven of which carry incoming air and six of which carry exhaust gas. Heat is transferred from the exhaust gases to the incoming air in the adjacent passages. Heat exchangers of this type have been fabricated for operation up to 2700°K, and empirical data on their performance are shown in Figure 33. This curve gives heat transfer coefficient (plotted as Coburn (j) factor) and pressure drop (plotted as Fanning friction factor f) as a function of G/μ, which is the Reynolds number without the characteristic dimension.

Using this heat exchanger with a flow length of 4 inches and assembled as shown in Figure 32, performance and volume curves are determined (Figure 34). The improvement in performance which results with the use of regenerator is produced with a relatively modest expenditure of weight, volume, and fan power. Peak performance occurs at a hot-junction temperature of approximately 1275°K, where the overall conversion efficiency is 6.3 per cent and the volume of the generator is about 11.7 cubic feet. At this point, it is interesting to note that heat is being recovered at the rate of 465,000 BTU/hr at the expenditure of 750 watts of fan power. Since the thermocouple have a conversion efficiency of 10.0 per cent at this temperature, the recovered heat can be converted to 13.6 kilowatts of electrical power. An 85 per cent increase in efficiency is possible compared to the unregenerated design. Further improvement can be made in performance by making the regenerator larger since, if weight and volume requirements are not of primary importance from an efficiency point of view, a net increase in performance results until the increased fan power exceeds the recovered thermal energy.

GENERATOR SYSTEM CHARACTERISTICS

General Construction

The proposed design is modular in construction, each module consisting of four water jackets onto which are bonded 81 silicon-germanium thermocouples. The modules are bound together in a square or rectangular array by inlet and outlet water manifolds. The water jackets of each module are arranged so that the hot junctions of the thermocouples form a square passage into which is placed a radiator heat source. A regenerator is placed in the stack of each subassembly with provision for bringing preheated air into a hot air plenum at the base of each combustion chamber. The regenerators are manifolded on the inlet air side so that a single blower can service the entire generator assembly.

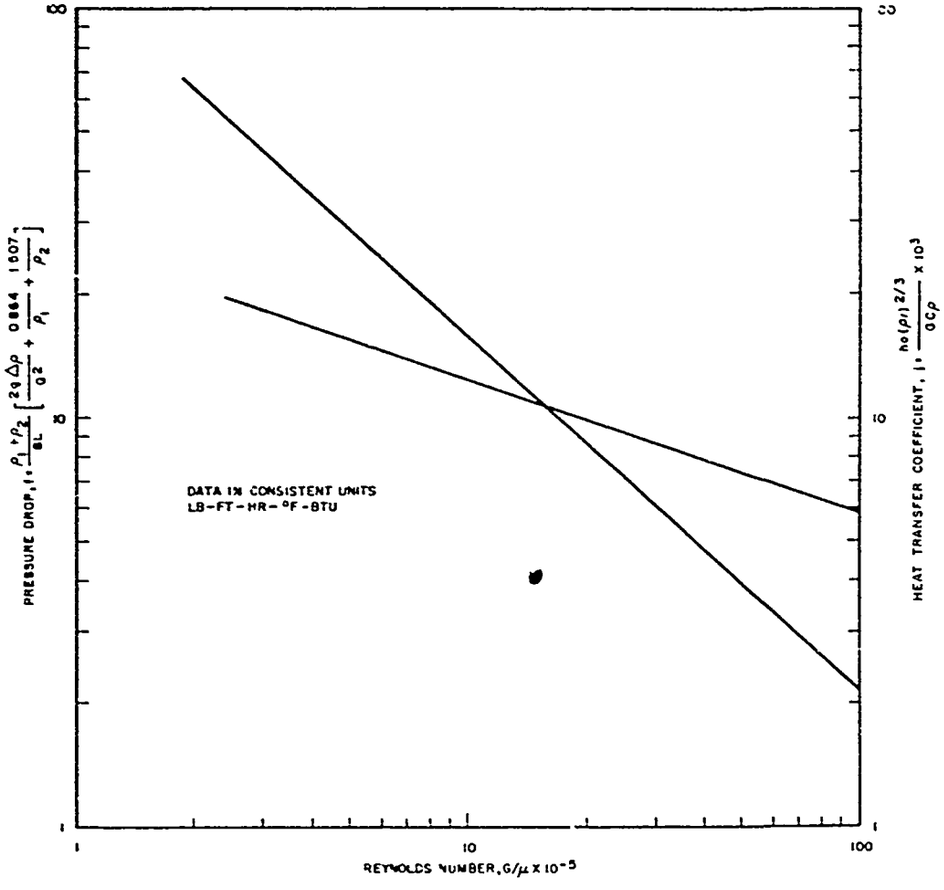

Figure 33. Correlated Heat Transfer and Flow Friction Data for Brazed Fin Surface.

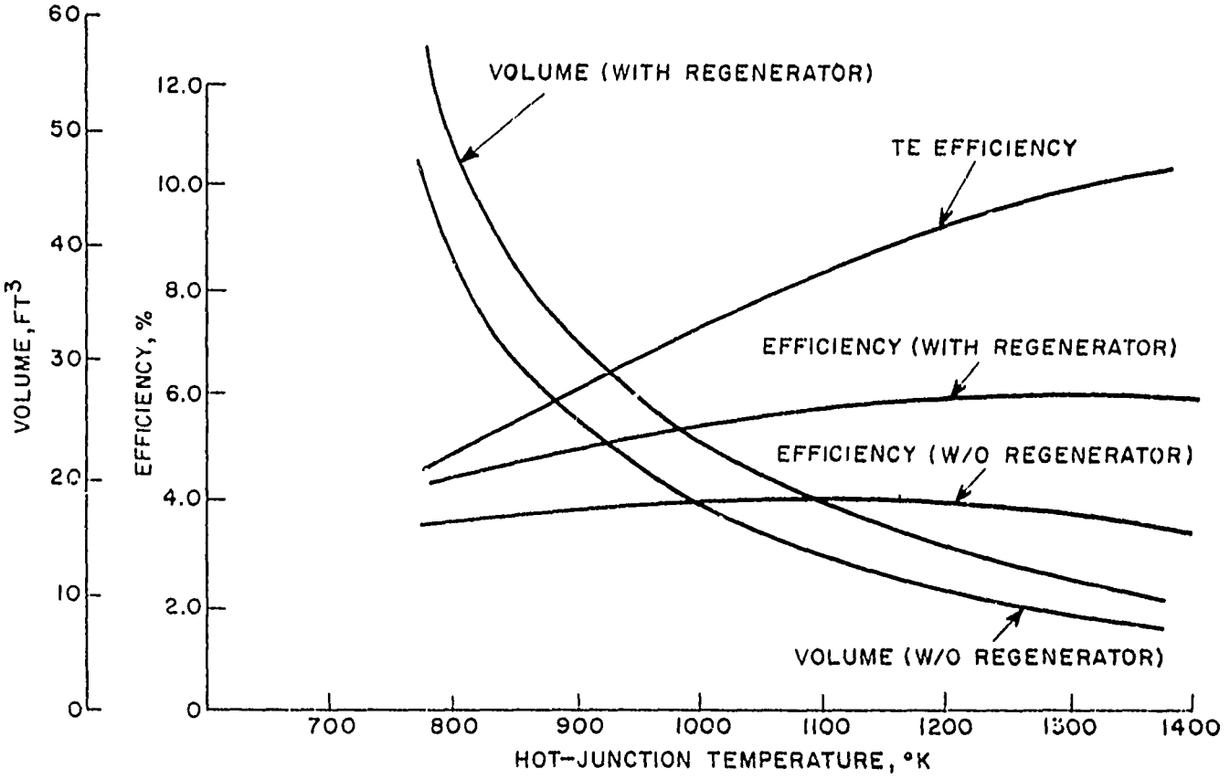

Figure 34. Heat Exchanger Performance Curves.

Thermocouple Design

The thermocouple configuration shown in Figure 15 has an electrical output of 2.3 watts with a conversion efficiency of 10 per cent when operating at a hot-junction temperature of 1000°C. The voltage output is 0.225 volt with a current drain of approximately 10 amperes; 13,000 couples are necessary to produce 30 kilowatts of electrical power.

Generator Module Design

The basic generator module (Figure 35) consists of a metal water jacket made from a 1/8 serrated fin, 0.220 inch high and containing 10 fpi. The flow rate through each water jacket is 0.16 GPM, which results in a 100°F water temperature rise in the heat sink. Each module contains 81 SiGe thermocouples which have an electrical output of 18 volts and 10 amperes at design conditions.

Generator Subassembly

A generator subassembly consists of four generator modules and a radiation heat source. The heat source must radiate at 2360°F and have a useful heat flux of 40,000 BTU/hr. Each generator subassembly is self-contained with an electrical capacity of 720 watts. Fuel consumption of each subassembly is approximately 2 pounds per hour.

Regenerator

Preheating of the incoming air will be accomplished by abstracting energy from the exhaust gases in a stainless steel heat exchanger (Figure 32). The heat exchanger is of the counter-flow type, with the active heat exchange surface occupying a space 4 x 4 x 4 inches. Distribution plenums cause the unit to grow in size to 4 x 4 x 5 1/2 inches. The heated air is carried to the combustion chamber through square ducts located in diagonally opposite corners of the generator subassembly.

Overall Generator

The generator assembly has an electrical output of 30,000 watts of d-c power (Figure 36). It occupies a space 31 x 31 x 20 inches, or 11 cubic feet. Total weight of the generator is approximately 1000 pounds. The fuel consumption rate is approximately 90 pounds per hour of diesel oil or other logistically available fossil fuel. The air supply must deliver 430 CFM against a static pressure head of 2 inches of water. The heat sink water flow requirements

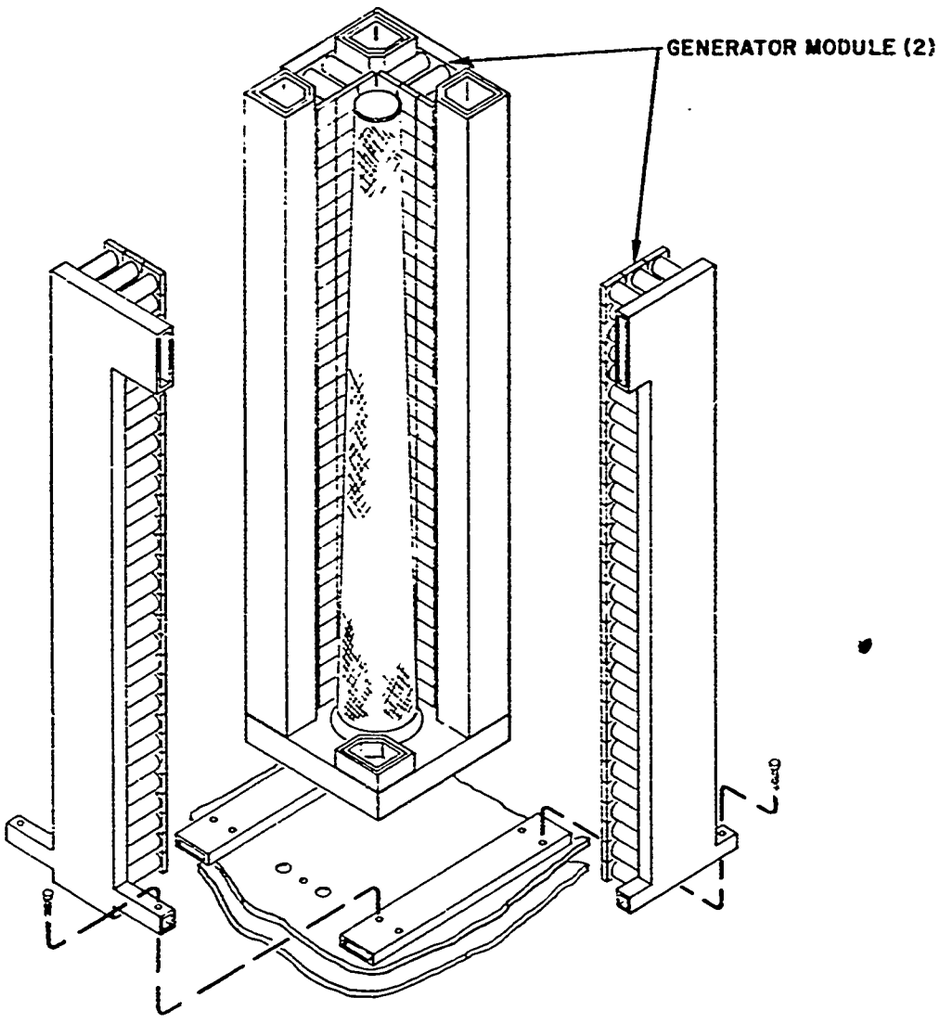

Figure 35. Generator Subassembly.

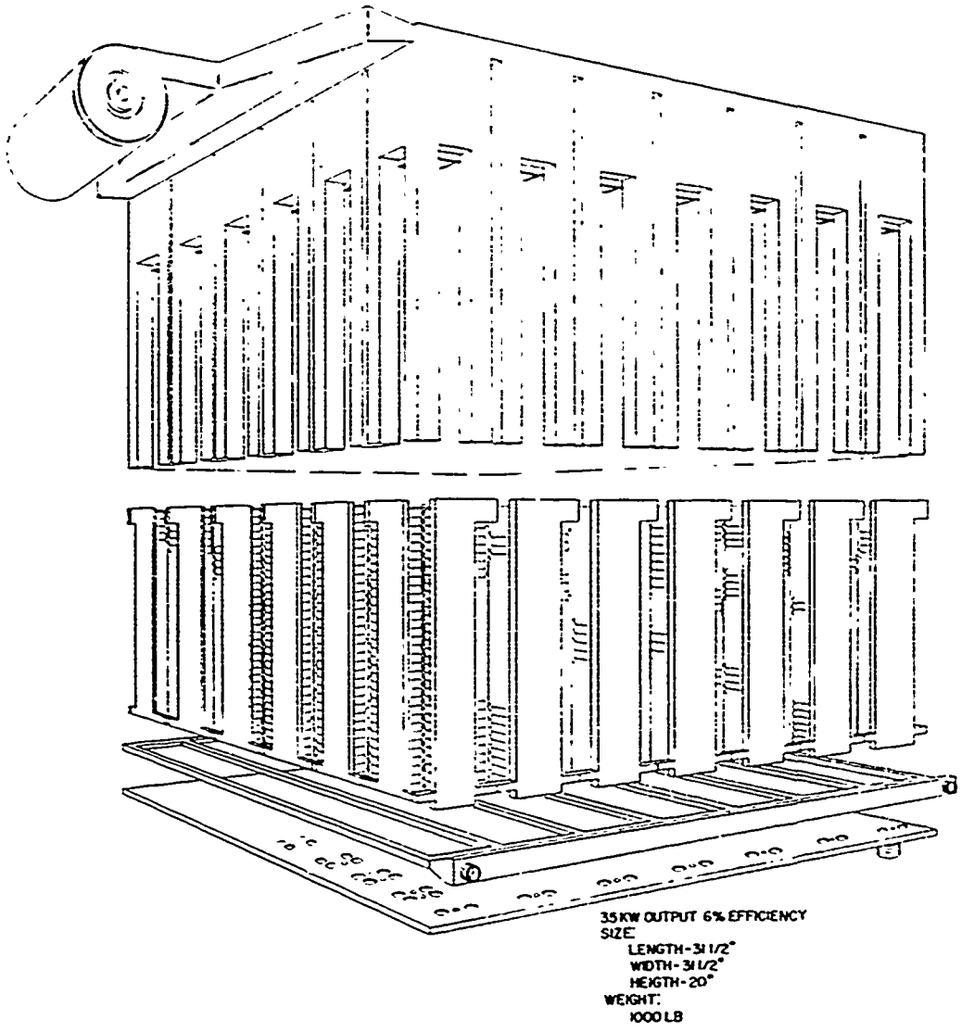

Figure 36. Thermoelectric Generator Assembly.

calls for 30 GPM against a 5-psi pressure drop.

The power from this generator can be made available in multiples of 10 amperes, so that 200 volts and 150 amperes (30 kilowatts) is a possible combination.

CONCLUSION

While it is clear that a 30-KW generator can be fabricated using SiGe thermoelements, it is equally obvious that real fabrication problems exist as compactness and high efficiency are pursued by increasing operating temperatures. The heat source requirements spelled out in this report are such that the limitations imposed by material properties must be considered. While thermoelectric materials are available to operate as specified in this report and regenerators have been built and tested to the requirements used, a considerable amount of effort is still required to develop a complete prototype unit conforming to the requirements dictated by this application. It is in this direction that further development could be usefully applied.

APPENDIX

THE OXIDATION AND PROTECTION OF TUNGSTEN AT ELEVATED TEMPERATURES

INTRODUCTION

One of the areas of study in this contract was the performance of SiGe thermocouples with tungsten metal parts at the hot junction. This approach was eventually abandoned because the tungsten could not be satisfactorily protected from oxidation. Nevertheless, since work in this area was performed during the TRECOM study, the results of a literature survey on the oxidation of tungsten are included in this Appendix for completeness. The recommended thermocouple design for TRECOM applications contains no tungsten parts at the hot junction, and so this literature survey is not applicable to the present thermocouple design.

Because tungsten oxidizes catastrophically in air in the temperature range of TRECOM device applications, it was clear at the start of the present program that if thermocouples with a tungsten hot-junction construction were to be employed, then protective coatings would be required for the tungsten metal parts. Accordingly, a literature search was made to evaluate possible protective coating systems for tungsten.

On the whole, the results of the present literature survey were less promising than might have been anticipated. Little concrete guidance was available, and the literature suggested that development of stable protective coatings for tungsten at temperatures higher than 800°C is a major problem. As a direct result, the tungsten hot-junction thermocouple construction was ultimately abandoned (mainly because of a lack of suitable protective coatings for air operation of tungsten above 750°C) in favor of the all-SiGe construction, in which oxidation problems were automatically resolved. The findings of this literature search support this decision, for they clearly indicate that the protection of tungsten for air operation is clearly not resolved by present-day technology.

In the past, tungsten metal has been primarily a material to be used for lamps and electron tubes. The properties which make its use as incandescent filaments possible are its high melting point (3410°C) and related strength properties at extremely high temperatures. In these applications, great care has been taken to provide a carefully purified atmosphere to avoid oxidation.

More recently, other properties, such as the low coefficient of thermal expansion, have made tungsten an attractive metal to be used at relatively low temperatures. In spite of commercial needs for a low-expansion metal which will operate with a protective atmosphere at elevated temperature, the technology of tungsten has as yet been unable to cope with stringent oxidation problems involved in the use of the metal at high temperatures. However, a considerable understanding of the complexity of the oxidation of tungsten has been developed. Use of this knowledge has aided research in the evaluation of protection methods, which are satisfactory for a few specialized applications.

OXIDATION RATES OF TUNGSTEN

Tungsten, like most refractory metals, lacks resistance to oxidation at high temperatures. The tungsten oxides formed are not protective because of their thermal instability, low melting point, and high volatility. In view of the disagreements in the literature concerning the oxidation behavior of tungsten, the general picture is still incomplete. The discussion is simplified by describing the oxidation behavior in three temperature ranges.

At temperatures below 600°C, tungsten is nearly inert. Tungsten resists attack by oxygen as well as by many acids and bases at room temperature, and does not tarnish or oxidize appreciably up to 300°C. Above this temperature, oxide films of various colors form and grow progressively thicker with increasing time and/or temperature. These films consist of WO initially and gradually oxidize to form higher oxides and eventually WO_3 at the surface. The oxidation reactions may be condensed and expressed by the equation

$$2W + 3O_2 \longrightarrow 2WO_3$$

which results in a weight gain. In the temperature range 300 to 600°C, the tungsten oxide is quite protective since its formation is diffusion-controlled and follows a parabolic rate law.

In the temperature range of approximately 600 to 1200°C, the oxidation of tungsten becomes progressively more rapid. It is generally recognized that the oxidation products consist of a loose yellow WO_3 outer layer and a thin intermediate layer of the lower tungsten oxides (WO, W_2O_3, WO_2, and W_2O_5 are the most probable). As indicated in Figure 37, discontinuities in some of the physical properties of WO_3 in the range 700° to 900°C indicate the existence of an allotropic transformation which involves a volume change, causing the oxide to crack and scale. Resulting defects in the oxide

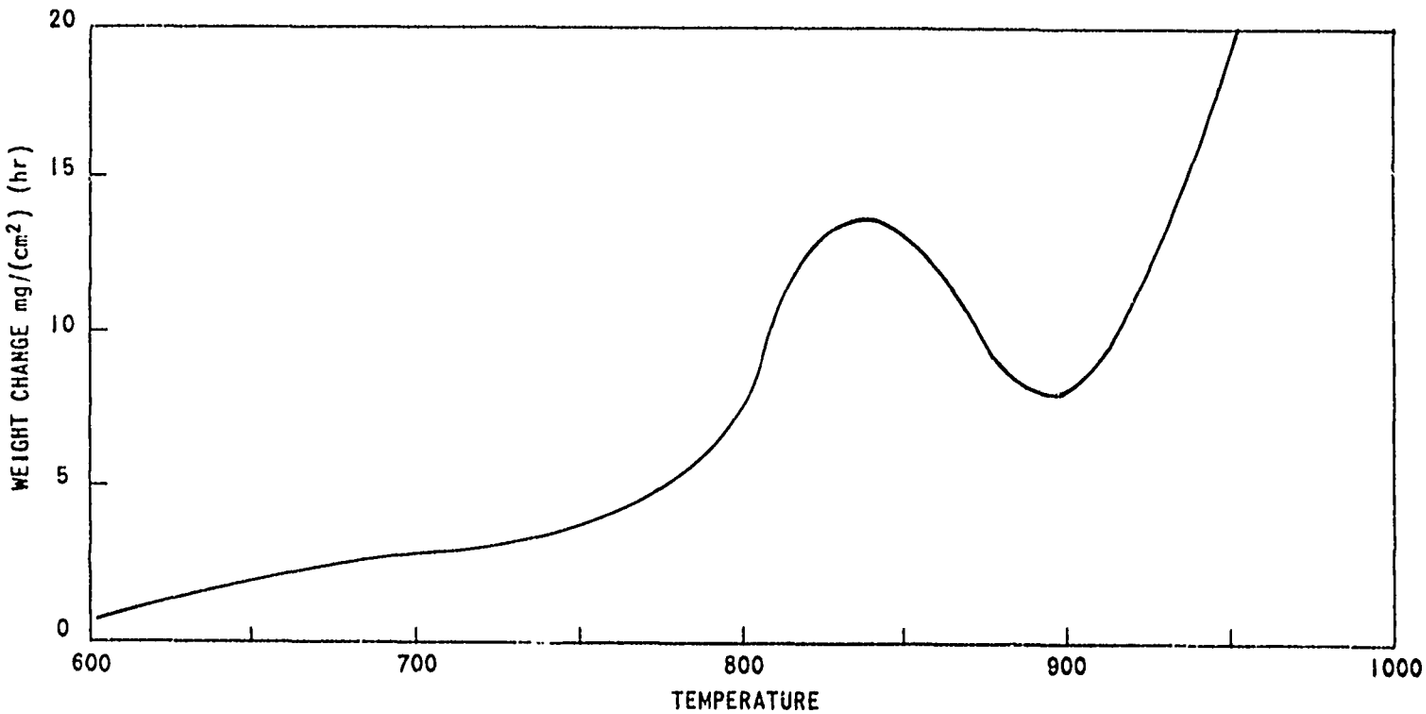

Figure 37. *Observed Rate of Oxidation of Tungsten in Air as a Function of Temperature Between 600 and 950 °C, Showing the Allotropic Transformation Between 850 and 900 °C.*

are not self-healing, thus allowing oxygen to penetrate to the bare metal substrate. These phenomena cause the oxidation rate through the porous oxide to depart from the "protective oxide" parabolical rate laws and ultimately approach a nonprotective linear law. In the temperature range of 600°C to 1200°C, tungsten has more resistance to oxidation than molybdenum, but is less resistant than columbium and tantalum. As an additional comparison, the oxidation rates of tungsten and iron in dry air at 1000°C are similar.

Above 1200°C, tungsten oxidizes catastrophically because of oxide removal by melting and vaporization of WO_3. The presence of water vapor greatly accelerates the evaporation of WO_3; in fact, in an atmosphere containing 30 per cent water vapor, the volatility of WO_3 is increased by two orders of magnitude at temperatures above 1000°C. The lower oxides of tungsten are similarly affected by water vapor but to a lesser extent.

PROTECTIVE SYSTEMS FOR TUNGSTEN

There exists extensive literature on protective coating systems for tungsten.[1-22] Much of the literature appears to result from the needs of the jet engine and rocket industries for short-term operational requirements at temperatures in excess of 1200°C. In these instances, satisfactory oxidation protection may be defined as several hours of operation with permissible surface erosions of many thousandths of an inch. In no case does any protective coating system appear to offer indefinite protection at elevated temperatures.

Relatively little information is available in the literature concerning the oxidation protection of tungsten at temperatures below 1100°C. Interestingly, many of the more promising coatings which are useful at elevated temperatures do not offer protection at temperatures in the range 700°C to 1200°C. A dramatic instance of this effect is the "pest" phenomenon which limits the use of many intermetallic compounds; for example, WSi_2. At high temperatures, a viscous "self-healing" layer of silica forms on the surface and protects the substrate. This layer, however, is not self-healing at lower temperatures, and oxygen penetration is rapid.

Examination of the application techniques employed for the protective coatings described in the literature shows that high application temperatures are the general rule. It may be noted that excessive application temperatures will eliminate many of the possible protective coating systems for tungsten-SiGe systems since the melting point of the SiGe alloy cannot be exceeded. A

further point to be considered is that many of the protective coating systems for tungsten may react excessively with SiGe alloys at high temperature and, hence, may not be compatible with a tungsten-SiGe thermocouple system.

The wide variety of protective measures for tungsten which are now being pursued actively in current researches indicates more clearly than the technical details in the various articles that the problem of tungsten oxidation is far from resolved. Among the areas of major current interest are:

A. Mechanical Cladding

This technique is one in which a coating of an oxidation resistance material is mechanically applied to the substrate by rolling, hammering, etc. It is obvious that the substrate must be of a reasonable ductile material and very simple in shape.

B. Electro-Deposition

A wide variety of materials can be electroplated to form protective coatings. A popular choice is the platinum group which has good oxidation resistance and is compatible with both tungsten and silicon-germanium at the temperatures involved in this application.

Metals such as chromium can be deposited and then have the surface converted to the protective oxide. Two or more metals may be co-deposited and converted to a protective alloy or intermetallic compound. Metals and ceramics ($Cr + ZrO_2$) can also be co-deposited in order to have the ductility of the metal plus the protection of the oxide.

One major shortcoming of this method is that the deposits are apt to be porous as applied, and should be densified by firing at high temperatures, preferably above the melting point. A second shortcoming, in the case of chromium, is that the vapor pressure at 950°C is high enough to crack the protective oxide. This factor, for example, can limit the usefulness of chromium platings on tungsten.

C. High Temperature Spraying

1. Flame Spray: This process consists of introducing the material to be sprayed (in powder or wire form) into an oxyacetylene or oxyhydrogen flame where it is heated and expelled with some force. The maximum temperature obtainable by this process is approximately 2760°C. The

sprayed material strikes the surface being sprayed as either molten droplets or as hot semiplastic particles. A wide variety of metals, ceramics, or combinations of them can be sprayed by this process. There as been some success in the protection of molybdenum using a flame-sprayed $MoSi_2$ coating.

2. Plasma Jet: The plasma jet operates by using a high-intensity spark to heat a stream of gas to temperatures in excess of 11,000°C. The sprayed material, in powder form, is fed into the gas stream just ahead of the spark gap. It is then expelled as fine liquid droplets. Any powder material which does not decompose at high temperature can be sprayed by this method. The main advantages of this method over flame spraying are wider choice of materials and a more dense deposit. For example, a typical metal-metal oxide combination is 90 per cent dense by the flame spray process and 98 per cent dense using the plasma jet.

D. Enamels

Enamel coatings consist of ceramics or cermets in liquid or viscous suspension. They are dipped, sprayed, or brushed onto the surface, then fired at temperatures from 1050°C to 1650°C. The proprietary literature frequently does not specify detailed enamel analyses, but states that it is necessary to formulate specific compositions for each application. One important point which must be considered is that the enamels lack ductility and therefore must have a thermal expansion very close to that of the substrate.

E. Sealing Glass

There has been some limited success using a number of glasses. Both the vitreous and the devitrified glasses (Pyroceram type*) have been used with and without the addition of fillers. Here, as with the enamels, it is necessary to have a close thermal expansion match between the glass and the substrate.

F. Hot Dipping

Three main techniques are used in hot dipping. In the first, a low melting point metal or alloy is employed. The substrate is dipped into the molten material and withdrawn with a cladding or coating of the melt material.

---

* Trademark -- Corning Glass Works.

Aluminum and aluminum-silicon are the most commonly used materials. A .007-inch coating of Al-Si eutectic has protected tungsten up to 1680°C, even though this is far above the melting point of the coating. The reason is that diffusion into the tungsten takes place at these high operating temperatures, forming the higher melting alloy which is protective. However, it is believed that if this procedure were to be applied to tungsten-SiGe systems, the thermoelectric material would have to be protected because it would react with the molten bath.

A second technique is the diffusion of a high-temperature material, such as chromium or silicon, from a lower melting point alloy. Diffusion of chromium from a Cr-Sn alloy system has shown moderate success. Temperature control must be very accurate because the process is carried out close to the maximum allowable temperature for SiGe devices.

A third technique utilizes a liquid alloy which is super-cooled so that the higher temperature material precipitates from the solutions on the substrate. Chromium has been deposited by this method, but no oxidation data are available for such deposits.

G. Vapor Deposition

In the vapor deposition process, coating material is reduced or decomposed from a volatile compound onto a heated substrate. Many high melting metals, ceramics, and cermets can be deposited by this means. Materials which cannot be deposited directly may be formed by subsequent diffusion or oxidation of the as-deposited or co-deposited materials. The major shortcoming of this process for present applications is that the materials which would be most useful appear to require high substrate temperatures.

H. Pack Cementation

A coating may be formed through the diffusion of materials from a pack into a substrate using halides as the carrier. Extremely simple arrangements will produce coatings on complex shapes. This process also has the shortcoming that the temperatures required are high.

SUMMARY AND RECOMMENDATIONS

A survey of the literature has pointed out that there are many possible coating techniques. Adequate oxidation protection measures for tungsten are, however,

still poorly documented and understood. Because of the additional restrictions imposed by the requirements for protection of a tungsten-SiGe system, it is probable that long-term protection at temperatures higher than 700°C to 800°C may be difficult to achieve. It may be noted that no protective coating appears capable of indefinite life at temperatures higher than 800°C to 900°C.

Because of the complexity of the present application, it is impossible to confidently give specific recommendations; however, it is felt that the following techniques have the greatest possibility for success for air operation up to 800°C.

1. Electro-deposited chromium, substrate with alternate layers of nickel, rhodium, or platinum. These must be fired at a minimum of 1050°C for one-half hour to eliminate porosity and to diffuse the plated materials.

2. Sintered co-electro-deposited metal and ceramic coatings. A chromium-rich combination of chromium and ZrO_2 has been successfully used on both tungsten and molybdenum.

3. Flame-sprayed Al_2O_3 over chromium plate. The Al_2O_3 must be at least .010 inch thick in order to prevent the porosity from forming continuous openings from the surface to the substrate. This may, however, interfere with the heat transfer characteristics of thermocouples.

4. Metals in combination with ZrO_2 applied using the plasma jet have shown promise on all the refractory alloys. Chromium-15 per cent ZrO_2 has been very successful on tungsten. A diffusion treatment at 1050°C for one-half hour increases the adherence.

5. Enamels have shown success on all the refractory metals. At present, it is not possible to pick a particular composition compatible with tungsten and SiGe. It is anticipated, however, that the addition of chromium to the enamel and/or chromium plating the substrate will increase the adherence to tungsten by diffusing into the substrate during firing.

BIBLIOGRAPHY

1. Barth, V. D., "Oxidation of Tungsten", DMIC Report 155, July 17, 1961.

2. Barth, V. D., "Physical and Mechanical Properties of Tungsten and Tungsten Base Alloys", DMIC Report 127, OTS PB151084, March 15, 1960.

3. Bergeron, C. G., A. L. Friedberg, R. C. Anderson, V. E. Bradford, D. M. Maroney, R. W. Bohl, "Protective Coatings for Refractory Metals", WADC Technical Report 59-526, Part I, January 1960.

4. Bergeron, C. G., V. J. Tenery, A. L. Friedberg, "Reaction Studies of Ceramic-Coated Tungsten", J. Am. Ceram. Soc., Volume 44 (4), April 1961, pp. 156-160.

5. Bergeron, C. G., V. J. Tenery, A. L. Friedberg, D. M. Maroney, R. D. Shannon, "Protective Coatings for Refractory Metals", WADC Technical Report 56-526, Part II, August 1960.

6. Booker, J., R. M. Paine, A. J. Stonehouse, "The Investigation of Intermetallic Compounds for Very High Temperature Applications", WADD Technical Report 60-889.

7. Doan, D. V., "Oxidation Resistant Coatings for Molybdenum", WADD Technical Report 54-492.

8. Goetzel, C. G., P. Landler, "Refractory Coatings for Tungsten", WADD Technical Report 60-825, March 1961, ASTIA AD 258574.

9. Goetzel, C. G., P. S. Venkatesan, R. F. Bunshah, "Development of Protective Coatings for Refractory Metals", WADC Technical Report 59-405, February 1960.

10. Gulbransen, E. A., K. F. Andrew, J. Electrochem. Soc., Volume 107, 1960, p. 619.

11. Hansen, M., Constitution of Binary Alloys, McGraw-Hill, New York, 1958.

12. Huminik, J., Jr., "Investigation of Oxidation and Erosion Resistant Coatings on Molybdenum, Tantalum, and Tungsten", Summary Report under Contract DA36-034-ORD-3270 RD, March 6, 1961.

13. Kennedy, A. J., International Science and Technology, August 1962, p. 43.

14. Klopp, W. D., "Summary of the Fifth Meeting of the Refractory Composites Working Group", DMIC Report 167, March 12, 1962.

15. Krier, C. A., "Coatings for the Protection of Refractory Metals from Oxidation", DMIC Report 162, November 24, 1961.

16. Margrave, J. L., Proceedings of Symposium on "High Temperatures -- A Tool for the Future", Stanford Research Institute, 1956.

17. Neiman, A. S., O. Preston, D. A. Brown, "Tungsten and Rocket Motors", SRI Project No. US-2785, Contract No. NORD-18619 (FBM).

18. Norton, F. J., J. App. Physics, Volume 29, 1958, p. 1122.

19. Oxx, G. E., L. F. Coffin, Trans. AIME, Volume 218, 1960, p. 541.

20. Passmore, E. M., J. E. Boyd, L. P. Neal, C. A. Anderson, B. S. Lement, "Investigation of Diffusion Barriers for Refractory Metals", WADD Technical Report 60-343, August 1960, ASTIA AD 246559.

21. Proceedings of an International Symposium on High Temperature Technology, October 1959, McGraw-Hill, New York, 1960.

22. Wlodek, S. T., John Wulff, "Growth of Chromium Coatings from Liquid Metallic Solutions", Trans. Met. Soc. AIME, Volume 218, August 1960, pp. 716-722.

DISTRIBUTION

USA Command & General Staff College	1
The Research Analysis Corporation	1
Army Research Office, Durham	2
Army Research Office, OCRD	1
U. S. Army Engineer Research & Development Laboratories	2
U. S. Army Tank-Automotive Center	2
The Ordnance Board	1
Communications-Electronics Combat Developments Agency	1
U. S. Army Aviation and Surface Materiel Command	15
U. S. Army Transportation School	4
U. S. Army Transportation Research Command	21
U. S. Army Research & Development Group (Europe)	1
Chief of Naval Operations	1
Chief of Naval Research	3
Bureau of Yards & Docks, D/N	1
U. S. Naval Postgraduate School	1
Langley Research Center, NASA	2
Manned Spacecraft Center, NASA	1
Ames Research Center, NASA	2
Lewis Research Center, NASA	1
NASA Representative, Scientific and Technical Information Facility	1
U. S. Government Printing Office	1
Defense Documentation Center	10
U. S. Army Mobility Command	2
U. S. Army Materiel Command	1
Limited Warfare Laboratory	1

Radio Corp. of America, Harrison, N.J.
x RCA Tube Div.
x Direct Energy Conversion Dept.
OPTIMIZATION OF SILICON-GERMANIUM THERMOELECTRIC MODULES FOR TRANSPORTATION CORPS SILENT BOAT DESIGN - Andrew G. F. Dingwall, TCREC Technical Rept 63-17, May 1963, 100 pp. (Contract DA 44-177-TC-857) USATRECOM Task 1D010501A01408 (Formerly Task 9R99-20-001-08).

Unclassified Report
(over)

1. Silicon-Germanium Thermoelectric Modules
2. Contract DA 44-177-TC-857

Radio Corp. of America, Harrison, N.J.
x RCA Tube Div.
x Direct Energy Conversion Dept.
OPTIMIZATION OF SILICON-GERMANIUM THERMOELECTRIC MODULES FOR TRANSPORTATION CORPS SILENT BOAT DESIGN - Andrew G. F. Dingwall, TCREC Technical Rept 63-17, May 1963, 100 pp. (Contract DA 44-177-TC-857) USATRECOM Task 1D010501A01408 (Formerly Task 9R99-20-001-08).

Unclassified Report
(over)

1. Silicon-Germanium Thermoelectric Modules
2. Contract DA 44-177-TC-857

Radio Corp. of America, Harrison, N.J.
x RCA Tube Div.
x Direct Energy Conversion Dept.
OPTIMIZATION OF SILICON-GERMANIUM THERMOELECTRIC MODULES FOR TRANSPORTATION CORPS SILENT BOAT DESIGN - Andrew G. F. Dingwall, TCREC Technical Rept 63-17, May 1963, 100 pp. (Contract DA 44-177-TC-857) USATRECOM Task 1D010501A01408 (Formerly Task 9R99-20-001-08).

Unclassified Report
(over)

1. Silicon-Germanium Thermoelectric Modules
2. Contract DA 44-177-TC-857

Radio Corp. of America, Harrison, N.J.
x RCA Tube Div.
x Direct Energy Conversion Dept.
OPTIMIZATION OF SILICON-GERMANIUM THERMOELECTRIC MODULES FOR TRANSPORTATION CORPS SILENT BOAT DESIGN - Andrew G. F. Dingwall, TCREC Technical Rept 63-17, May 1963, 100 pp. (Contract DA 44-177-TC-857) USATRECOM Task 1D010501A01408 (Formerly Task 9R99-20-001-08).

Unclassified Report
(over)

1. Silicon-Germanium Thermoelectric Modules
2. Contract DA 44-177-TC-857

Mechanical strength tests, as well as life tests in air and vacuum environments, were performed on silicon-germanium thermoelectric modules with different construction features. The optimized thermocouple configuration withstood 100-g shock tests, 60-g vibration tests, and was operated stably in air at 1025°C at a conversion efficiency of 10 per cent. A study of a 30-KW generator utilizing silicon-germanium thermoelements indicated that such a generator is technically feasible.

Mechanical strength tests, as well as life tests in air and vacuum environments, were performed on silicon-germanium thermoelectric modules with different construction features. The optimized thermocouple configuration withstood 100-g shock tests, 60-g vibration tests, and was operated stably in air at 1025°C at a conversion efficiency of 10 per cent. A study of a 30-KW generator utilizing silicon-germanium thermoelements indicated that such a generator is technically feasible.

Mechanical strength tests, as well as life tests in air and vacuum environments, were performed on silicon-germanium thermoelectric modules with different construction features. The optimized thermocouple configuration withstood 100-g shock tests, 60-g vibration tests, and was operated stably in air at 1025°C at a conversion efficiency of 10 per cent. A study of a 30-KW generator utilizing silicon-germanium thermoelements indicated that such a generator is technically feasible.

Mechanical strength tests, as well as life tests in air and vacuum environments, were performed on silicon-germanium thermoelectric modules with different construction features. The optimized thermocouple configuration withstood 100-g shock tests, 60-g vibration tests, and was operated stably in air at 1025°C at a conversion efficiency of 10 per cent. A study of a 30-KW generator utilizing silicon-germanium thermoelements indicated that such a generator is technically feasible.